CHAPTER 1

INTRODUCTION

Managing a reservoir and well delivery requires continuous availability of reservoir pressure data. However, continuous reservoir pressure data acquisition is always a problem due to several economical and operational constraints, such as economically unjustifiable downhole monitoring or measuring devices, and risk of fishing and well downtime from measurement through well intervention (Hurzeler, 2010). For offshore operations, the situation can be further compounded due to downtime caused by bad weather making well locations inaccessible.

An alternative to downhole reservoir pressure data acquisition is to employ transient flow modeling technique (Hu *et al.*, 2007). In this modeling technique, the near wellbore reservoir pressure is estimated from surface data and then fluid redistribution during well shut-in is modeled. When a shut-in well reaches equilibrium, the reservoir pressure is obtained by the adding the closed-in tubing head pressure (CITHP) to the fluids' hydrostatic pressure (Hassan and Kabir, 2002). The fluids' hydrostatic pressure is calculated from the fluids' contact levels and the respective fluids' gradients as shown in Figure 1.1.

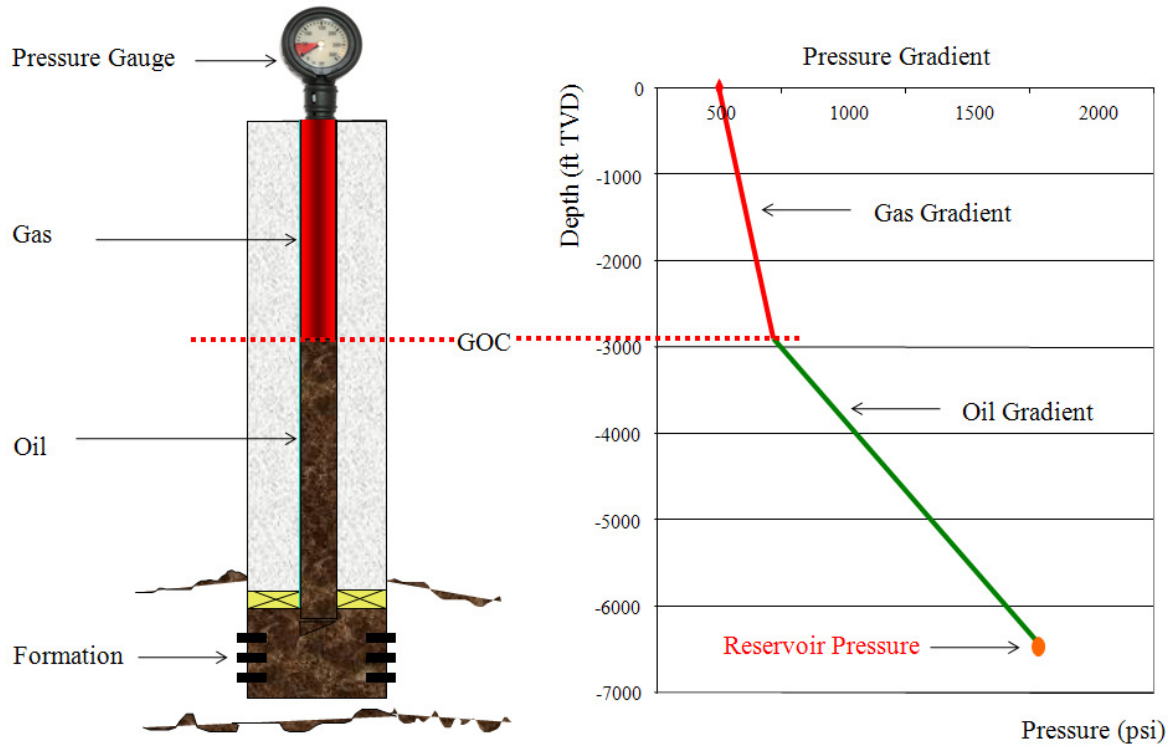

Figure 1.1: Reservoir pressure determination from fluids contact levels and gradients (Ahmed, 1989)

Hassan and Kabir (1994) employed the transient flow modeling technique to develop a physically realistic model for phase redistribution to estimate an accurate volume of each fluid phase at any cell in the well over time. However, Hassan and Kabir (1994) model is used to investigate the wellbore storage coefficient during pressure build-up survey rather than to estimate the reservoir pressure. Therefore, model refinement is required to demonstrate its applicability to estimate reservoir pressure.

1.1. Problem Statement

The lack of reservoir pressure data has always posed a problem in production planning and oil recovery optimization. Subsurface reservoir pressure data acquisition through intrusive well intervention method might lead to loss of production, increased risk, inconvenience and logistical problems and might involve additional expense and time (Chamoux and Patrick, 1998, Jordan *et al.*, 2006, Reeves *et al.*, 2003). An alternative to

well intervention is to employ transient flow modeling to estimate the near wellbore reservoir pressure.

Transient flow modeling technique is a proven tool which has been applied for years by facilities engineers for pipeline and slug-catcher design (Mantecon, 2007). However, transient flow modeling for estimating reservoir pressure requires further investigation to evaluate its applicability in wellbore condition. For wellbore transient behavior application, the overall goal is to obtain a better understanding of the physics of transient flow in the wellbore (Xiao *et al.*, 1995). Transient flow model should account for the dynamic wellbore and reservoir interaction (Hassan and Kabir, 1994). Neither reservoir models nor well flow models can account for the dynamic wellbore and reservoir interactions (Bin et al., 2007). Reservoir models use steady state lift curves to represent tubing performance relationships which ignore the flow dynamics in the wellbore (Bin et al., 2007). Well flow models use steady state inflow performance relationships (IPR) to describe the influx of oil and gas from the reservoir, which ignore the flow transients in the near-wellbore area (Hu et al., 2007). Hassan and Kabir (1994) proposed an integrated modelling of the combined wellbore and reservoir system in transient flow modelling. Hassan and Kabir (1994) model used a hybrid approach to couple both wellbore and reservoir system for phase redistribution. However, Hassan and Kabir (1994) model aimed to investigate the wellbore storage coefficient during pressure build-up survey rather than to estimate the reservoir pressure, suggesting the needs for this research.

1.2. Scope of Work

This research aims to model the transient flow in a shut-in well for the estimation of reservoir pressure. The investigation comprises four phases. The first phase is a detailed literature study in multiphase flow for both steady state flow and transient flow models. The applications and limitations of established steady state and transient flow models are also studied. In addition, pressure-volume-temperature (PVT) correlations and Equation of States (EoS) are studied in-depth because of their importance in determining volumetric and phase behavior of the hydrocarbon fluids in the well.

The second phase is to refine and modify Hassan and Kabir (1994) model to model the transient flow in shut-in well. A mathematical workflow to describe the underlying

physics of the model is developed. The mathematical workflow describes the fluid redistribution period in a shut-in well from the beginning of shut-in until equilibrium conditions are met. The mathematical workflow will account for continually decreasing reservoir fluid influx after shut-in, variation of void distribution within the wellbore with depth and time, and the combined effects of reservoir fluid influx and gas bubble migration on the wellhead and bottom-hole pressure.

This is followed by the third phase in which the mathematical workflow is programmed into separate calculation modules in visual basic codes. These modules are then seamlessly linked with the steady state flow model to become a fully functional transient flow model capable to estimate the reservoir pressure in a shut-in well.

The final phase is a verification phase to demonstrate the transient flow modeling capability and accuracy. Actual field data are collected and matched with the transient flow modeling-generated pressure build-up data. The variance between the actual and modeling-generated data is desired to be within 10% variation as per the standard industry acceptable limit (Zainal, 2010).

1.3. Objective

The three main objectives of this research are:

- To develop a transient flow model to estimate the reservoir pressure with modification on the Hassan and Kabir (1994) model.
- To transform the developed transient flow model mathematical workflow into visual basic code and link with steady state flow model, to become a fully functional transient flow model.
- To validate the developed transient flow model against real production data.

CHAPTER 2

LITERATURE REVIEW

Firstly, PVT correlations are studied in-depth as their use is essential in determining the volumetric and phase behavior of petroleum reservoir fluids. Secondly, a comprehensive literature review has been conducted to understand the multiphase flow theories, comprising important concepts on flow velocities, void fractions and their relations with pressure gradient in a well. Modeling flow in non-conventional situation, in particular countercurrent two-phase flow as occurred in shut-in well is discussed in detailed. In addition, the applications of established multiphase flow model for both steady state flow and transient flow are presented to examine the applicability of both models.

2.1. PVT Correlations

PVT correlations are essential in determining the volumetric and phase behavior of petroleum reservoir fluids. PVT correlations comprise of black oil PVT correlations and Equation of States, (EoS). The dependant parameters for both black oil PVT correlations and EoS are shown in the functions below:

$$\text{Back Oil PVT correlations} = f\ (\ P_B, T_{res}, R_s, API, SG_g, Bo\ ) \tag{2.1}$$

$$\text{EoS} = f\ (\ P, T, \text{gas \& oil composition}\ ) \tag{2.2}$$

2.1.1. Description of Black Oil PVT Correlations

When fluid properties are required for petroleum engineering calculations it is advisable to use values which have been measured on representative samples of the actual fluids

involved. However, such measurements are not always available. For these cases correlations of the required properties with other known properties have been developed.

The physical properties of primary interest that describes black oils includes fluid densities, isothermal compressibility, solution gas-oil ratio, oil formation volume factor, fluid viscosities, bubble point pressure and surface tension. These values of properties are employed in the calculation of material balance, allowing integrating the information from the reservoir to the information at surface through conservation of mass.

All the correlations use the reservoir temperature, gas and oil specific gravity and the solution gas to oil ratio to determine the properties of saturated oil. Several authors have provided correction factors to include the effects of non-hydrocarbon compounds and separator conditions. All the authors have used a large number of experimental data to regress the parameters of their proposed correlations to minimize the differences between the predicted and measured values (Ali, 1998).

Standing (1947) used a total of 105 data points on 22 different crude oils from California to develop his correlations. Lasater (1958) presented a bubble point correlation using 158 measured bubble point data on 137 crude oils from Canada, Western and Mid-Continental United States and South America. Vasquez and Beggs (1980) developed correlations for the solution gas to oil ratio and formation volume factor using 6004 data points. Glaso (1980) used data from 45 oil samples mostly from the North Sea region to develop his correlations.

Table 2.1 to 2.3 summarizes established black oil PVT correlations commonly used in the oil and gas. It is important to note that these correlations represent averages for a limited number of fluids and that sometimes large deviation might occur (Abdul, 1985; Ghetto, 1994). Therefore, these correlations should not be applied for conditions outside their application ranges. Table 2.4 tabulates the operating conditions for the respecting black oil PVT correlations.

Table 2.1: Examples of black oil PVT correlations for estimating bubble point pressure

No.	Correlation	Equation
1	Standing (1947)	$P_B = A\left[\left(\frac{GOR}{\gamma_g}\right)^B \times 10^{CT-API} - E\right]$
2	Lasater (1958)	$P_B = \frac{A(T+459.67)}{\gamma_g}\left[\exp\left(B\gamma_g\right) - C\right]$
3	Vasquez-Beggs (1980)	$P_B = \left[\frac{GOR}{A\gamma_g \exp\left(\frac{B \times API}{T+459.67}\right)}\right]^{D\left(\frac{1}{C}\right)}$
4	Glaso (1980)	$P_B = 10^x,$ $x = A + B\log_{10}(P_B *) - C[\log_{10}(P_B^*)]^2,$ $P_B * = \frac{D \times T^F GOR^E}{{\gamma_g}^G API^H}$
5	Petrosky-Farshad (1998)	$P_B = I\left[A\left(\frac{GOR}{\gamma_g}\right)^B {\gamma_g}^{-C} 10^{\delta} - D\right],$ $\delta = E \times T^F - G \times API^H$
6	Macary (1993)	$P_B = A[\exp\left(B \times T - L\left(C \times API + D\gamma_g\right)\right] \times [GOR^E - F]$

Note: Please refer to the complete nomenclature on page xiii.

Table 2.2: Examples of black oil PVT correlations for gas solubility

No.	Correlation	Equation
1	Standing (1947)	$R_s = \gamma_g \times \left[\left(\frac{P}{18.2} + 1.4\right) \times 10^{0.0125API - 0.00091(T-460)}\right]^{1.2048}$
2	Glasso (1980)	$R_s = \gamma_g \times \left[\left(\frac{API^{0.08}}{(T-460)^{0.172}}\right) \times P_b\right]^{1.2255}$
4	Vasquez-Beggs (1980)	$R_s = A\gamma_g P^B exp\left[C\left(\frac{API}{T}\right)\right]$

Note: Please refer to the complete nomenclature on page xiii.

Table 2.3: Examples of black oil PVT correlations for estimating oil formation volume factor

No.	Correlation	Equation
1	Standing (1947)	$B_o = G\left[A + B\left(R_s\left(\frac{\gamma_g}{\gamma_o}\right)^C + (DT + E)\right)^F\right]$
2	Lasater (1958)	$B_o = G\left[A + B\left(R_s\left(\frac{\gamma_g}{\gamma_o}\right)^C + (DT + E)\right)^F\right]$
3	Vasquez-Beggs (1980)	$B_o = D\left[1 + AR_s + B(T-60)\left(\frac{API}{\gamma_g}\right) + CR_s(T-60)\left(\frac{API}{\gamma_g}\right)\right]$
4	Glaso (1980)	$B_o = D\left(1 + 10^{-A+B\beta-C\beta^2}\right)$, $\beta = \log_{10}\left(ER_s\left(\frac{\gamma_g}{\gamma_o}\right)^F + GT\right)$
5	Petrosky-Farshad (1998)	$B_o = K\left(A + B\left[CR_s{}^D\left(\frac{\gamma_g}{\gamma_o}\right)^E \gamma_o^{-F} + GT^H + I\right]^J\right)$
6	Macary (1993)	$B_o = Aexp\left[F\left(BR_s + C\frac{\gamma_o}{\gamma_g}\right)\right](D + ET)$

Note: Please refer to the complete nomenclature on page xiii.

Table 2.4: Operating conditions for black oil PVT correlations

No.	PVT Properties	Standing (1947)	Lasater (1958)	Vasquez-Beggs (1980)	Glaso (1980)	Petrosky-Farshad (1998)	Marcary (1993)
1	P_B (psia)	130-7000	48-5780	15-6055	165-7142	1574-6523	1200-4600
2	B_o (rb/stb)	1.042-1.15	-	1.028-2.226	1.087-2.588	1.1178-1.6229	1.2-2.0
3	R_s (scf/stb)	20-1425	3-2905	0-2199	90-2637	217-1406	200-1200
4	Res. Temp. (^{o}F)	100-258	82-272	75-294	80-280	114-288	180-290

5	Oil API Gravity	16.5-63.8	17.9-51.1	15.3-59.5	22.3-48.1	16.3-45.0	25-40
6	Gas Specific Gravity	0.59-0.95	0.574-1.223	0.511-1.351	0.65-1.276	0.5781-0.8519	0.7-1.0

2.1.2. Description of Equation of States (EoS)

EoS is an analytical expression relating the pressure, P to the temperature, T and the volume, V (Ahmed, 1989). A proper description of this PVT relationship for real hydrocarbon fluids is essential in determining the volumetric and phase behaviour of petroleum reservoir fluids and in predicting the performance of surface separation facilities.

EoS originated from concept of the combined gas law which combines Charles's law, Boyle's law, and Gay-Lussac's law. In each of these laws pressure, temperature, and volume must remain constant for the law to be true. In the combined gas law, any of these properties can be found mathematically.

The best known and simplest example of an equation of state is the ideal gas equation, expressed mathematically by the expression:

$$P = \frac{RT}{V} \tag{2.3}$$

where V is the gas volume in ft^3 per one mole of gas.

This PVT relationship is only used to describe the volumetric behavior of real hydrocarbon gases at pressures close to the atmospheric pressure for which it was experimentally derived.

The extreme limitations of the applicability of the above equation prompted numerous attempts to develop an EoS suitable for describing the behavior of real fluids at extended ranges of pressures and temperatures. There are hundreds of these equations ranging from those for a specific pure compound to generalize forms that claim to relate the properties of multi-component mixtures (Ahmed, 1989). There is a large range of complexity from

the simple ideal-gas law to modern equations with 15 or more universal constants plus adjustable parameters.

The following describes established EoS and their respective applications in petroleum engineering. All EoS are generally developed for pure fluids first, and then extended to mixtures through the use of mixing rules. These mixing rules are simply means of calculating parameters equivalent to those of pure substances (Ahmed, 1989).

2.1.2.1.Van der Waals' EoS

In developing the ideal gas EoS, two assumptions were made. Firstly, the volume of the gas molecules is insignificant compared to the container and distance between the molecules. Secondly, there are no attractive or repulsive forces between the molecules or the walls of the container.

Van der Waals (1873) attempted to eliminate these two assumptions in developing an empirical EoS for real gases, the equation becomes:

$$\left(p + \frac{a}{V_M{}^2}\right)(V_M - b) = RT \tag{2.4}$$

where V_M is the molar volume and a and b are constants characteristic of the gas.

The term b is a constant to correct for the volume occupied by the molecules themselves. The term $\frac{a}{V_M^2}$ is a correction factor to account for the attraction between molecules as a function of the average distance between them, which is related to the molar volume. When an EoS such as the Van der Waals' equation is applied to mixtures, either special constants for a and b must be developed for each mixture or constants for each gas in the mixture must be included in the equation along with adjustments for the interaction between unlike gases. The latter is the more common approach.

Van der Waals' law extends the range of pressures and temperatures for describing gas behavior beyond that of the ideal-gas law (Ahmed, 1989). However, study by Ahmed (1988) showed that Van der Waals' law has two disadvantages in actual application.

Firstly, the correction factors are inadequate at very high pressures and it is not always easy to obtain the mixture coefficients and interaction constants. Secondly, this two-parameter formulation does not really treat the attractive and repulsive forces correctly. Despite these criticisms, modifications of the Van der Waals' equation have been used successfully in industry for many years (Ahmed, 1988).

2.1.2.2.Extension of EoS

Redlich and Kwong (1948) developed the first major extension of the two-parameter EoS when it was proposed the a and b terms to R, P_c, and T_c. Redlich and Kwong (1948) demonstrated that by a simple adjustment, the Van der Waals' attractive pressure term, $\frac{a}{V_M^2}$, could considerably improve the prediction of the volumetric and physical properties of the vapor phase.

Other researchers since have modified the original Redlich and Kwong equation to improve its accuracy and generality further. Most notable of the modifications are those of Soave, Zudkevitch and Joffe, and Peng and Robinson (Ahmed, 1989). The most common EoS in use today and the computer programs available are: 1) Starling-Hon extension of the Benedict-Webb-Rubin EoS, 2) Peng-Robinson EoS, and 3) Soave modification of the Redlich-Kwong EoS.

Equation 2.5 shows the Starling-Hon extension of the Benedict-Webb-Rubin EoS:

$$\begin{aligned} P = RT_{pM} &+ \left(B_o RT - A_o - \frac{C}{T^2} + \frac{D_o}{T^3} - \frac{E_o}{T^4} \right) P_M{}^2 \\ &+ \left(bRT - a - \frac{d}{T} \right) P_M{}^3 + \alpha(a+d) P_M{}^6 + \left(\frac{cP_M{}^2}{T^2} \right) \left(1 + \gamma P_M{}^2\right) \exp\left(-\gamma P_M{}^2\right) \end{aligned} \tag{2.5}$$

where A_o, B_o, C, D_o, E_o, a, b, c, d, α and γ are empirical constants, and P_M equals $\frac{n}{V_M}$ (subscript M refers to molar values). This equation is usually called "BWRS".

The Peng-Robinson EoS is:

$$P = \frac{RT}{V_M - b} - \frac{a(T)}{V_M(V_M + b) + b(V_M - b)} \tag{2.6}$$

where a and b are constants characteristic of the fluid, $a(T)$ is a functional relationship, and V_M, is the molar volume.

The Soave modification of the Redlich-Kwong EoS is:

$$P = \frac{RT}{V_M - b} - \frac{a(T)}{V_M(V_M - b)} \tag{2.7}$$

where $a(T)$ is a functional relationship.

The first equation, BWRS, is an empirical form using 11 constants. The values of these constants have been determined from properties measured on many different fluids. It is very accurate in the prediction of most thermodynamic properties. Equations 2.6 and 2.7 are variations of the original equation proposed by Van der Waals and as such are not as accurate as the BWRS for calculation of pure component properties or properties of mixtures of light hydrocarbons. Both the Peng-Robinson and the Soave RK EoS's are more reliable for phase equilibrium calculations or for calculation of properties of gas condensate systems. Their accuracy cannot be assessed directly because it is dependent on how well the constants represent the specific components (Ahmed, 1989).

2.1.2.3.The Generalized Form of EoS

Scmidt and Wenzel (1980) have shown that almost all cubic EoS can be expressed in a generalized form by the following four-constant EoS:

$$P = \frac{RT}{V - b} - \frac{a}{V^2 + ubV + wb^2} \tag{2.8}$$

When the parameters u and w are assigned certain values, equation 2.8 is reduced to a specific EoS. The relationship between u and w for a number of cubic EoS is given in Table 2.5 below:

Table 2.5: Equation of states relationships

Type of EoS	u	w
Van der Waals	0	0
Redlich-Kwong	1	0
Soave-Redlich-Kwong	1	0
Peng-Robinson	2	-1
Heyen	1-w	$f(w,b)$
Kubic	$f(w)$	$U^2/4$
Patel-Teja	1-w	$f(w)$
Schmidt-Wenzel	1-w	$f(w)$
Yu-Lu	$f(w)$	u-3

2.2. Multiphase Flow

Fluid flow in wellbores occurs during various phases of a well's life. Fluid flow, in a variety of forms and complexities, is a basic entity that must be dealt with in the production of hydrocarbons. Though multiphase production systems are complex, an accurate prediction of their behavior is essential for successful design and operation of offshore facilities (Danielson *et al.*, 2000). Interest in multiphase flow is not restricted to the oil industry. Nuclear, geothermal and chemical processing plants routinely requires two-phase flow modeling in their system design (Kaya *et al.*, 2001). The diverse interest in multiphase flow is reflected by a large number of publications in this area. At the same time, the excess of publications indicates that the basics of multiphase flow are not completely understood. Often, correlations are published that have no general applicability to any situation other than specific conditions under which those were developed (Hassan and Kabir, 2002).

One of the reasons multiphase flow is more complicated than single phase flow is that two or more fluids compete for the available flow area. To model flow behavior, one needs to know how the flow across section is occupied by each fluid phase. Therefore,

understanding physics of multiphase flow demands grasping important concepts such as flow velocity and volume fractions (Hassan and Kabir, 2002).

2.2.1. Superficial and In-Situ Velocities

Superficial velocity of any phase is the volumetric flow rate of that phase, divided by the total cross-sectional area of the channel. Thus, the superficial liquid velocity, v_{sL}, is given in terms of the volumetric liquid flow rate, q_L, and cross-sectional area, A, of the pipe (Hassan and Kabir, 2002):

$$v_{sL} = \frac{q_L}{A} \tag{2.9}$$

Similarly, superficial gas velocity, v_{sg}, is defined in terms of the volumetric gas flow rate q_g. It is important to note that superficial velocity is a quantity averaged over the flow cross section. Even for single-phase flow, fluid velocity across the channel varies; elements of fluid flowing close to the wall have much lower velocity than those flowing near the center.

2.2.2. Gas-Volume Fraction and Liquid Hold-Up

The relative amount of each fluid phase in the wellbore may be expressed in many ways. We can express the volumetric flow of the gas or liquid phase as a fraction of the total volumetric flow. This volume fraction can be calculated from the known flow rates. For instance, the gas volume fraction, f_g, can be calculated from superficial gas velocity, v_{sg}, and mixture velocity, v_m, as (Hassan and Kabir, 2002):

$$f_g = \frac{q_g}{(q_g + q_L)} = \frac{v_{sg}}{v_m} \tag{2.10}$$

Figure 2.1 depicts the in-situ volumetric fractions of the two phases in a pipe cross-sectional area of flow during transient behavior, where v_m, v_{sg} and v_{sL} respectively stands for the mixture, superficial gas and liquid velocities, f_g and f_L are the gas volume fraction and liquid hold-up, V, V_L and V_g are the pipe, liquid and gas volumes respectively. The

figure illustrates the relative portions of the two phases upon segregation. The liquid in-situ velocity is generally less than that of the gas phase, which means the liquid is held-up. This is the reason liquid fraction is known as the liquid hold-up in the petroleum industry.

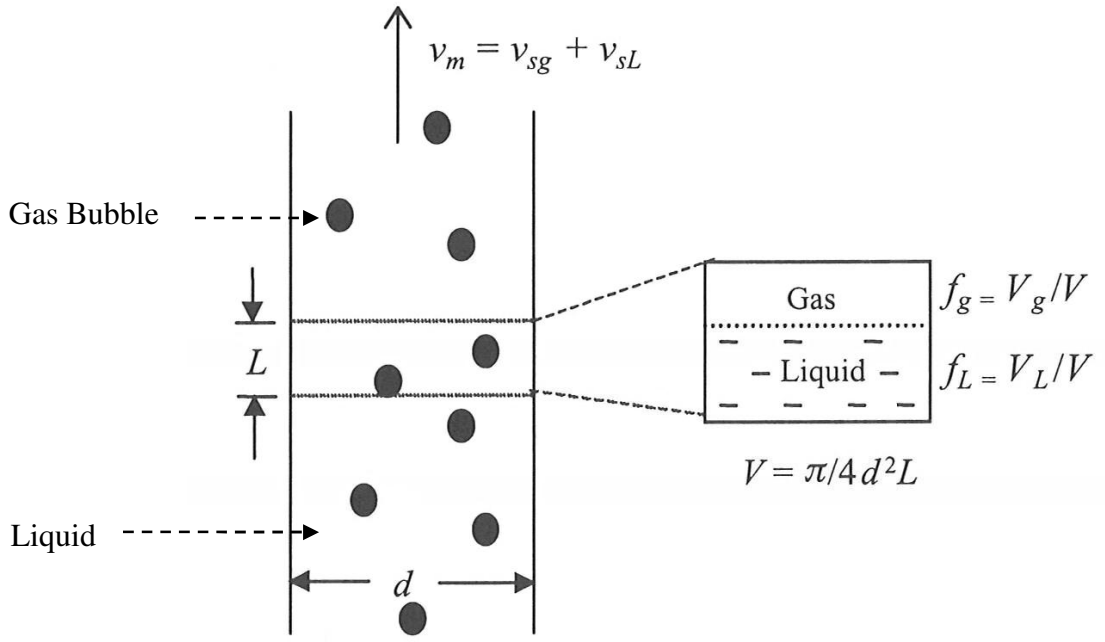

Figure 2.1: Schematic of in-situ and liquid volume fractions in two-phase flow

2.2.3. Mixture Density

Numerous equations have been proposed to describe the physical properties of gas and liquid mixtures. By definition, mixture density is the mass of gas and liquid in a unit volume of the mixture. Therefore, in a cubic foot of the mixture, there is liquid volume fraction, f_L ft^3 and gas volume fraction, (1-f_L) ft^3 of gas. Hence, in-situ density of the two-phase mixture, ρ_m, is based upon the in-situ volume fraction of each phase and is given by (James and Hemanta, 1999):

$$\rho_m = f_L \rho_L + (1 - f_L)\rho_g \tag{2.11}$$

2.2.4. Pressure Drop Prediction

The pressure drop in a multiphase pipeline can be separated into three distinct components: the frictional gradient, $\left(\frac{dp}{dz}\right)_F$, the hydrostatic gradient, $\left(\frac{dp}{dz}\right)_H$, and the accelerational gradient, $\left(\frac{dp}{dz}\right)_A$, (Danielson *et al.*, 2000):

$$\left(\frac{dp}{dz}\right)=\left(\frac{dp}{dz}\right)_F+\left(\frac{dp}{dz}\right)_H+\left(\frac{dp}{dz}\right)_A \tag{2.12}$$

The frictional pressure gradient is calculated from the Moody chart, using a modified Reynolds number based on a combination of slip and no-slip mixture properties (Moody, 1944). In general, for even mildly inclined pipelines, the gravitational pressure gradient quickly exceeds the frictional pressure gradient (Danielson *et al.*, 2000). For a shut-in well, the flow rate declines quickly after shut-in and the frictional pressure gradient soon becomes negligible (Hassan and Kabir, 1994). Computations by Xiao *et al.* (1995) also indicate that the addition of a frictional gradient has a negligible effect on pressure build-up data.

The acceleration pressure gradient becomes important if there is a sudden change in pipeline diameter, such as the presence of a choke, or if the gas density is changing very rapidly, resulting in a large change in gas velocity (Danielson *et al.*, 2000). The forming of liquid into a slug can also be an important source of acceleration pressure drop, but this presently ignored in all steady state flow and transient flow models (Danielson *et al.*, 2000).

Of these three terms, perhaps the hydrostatic gradient is the easiest to estimate because it only requires knowledge of the fluid density and well deviation angle (Hassan and Kabir, 2002). The static term will vary along the well because gas density depends on pressure.

In the analysis of multiphase flow in vertical and near vertical systems, the estimation of hydrostatic head becomes very important. In most vertical flow situations, the hydrostatic head is the major contributor to the total pressure gradient and can account for more than 90% of the total pressure drop. The hydrostatic head is directly dependent on the liquid hold-up, f_L, because of the mixture density. Therefore an accurate estimation of liquid hold-up is very important (Hassan and Kabir, 2002).

2.3. Countercurrent Two-Phase Flow

Countercurrent two-phase flow, in which liquid flows downward and the gas phase moves upward, occurs during transient testing. Transient tests that are performed by shutting the well at surface often lead to interpretation problems when high gas or liquid productions occur. The preferential movement of the gas may cause severe segregation, resulting in wellbore pressure increase (Hassan and Kabir, 1994). The increased pressure can cause the liquid to flow back into the formation, while the gas phase moves in the upward direction.

Very few works exist in the petroleum literatures that examined countercurrent two-phase flow (Hassan and Kabir, 2002). The work of Shah *et al.* (1978), among others, is essentially empirical in nature. Taitel and Bornea (1983) were the first to report the existence of three flow regimes – bubbly, slug and annular, and presented a map delineating the boundaries.

The behavior of countercurrent flow may be viewed as a combination of simultaneous flow of two phases in the upward and downward directions. For a bubbly flow regime, in which the gas hold-up is less than 0.25, Harmathy correlation (Harmathy, 1960) is used to estimate the gas bubble rise velocity, v_g, in a countercurrent flow:

$$v_g = 1.53\left[\frac{g\cdot(\rho_L-\rho_g)\cdot\theta_L}{\rho_L^{\,2}}\right]^{\frac{1}{4}} \tag{2.13}$$

In equation 2.13, g is the gravity force of 9.81 m/s^2, θ_L is the gas-liquid interfacial tension, whereas ρ_l and ρ_g are the liquid and gas densities respectively.

If the gas hold-up is more than 0.25, the flow regime is slug flow, the gas bubble rise velocity, v_g, is calculated from equation 2.14 below (Bikbulatov et al., 2005):

$$v_g = 0.35\cdot\sqrt{g\cdot ID\cdot\frac{(\rho_L-\rho_g)}{\rho_L}}\cdot Dev \tag{2.14}$$

ID is the tubing diameter and the flow deviation angle, *Dev*, is calculated from:

$$Dev = \sqrt{\sin\left(\frac{incl \cdot \pi}{180}\right)} \cdot \left[1 + \cos\left(\frac{incl \cdot \pi}{180}\right)\right]^{1.2} \quad (2.15)$$

The inclination, *incl*, is 90 degree minus the well angle from vertical.

2.4. Multiphase Flow Model

The analysis of multiphase flow phenomena in pipeline systems is classified along two levels of complexity (Ellul *et al.*, 2004). The first is that associated with steady state flow where there is no major changes transgressing the pipeline network. The second related to transient or dynamic flows where the flow behavior is changing on a regular and significant basis (Ellul *et al.*, 2004). Both steady state and transient flow models can be viewed as complementary rather than competitive. There are specific situations where each would be greatly favored over the other (Danielson *et al.*, 2000). Details descriptions on both the steady state flow model and transient flow model are described in the following sections.

2.4.1. Steady State Flow Model

In a producing well, the fluids are flowing in steady-state flow condition whereby the fluid properties at any single point in the tubing do not change over time (Ellul *et al.*, 2004). There is no accumulation of mass in the tubing. There are many established multiphase flow correlations that have become integral element of steady-state flow modeling, which is well established and implemented in software (Orkiszewski, 1967, Duns and Ros, 1963, and Mukherjee and Brill, 1983).

Fluid properties change with the location-dependent pressure and temperature in the oil and gas production system. To simulate the steady state fluid flow in the system, it is necessary to "break" the system into discrete nodes that separate system elements or equipment components. Fluid properties at the elements are evaluated locally. The system analysis for determination of fluid production rate and pressure at a specific node is called "nodal analysis" in petroleum engineering (Boyun *et al.*, 2007).

Figure 2.2 depicts the steady state flowing condition in a producing well towards an equilibrium condition upon well shut-in. Note that the fluid flow goes through a transient flow period from the steady state flow condition before reaching equilibrium condition.

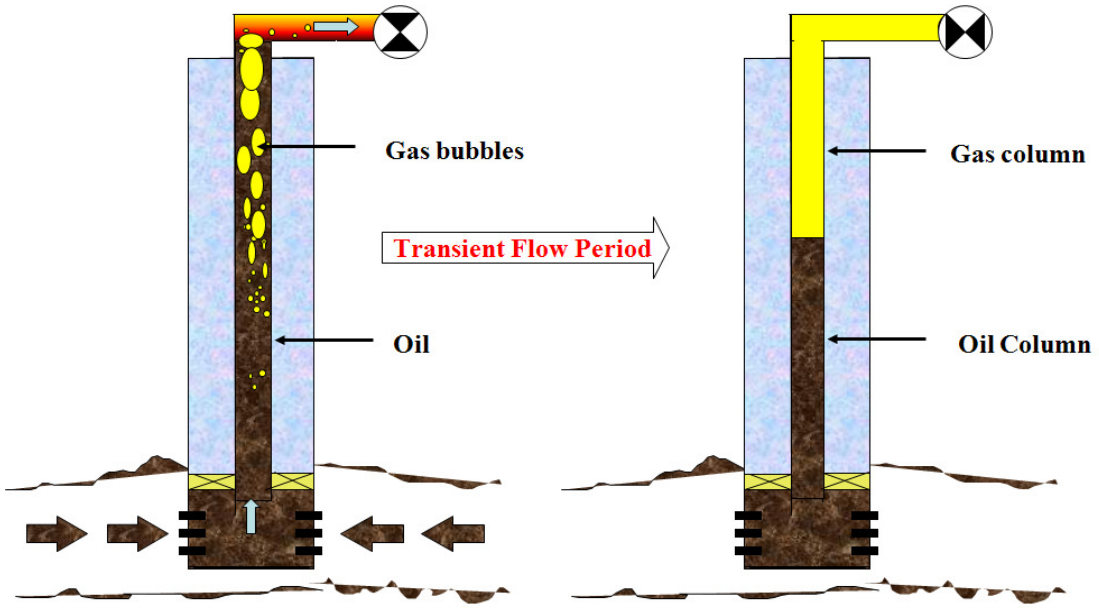

(a) Producing well (b) Shut-in well

Figure 2.2: (a) Producing well at steady state flow; (b) Shut-in well at equilibrium

2.4.2. Transient Flow Model

Transient flow model is applied where the fluid flow in the system is no longer flowing in steady state condition. Contrary to the steady state flow condition, fluid properties at any single point in the tubing are changing on a regular and significant basis during a transient flow condition (Ellul *et al.*, 2004). The rapid uptake of transient flow model demonstrates the recognized value to the industry of this relatively new technique (James and Hemanta, 1999). It is an excellent modeling technique to understand transient well behavior and determine the optimum process to eliminate or minimize potential transient problems. It does not replace nodal analysis used in steady state flow model but fills gap where nodal analysis techniques cannot provide solutions (James and Hemanta, 1999).

The emergence of complex operational situations has caused demand in transient flow modeling technique (Ellul *et al.*, 2004). Several common applications of transient flow modeling technique are well understood and documented, such as for application in pipeline hydrate formation prediction (Davies *et al.*, 2009, Boxall *et al.*, 2008, Harun *et al.*, 2006, Zabaras and Mehta, 2004), pipeline slug modeling (Fard *et al.*, 2006, Tang *et al.*, 2006, Meng and Zhang, 2001, Havre and Dalsmo, 2001, Taitel *et al.*, 2000), flow assurance modeling for gas condensate well and pipeline (Hagesæter *et al*. 2006, Eidsmoen and Roberts, 2005) as well as in understanding of well liquid loading (Chupin *et al.*, 2007). The dynamic simulation used in these transient flow models is capable of modeling the well multiphase flow behavior from the static initial conditions (zero rates) to the steady state flow conditions, confirming if such conditions can be reached. Therefore, the area of application is dramatically increased over steady state techniques (Mantecon, 2007). Table 2.6 summarizes the common applications of transient flow model.

Table 2.6: Areas of application of transient flow model as reviewed by Mantecon (2007)

Flow Assurance Threat	Wells	Pipelines	Process Facilities
Flow delivery through field-life	• Verification of planned production • Optimal routing to pipelines • Ability to restart wells • Time to re-establish full flow potential • Water accumulation	• Pipeline packing / unpacking • Start-up / Shut-in • Operation of twin parallel lines • Application of multiphase pumps • Product composition from co-mingled fields • Component tracking	• Control stability • Production optimization • Hot oil circulation • Subsea separation
Liquid surges	• Optimal use of gas lift • Flow stability	• Slug break-up • Designing successful pigging operations	• Vessel sizing • Surge control
Hydrates & wax	• Inhibitor deployment • Sub-surface safety valve placement	• Design of insulation/bundle/heating medium • Inhibitor deployment • Water accumulation	• Handling wax volumes
Integrity & safety	• Drilling operations • Water accumulation	• Pressurization or depressurization within material limitations • Identification of high corrosion risk areas • Location and conditions of reverse flow	• Flare system requirements and capabilities • Identification of leaks from routine data

When actual surface and subsurface data measurements are available for matching the transient flow modelling results, it is possible to convert the transient flow model into a virtual downhole gauge and multiphase flow meter (Mantecon, 2007). Transient flow model can be

used initially as a predictive tool when the reservoir boundary input is estimated and the modelling results cannot be compared with the actual data. However, when actual data measurements are available, the model can be validated by matching the measured data. Once validated, the model becomes a virtual well simulator. Depending on the type of actual data available for model validation, the model can be converted into 1) a virtual downhole gauge if only surface data available, or 2) a virtual downhole gauge and multiphase flow meter if both surface and subsurface data are available. In both cases, when using the model as a virtual well, the model should be able to match the well-reservoir interaction which is transient in nature (Mantecon, 2007). The virtual downhole gauge and multiphase flow simulator can calculate all the bottom-hole flowing conditions including downhole multiphase flow rates, from available wellhead temperature and pressure, oil, gas and water flow rates, subsurface bottom-hole pressure and temperature measurements. Surface and downhole measurements should be matched by the transient flow modelling results (Mantecon, 2007).

Meanwhile, transient flow model should account for the dynamic wellbore and reservoir interaction (Hassan and Kabir, 1994). Neither reservoir models nor well flow models can account for the dynamic wellbore and reservoir interactions (Bin *et al.*, 2007). Reservoir models use steady state lift curves to represent tubing performance relationships which ignore the flow dynamics in the wellbore (Bin *et al.*, 2007). Well flow models use steady state inflow performance relationships (IPR) to describe the influx of oil and gas from the reservoir, which ignore the flow transients in the near-wellbore area (Hu *et al.*, 2007). In addition, a typical steady state flow IPR uses Vogel (1968) and Standing (1970) derived correlations for oil reservoirs. These idealized mathematical equations are sensitive to actual field data and often results in misinterpretation (Mattar, 1987). Most importantly, the dynamic wellbore and reservoir interactions are not accounted for in using these equations (Hu *et al.*, 2007). For example, Gaspari *et al.* (2006) verified the performance of an advanced transient flow model with the field data from an offshore well in Brazil. Even though the simulation matched the steady state production perfectly, the model failed to simulate the shut-in and start-up operations by a big deviation in the downhole shut-in pressure prediction (Hu *et al.*, 2007).

Gaspari *et al.* (2006) concluded that a reservoir model based on IPR may not be reasonable for modelling the pressure transient in the well and recommended that a more complex, time-dependent model is needed for better simulation results. Hu *et al.* (2007) highlighted that pressure transient results deviation in the work by Gaspari *et al.* (2006) was attributed to the strong pressure transient in the tight reservoir, which was not considered in the modelling.

To bridge this gap, an alternative might lie in an integrated modelling of the combined wellbore and reservoir system in transient flow modelling (Hassan and Kabir, 1994). Hassan and Kabir (1994) recommended a hybrid approach to couple both wellbore and reservoir system. The principle of superposition in time is used to relate the sandface flow rate to the formation properties, wellbore shut-in pressure and shut-in time (Hassan and Kabir, 1994).

$$q(t_{j+1}) = q(t_j) + \frac{\Delta p(t_{j+1})}{m'[p_D(t_{D,j+1} - t_{D,j}) + s]} - \frac{1}{p_D(t_{D,j+1} - t_{D,j} + s)} \sum_{i=1}^{j} [q(t_i) - q(t_{i-1})][p_D(t_{D,j} - t_{D,j-1})] \quad (2.16)$$

where

$$t_D = \frac{0.000264\, kt}{\phi \mu C_t A} \quad (2.17)$$

Note that t_D is calculated based on each time-step j.

$$p_D = \frac{1}{2} \ln\left(\frac{4t_D}{1.781}\right) \quad (2.18)$$

$$m' = 162.6 \frac{Bo\,\mu}{kh} \quad (2.19)$$

t_D represents the dimensionless time argument during pressure build-up period in the shut-in well, whereas the p_D equation is the dimensionless pressure applicable to the early steady state or linear period for the build-up phase (Dake, 2001). Dake (2001) stated that the effect of

reservoir fluid influx is only significant at the beginning of the build-up, therefore, the use of equation 2.18 in calculating the reservoir fluid influx is a valid assumption.

Equation 2.16 is completely general, in which for any analytical reservoir model, the dimensionless pressure, p_D, can be used to represent the reservoir response. For instance, when the logarithmic approximation of the line-source solution applies, equation 2.16 becomes very similar to the expression developed by Muenier et. al. (1985). It forms the basis for calculating the sandface flow rate at any time after shut-in, which depends on prior knowledge of the shut-in pressure. Thus, the mathematical workflow for the transient flow model entails the use of shut-in pressure, p_{ws}, calculated at the earlier time-step to establish the flow rate at the present time-step (Hassan and Kabir, 1994).

One difficulty with the use of equation 2.16 is that numerical rounding off may make the calculated reservoir fluid influx not equal to zero when $p_i - p_{ws} = 0$. As the wellbore shut-in pressure approaches the reservoir pressure, flow rates calculated with equation 2.16 may cause numerical stability problems. Therefore, it was suggested that selecting small time-steps is required to avoid this problem (Hassan and Kabir, 1994).

Hassan and Kabir (1994) proposed a physical realistic transient flow model for phase redistribution based on integrated modelling of the combined wellbore and reservoir system. Meanwhile, Xiao *et al.* (1995) proposed a mechanistic transient flow model to simulate wellbore phase segregation. The Xiao *et al.* (1995) model accounted for wellbore and reservoir flow interaction, and handled the effect of interface mass transfer through black-oil approach. The black-oil formulation, commonly used in reservoir simulation, is applied to account for the interphase mass transfer in Xiao *et al.* (1995) model. A variable bubble-point procedure is included in the calculation. Single-phase flow of oil in the reservoir is assumed to allow rigorous couple of the reservoir and wellbore with a convolution integral (Duhamel's principle).

Both proposed transient flow models by Hassan and Kabir (1994) and Xiao *et al.* (1995) are aimed to investigate the wellbore storage coefficient during pressure build-up survey. They concluded that the wellbore storage coefficient is affected by both phase segregation and gas compression.

In summary, transient flow modeling for wellbore is a new application of multiphase flow, which requires different understanding and expertise (Mantecon, 2007). The literature search showed that there are several reported works on transient flow modelling for application in pipeline hydrate formation, pipeline slug modeling, flow assurance modeling for gas condensate well, understanding of well liquid loading as well as determination of wellbore storage coefficient. There appeared to be no reported work on application of transient flow modelling in simulating reservoir pressure, suggesting the needs for this research. To develop a wellbore transient flow modelling technique, it is essential to rigorously model transient flow in the wellbore emphasizing the phase segregation on pressure build-up data (Xiao et al., 1995). In addition, PVT calculation is an essential integral element in determining the wellbore fluids' PVT properties during transient flow. Meanwhile, it is equally important to account for the dynamic wellbore and reservoir interactions in developing wellbore transient flow modeling technique (Hassan and Kabir, 1994).

CHAPTER 3

METHODOLOGY

The aim of this research is to modify Hassan and Kabir (1994) transient flow model for the estimation of reservoir pressure. The first section of this methodology chapter presents the framework of the mathematical workflow of the modified Hassan and Kabir (1994) transient flow model to simulate fluid redistribution in a shut-in well. This includes the input and output parameters with the complete set of equations and theories. The mathematical workflow captures all the underlying physics of the transient period when a well is shut-in until equilibrium condition is met. The mathematical workflow is then transformed into visual basic code and linked with the steady state flow model to become a fully functional transient flow model.

The second section presents the well selection criteria to validate the capability of the transient flow model. Careful selection of candidate well is important to ensure that it meets the working condition and range of applicability of the modeling technique.

3.1 Transient Flow Model Mathematical Workflow

Steady state flow model for well is used to model the inflow performance relationship of the well by generating the pressure traverse curve of a production well flowing in a steady state condition. When the producing well is shut-in, there is a transient flow period before reaching equilibrium, whereby during this period the fluid velocity and pressure changes over time, resulting in a very complex system to model. This section presents on the mathematical workflow developed for the transient flow model to simulate the transient flow behavior in a shut-in well. This transient flow modeling is a modeling technique that transfers the steady state flowing fluids' pressure gradient as shown in

Figure 3.1b into the static fluids' pressure gradient as shown in Figure 3.1a. The latter is used to obtain the reservoir pressure when the fluid columns are fully segregated upon equilibrium.

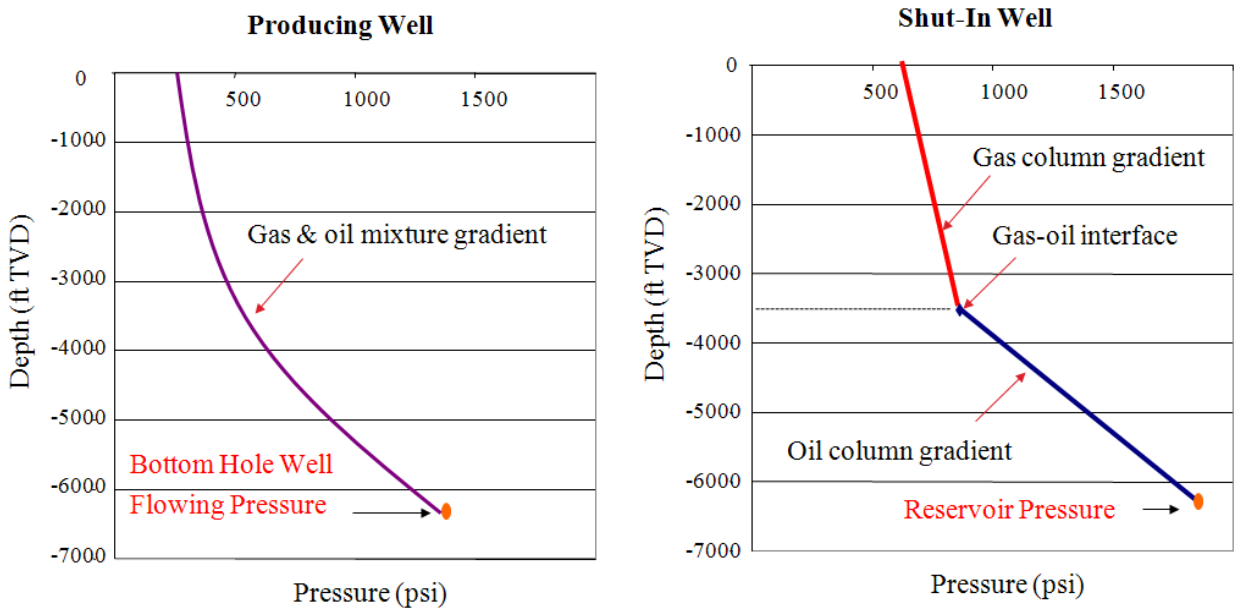

(a) Producing well: Steady state flowing fluids' pressure gradient profile

(b) Shut-in well: Static fluids' pressure profile

Figure 3.1: Fluids' pressure gradient profiles

The mathematical workflow to obtain the fluids' pressure gradient profile from steady state flow until shut-in equilibrium condition is illustrated in Figure 3.2.

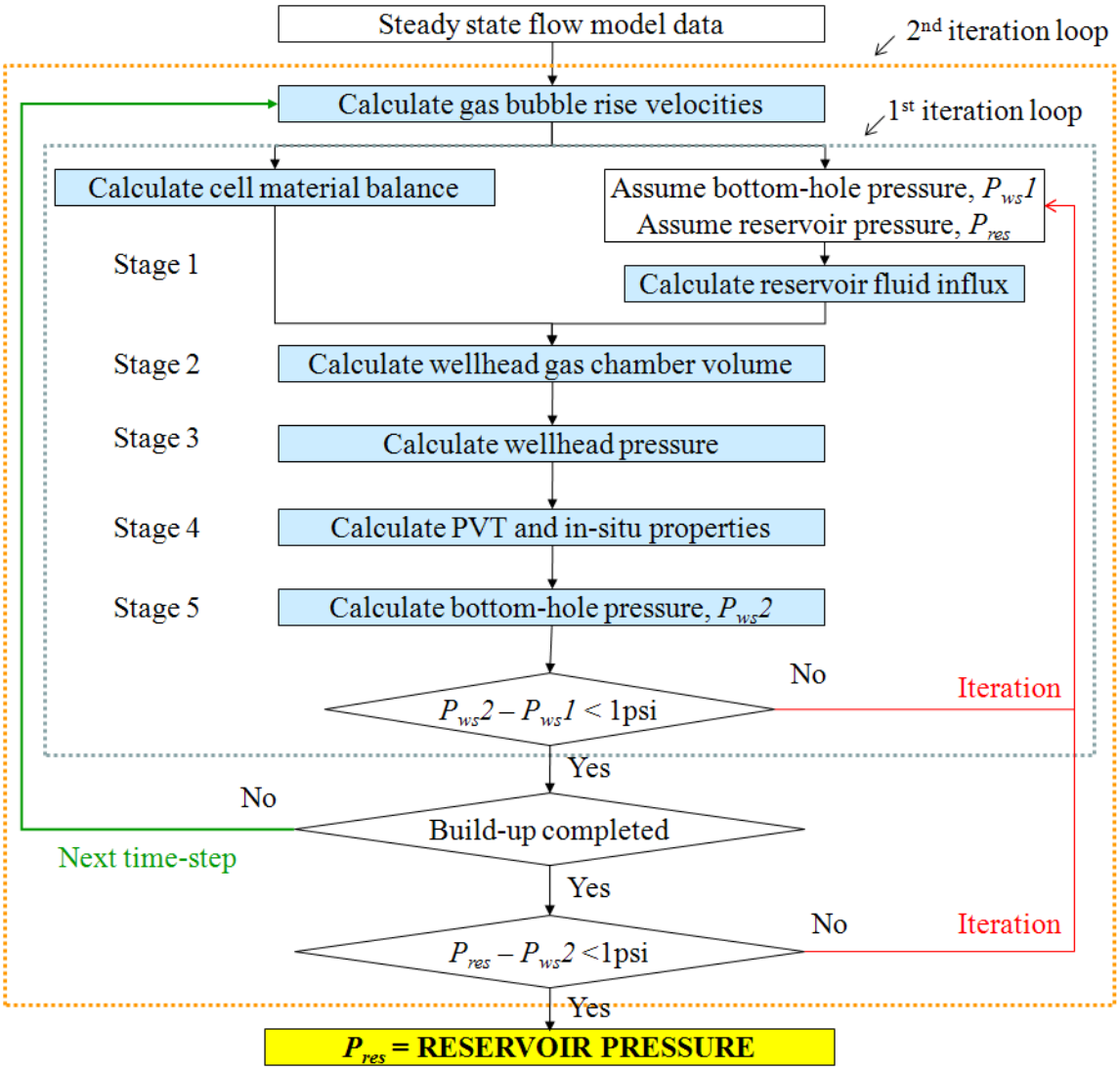

Figure 3.2: Overall mathematical workflow

The subsequent calculation procedures describe the overall mathematical workflow in Figure 3.2:

Step 1: Inputs initialization

- Once the well shut-in option is initiated, all the required steady state flow model data is read. The well is descretized into numerous cells and each of the cell will be assigned a set of fluid properties corresponding to its temperature and pressure.

Step 2: Bubble rise velocities calculation

- The oil density, gas density and the gas-oil interfacial tension from previous time-step is used to calculate the current time-step bubble rise velocity in each of the cell.

Step 3: Cell material balance calculation

- To account for the accurate gas-liquid interface movement at any time-step as shown in Figure 3.3, the adjacent cell, denoted as *NN* cell, right below the gas chamber is set to be flexible and changeable in cell size. When the gas chamber is increasing, the size of the *NN* cell should be reduced accordingly so that the total tubing volume is maintained throughout.

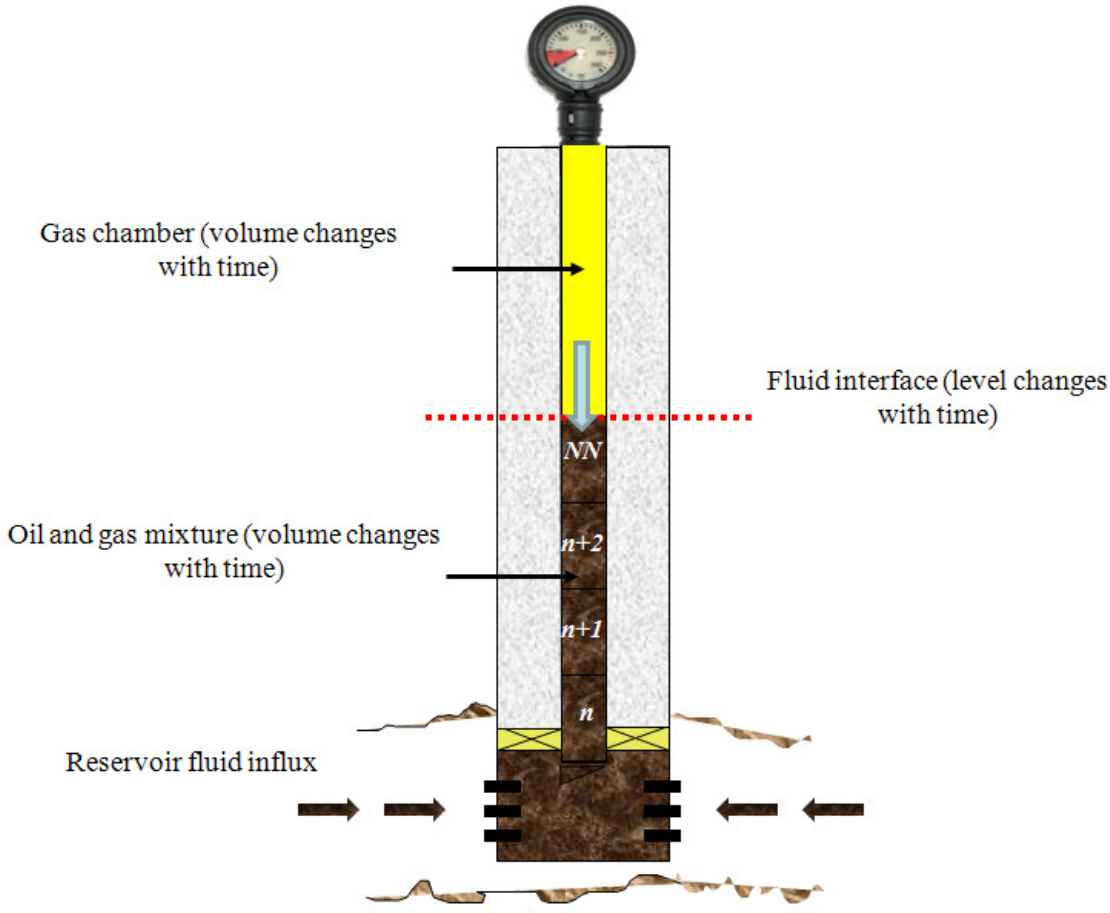

Figure 3.3: Schematic of fluid interface movement

Step 4: Reservoir fluid influx calculation

- The reservoir fluid influx calculation is performed by using the wellbore shut-in pressure, $P_{ws}1$, obtained from the previous time-step. This initial guess $P_{ws}1$ is indeed arbitrary and any other value can be used as the initial guess value. The calculation will eventually reach to the same solution point after iterations to match the calculated wellbore shut-in pressure, $P_{ws}2$ derived from gradient calculation. The previous time-step $P_{ws}1$ is used as the first guess $P_{ws}1$ to reduce the calculation time.

- The reservoir fluid influx takes into account the volume of the associated gas that will evolve from liquid solution as pressure in the wellbore is lower than in the reservoir.

Step 5: Wellhead gas chamber volume calculation

- Due to the lighter gas density than that of water and oil, the gas bubbles ascend upwards and accumulate at the well top forming a gas chamber. The gas chamber volume may be increasing or decreasing in size. After each time-step, the wellhead gas chamber volume will be recalculated from the remaining gas volume in the rest of the tubing length (except the wellhead gas chamber), total reservoir fluid influx volumes (and its associated gas) and compressibility effect.

Step 6: Wellhead pressure calculation

- The wellhead pressure is derived from the volume-pressure gas law relationship for real gas system. As the calculation requires the gas compressibility factor, z, for the current wellhead pressure, an internal iteration loop is used within this step to deduce the representative z factor at the current time-step.

- The additional gas mole added to the wellhead gas chamber is calculated from the number of mole gas leaving the *NN* cell at the particular time-step.

Step 7: PVT and in-situ properties calculation

- After the wellhead pressure is estimated from the gas law, the fluid gradient of each cell is computed starting from the wellhead to wellbore. The fluid gradient from the upper cell will be used to deduce the fluid gradient for the subsequent cell located below it.

- To attain a reliable fluid gradient for each of the cell, PVT calculation module will be called each time and the fluid gradient in each cell is calculated. The PVT calculation module calculates the fluids' densities, volumes, solution gas, formation volume factors, and compressibility factors. The associated cell pressure will be iterated to match the fluid gradient calculation, which is assumed gradient equal to calculated gradient.

Step 8: Bottom-hole pressure calculation

- The fluid gradient calculation from top to bottom tubing leads to the calculation of shut-in wellbore pressure, $P_{ws}2$. The $P_{ws}2$ is compared to the initially assumed $P_{ws}1$ (for reservoir fluid influx calculation) until a good match is achieved between these two values. Bisectional programming approach is adopted to speed up the iteration calculation to attain the final shut-in wellbore pressure before the next time-step is embarked.

Overall, the entire calculation procedure describe in steps 1 to 8 is illustrated in Figure 3.2. It has two iteration loops. The first iteration loop is to converge the assumed bottom-hole pressure (input of the reservoir fluid influx calculation) with the calculated bottom-hole pressure (obtained at the end of the fluid redistribution calculation over the time-step). A tolerance of 1 psi is employed to ensure the accuracy of the calculation. The second iteration loop is to converge the assumed reservoir pressure (input of the reservoir fluid influx calculation) with the calculated reservoir pressure (obtained when the well has reached equilibrium at the end of the time-step).

This mathematical workflow accounts for continually decreasing reservoir fluid influx after shut-in, the variation of void distribution within the wellbore against depth and time,

and the combined effects of influx and gas bubble migration on the wellhead and bottom-hole build-up pressure. The following sections details the physics and the equations used in the mathematical workflow.

3.2 Steady State Flow Model Data

Prior to the well shut-in, the well is flowing at steady state flow condition. Capturing the initial steady state flow condition is essential to set-up the transient flow model for shut-in well. Therefore, the first step of well transient behavior prediction during shut-in period is to obtain the steady state flow data prior to the shut-in. These data will be the initialization inputs to model the transient flow in a shut-in well.

The calculation starts with constructing the steady state flow model using Multiflo^{TM} software, a nodal analysis tool. This steady state flow modeling was run using a standard well configuration at steady state flowing conditions. The well is divided into numerous cells according to the respective cell length generated from the steady-state model. Each cell has its respective steady-state flow data, exactly as before shut-in. These steady state flow model output data will be used as the input parameters for the transient flow modeling calculations. The key steady state flow model output data are:

1. Well depth (bottom measured depth and true vertical depth)
2. Well angle from vertical
3. Cell length (bottom measured depth)
4. Tubing diameter
5. Pressure
6. Temperature
7. Gas-oil interfacial tension
8. Gas and oil viscosities
9. Gas and oil densities
10. Gas and oil specific gravities

11. Gas and oil hold-up

12. Gas and oil formation volume factors

13. Solution gas

3.3 Gas Bubble Rise Velocities

When a well is shut-in, the gas bubble will rise towards the wellhead whereas the liquid will drop to the bottom of the well. The velocity of the rising gas bubble can be calculated from the initial PVT properties generated from the steady state flow model.

If the gas hold-up is less than 0.25, the flow regime is bubble flow (Hassan and Kabir, 2002). Evaluation by Hassan and Kabir (2002) showed that Harmathy correlation (Harmathy, 1960) is suitable in estimating the gas bubble rise velocity, v_g, in a countercurrent flow of a shut-in well:

$$v_g = 1.53 \cdot \left[\frac{g \cdot (\rho_L - \rho_g) \cdot \theta_L}{\rho_L^{\,2}} \right]^{\frac{1}{4}} \tag{2.13}$$

where

g ≡ gravity force, 9.81 m/s^2

θ_L ≡ gas-liquid interfacial tension (dynes/cm)

ρ_L ≡ liquid density (kg/m^3)

ρ_g ≡ gas density (kg/m^3)

If the gas hold-up is more than 0.25, the flow regime is slug flow (Hassan and Kabir, 2002). The work by Bikbulatov *et al.* (2005) showed that the flow deviation angle affects the gas bubble rise velocity, v_g, there equation 3.2 below is recommeded:

$$v_g = 0.35 \cdot \sqrt{g \cdot ID \cdot \frac{(\rho_L - \rho_g)}{\rho_L}} \cdot Dev \tag{2.14}$$

where

g ≡ gravity force, 9.81 m/s^2

ID ≡ tubing diameter (m)

ρ_L ≡ liquid density (kg/m^3)

ρ_g ≡ gas density (kg/m^3)

$$Dev = \sqrt{\sin\left(\frac{incl \cdot \pi}{180}\right)} \cdot \left[1 + \cos\left(\frac{incl \cdot \pi}{180}\right)\right]^{1.2} \tag{2.15}$$

where

$incl$ ≡ 90^o-deviation^o

$deviation^o$ ≡ well angle from vertical (^{o})

3.4 Reservoir Fluid Influx

The modelling of the transient flow in a shut-in well should include the well-reservoir interaction which is transient in nature. The interaction between the well and the near wellbore reservoir region can play a dominant role in the description of the dynamic behavior of the complete system (Mantecon, 2007). The principle of superposition in time is used to relate the sandface flow rate to the formation properties, shut-in bottom-hole pressure and shut-in time (Hassan and Kabir, 1994) as in equation 2.16. The pressure difference, Δp, between the shut-in bottom-hole pressure, p_{ws}, over time and the reservoir pressure, p_{res}, is accounted in the reservoir fluid influx calculation.

$$q(t_{j+1}) = q(t_j) + \frac{\Delta p(t_{j+1})}{m'[p_D(t_{D,j+1} - t_{D,j}) + s]} - \frac{1}{p_D(t_{D,j+1} - t_{D,j} + s)} \sum_{i=1}^{j} [q(t_i) - q(t_{i-1})][p_D(t_{D,j} - t_{D,j-1})] \tag{2.16}$$

where t_D is the dimensionless time during pressure build-up period in the shut-in well, whereas the p_D is the dimensionless pressure during the early steady state or linear period of the build-up phase. The details of equation 2.16 is discussed in section 2.4.2.

3.5 Cell Material Balance

To account for fluid movement in the wellbore, the wellbore is discretized into a number of cells, as shown in Figure 3.4 below, with the top cell completely filled with gas. This top cell is known as gas chamber thereafter in the latter discussion.

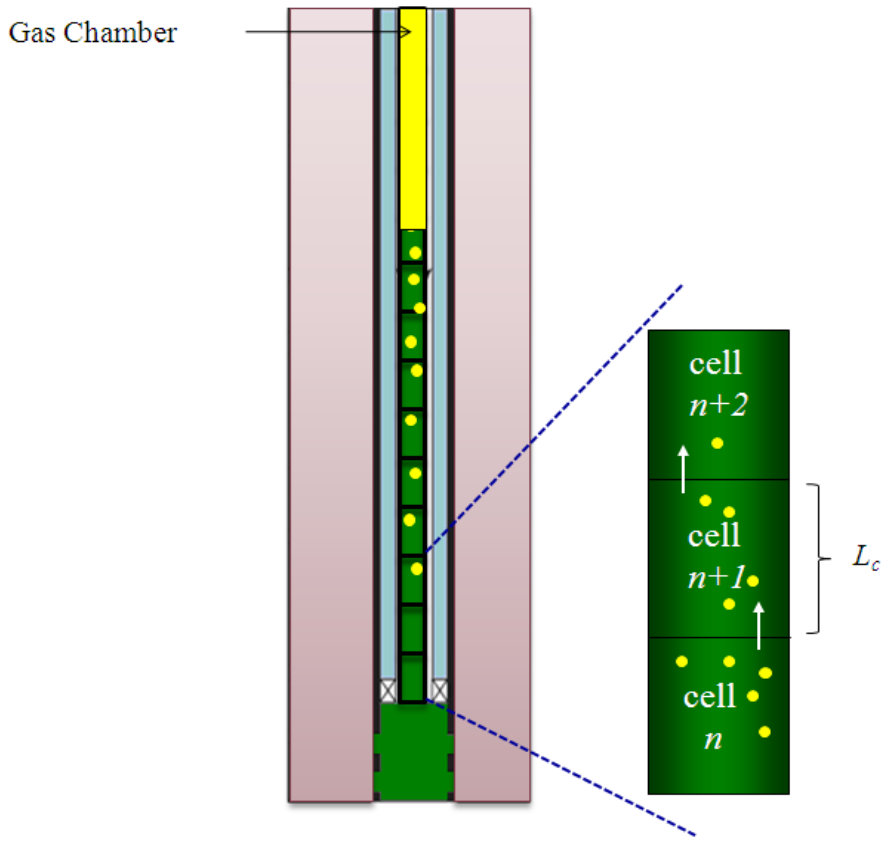

Figure 3.4: Schematic representation of the wellbore for cell material balance

Within a time-step, from time t_j to time t_{j+1}, cell $n+1$ receives gas from the cell below, cell n and losses it to the cell above, cell $n+2$. Over the elapse time, $\Delta t(t_{j+1} - t_j)$, cell $n+1$ receives gas from the lower cell from as far down as the bubbles can travel in that time period, which is from a distance of up to $v_g \Delta t$. Thus, the fraction of gas in the cell n that will migrate to cell $n+1$ is $v_g \Delta t / L_c$, where L_c is the length of each cell. This L_c remains constant throughout the transient calculation. The actual volume of the gas gained by cell $n+1$ from cell n below, $V_{R,n}$, also depends on the gas compressibility factors and the pressures and temperatures of the cells (Hassan and Kabir, 1994). Noting that v_g is obtained from equation 2.13 or 2.14 depending on the flow regime as explained in the section 3.3. The volume of gas received by cell $n+1$ is obtained by:

$$V_{R,n} = v_g \Delta t \left[\frac{V_{g,n}(t_j)}{L_c} \right] \left[\frac{p_n}{p_{n+1}} \frac{T_{n+1}}{T_n} \frac{z_{n+1}}{z_n} \right] \tag{3.1}$$

where

Ug ≡ gas bubble rise velocity (m/s)

Δt ≡ elaspse time (s)

$V_{g,n}(t_j)$ ≡ gas volume in cell n at time j (m^3)

L_c ≡ cell length (m)

P_n ≡ pressure at cell n (psi)

P_{n+1} ≡ pressure at cell $n+1$ (psi)

T_n ≡ temperature at cell n (^oF)

T_{n+1} ≡ temperature at cell $n+1$ (^oF)

z_n ≡ gas compressibility factor at cell n

z_{n+1} ≡ gas compressibility factor at cell $n+1$

Similarly, the volume of gas losses from cell $n+1$ to cell $n+2$ over the elapse time, $V_{L,n+1}$, is (Hassan and Kabir, 1994):

$$V_{L,n+1} = v_g \Delta t \left[\frac{V_{g,n+1}(t_j)}{L_c} \right] \tag{3.2}$$

where

Ug ≡ gas bubble rise velocity (m/s)

Δt ≡ elaspse time (s)

$V_{g,n+1}(t_j)$ ≡ gas volume in cell $n+1$ at time j (m^3)

L_c ≡ cell length (m)

Hence, the in-situ gas volume in cell $n+1$, or $V_{g,n+1}(t_{j+1})$, after Δt, in terms of volume at the earlier time-step, $V_{g,n+1}(t_j)$, is (Hassan and Kabir, 1994):

$$V_{g,n+1} = V_{g,n+1}(t_j) + (V_{R,n} - V_{L,n+1}) \tag{3.3}$$

where

$V_{g,n+1}(t_j)$ ≡ gas volume in cell $n+1$ at time j (m^3)

$V_{R,n}$ ≡ gas volume received in cell $n+1$ form cell n (m^3)

$V_{L,n+1}$ ≡gas volume loss from cell $n+1$ to cell $n+2$ (m^3)

In arriving equation 3.1 through 3.3, it is assumed that L_c is always longer than the distance traveled by the bubbles, $v_g \Delta t$; otherwise gas from n would migrate to $n+2$ or beyond.

3.6 Wellhead Gas Chamber Volume and Pressure

When the well is shut-in at surface, the gas near the top of the well separates from the liquid to form a gas chamber toward the wellhead top. This gas chamber is completely filled with gas and it cannot lose gas to any other cell although it receives gas from the cell below it.

The volume of this wellhead gas chamber changes with time. As the pressure build-up in the well continues during shut-in, a single phase gas zone propagates downward from the wellhead. At the same time, a single phase liquid zone is propagating upward from the bottom hole (Xiao *et al.*, 1995). The net effect of these two opposing processes might be a net increase or decrease in the wellhead gas chamber volume. The wellhead gas

chamber volume, $V_{wh}(t_j)$, at any time, t_j, is related to its volume at the earlier time-step, t_{j-1}, in the following manner (Hassan and Kabir, 1994):

$$V_{wh}(t_j) = V_{wh}(t_{j-1}) + \sum V_g(t_{j-1}) - \sum V_g(t_j) - q(t_j)\Delta t + \Delta V_l \qquad (3.4)$$

where

$V_{wh}(t_{j-1})$ ≡ wellhead gas chamber volume at the earlier time-step, t_{j-1} (m^3)

$\sum V_g(t_{j-1})$ ≡ total gas in the rest of the wellbore at the earlier time-step, t_{j-1} (m^3)

$\sum V_g(t_j)$ ≡ total gas in the rest of the wellbore at current time-step, t_j, (m^3)

$q(tj)$ ≡ reservoir fluid influx rate at current time-step, t_j, (m^3/s)

Δt ≡ elaspse time (s)

ΔV_l ≡ change in wellbore liquid volume (m^3)

Therefore, the wellhead pressure at any time-step, t_j, is related to the pressure at the earlier time-step, t_{j-1}, through the volume-pressure gas law relationship for real gas system (Hassan and Kabir, 1994):

$$p_{wh}(t_j) = \frac{p_{wh}(t_{j-1})n(t_j)V_{wh}(t_{j-1})z(t_j)}{n(t_{j-1})V_{wh}(t_j)z(t_{j-1})} \qquad (3.5)$$

where

$P_{wh}(t_{j-1})$ ≡ wellhead gas chamber pressure at the earlier time-step, t_{j-1} (psi)

$V_{wh}(t_{j-1})$ ≡ wellhead gas chamber volume at the earlier time-step, t_{j-1} (m^3)

$V_{wh}(t_{j-1})$ ≡ wellhead gas chamber volume at current time-step, (t_j) m^3

$z(t_j)$ ≡ gas compressibility factor at current time-step, t_j

$z(t_{j-1})$ ≡ gas compressibility factor at the earlier time-step, t_{j-1}

$n(t_j)$ ≡ number of gas mole in the wellhead gas chamber at current time-step , t_j

$n(t_{j-1})$ ≡ number of gas mole in the wellhead gas chamber at the earlier time-step, t_{j-1}

As the wellhead pressure calculation requires the gas compressibility factor that corresponds to the current wellhead pressure, an internal iteration loop is used within this step to deduce the likelihood gas compressibility factor at current time-step.

3.7 PVT and In-Situ Properties

After the wellhead gas chamber pressure is estimated from the gas law (equation 3.5), the fluid gradient of each cell is computed starting from the wellhead to wellbore. To obtain the fluid gradient for each of the cell, PVT and in-situ fluid properties must be calculated. Several established PVT correlations and EoS were used to calculate the critical PVT properties. These PVT properties are solution gas in oil, R_s, oil and gas formation volume factors, B_o and B_g, as well as oil and gas densities, ρ_o and ρ_g.

For solution gas calculation, empirical correlations by Standing, Glasso, Marhoun and Vasquez-Beggs are widely used. These correlations assume a flash-vaporization process (James and Hemanta, 1999). An example of correlation by Standing for solution gas, R_s, calculation is shown:

$$R_S = \gamma_g \times \left[\left(\frac{P}{18.2} + 1.4 \right) \times 10^{0.0125\,API - 0.00091(T-460)} \right]^{1.2048} \tag{3.6}$$

where

γ_g ≡ gas specific gravity

P ≡ reservoir pressure (psig)

API ≡ oil gravity (^{o})

T ≡ reservoir temperature (^{o}F)

Correlations by Standing, Glasso, Lasater, Petrosky-Farshad and Macary are available for oil formation volume factor calculation (Ahmed, 1989). An example of correlation by Standing for oil formation volume factor, B_o, calculation is shown:

$$Bo = G\left[A + B\left(R_s \left(\frac{\gamma_g}{\gamma_o} \right)^C + (DT + E) \right)^F \right] \tag{3.7}$$

where

R_s ≡ solution gas (scf/stb)

γ_g ≡ gas specific gravity

γ_o ≡ oil specific gravity

T ≡ reservoir temperature, (^{o}F)

A, B, C, D, E, F, G ≡ tuning parameters

Meanwhile, the gas formation volume factor, B_g, is calculated based on the real gas *EoS* (Ahmed, 1989):

$$B_g = \frac{14.7}{520}\left[(T+460)\frac{z}{P}\right] \tag{3.8}$$

where

T ≡ reservoir temperature (^{o}F)

z ≡ gas compressibility factor (z = 1 for a perfect gas)

P ≡ reservoir pressure (psig)

The fluids' densities can be calculated from several semi-empirical correlations, such as correlations by Standing, Vasquez-Beggs and Ahmed (Ahmed, 1989). Examples of correlations by Standing are shown;

Oil density, ρ_o

$$\rho_o = \frac{62.4\gamma_o \cdot + \left(\frac{0.0764\gamma_g R_s}{5.614}\right)}{B_o} \tag{3.9}$$

where

$$\gamma_o = \frac{141.5}{(131.5+API)} \tag{3.10}$$

γ_g ≡ gas specific gravity

γ_o ≡ oil specific gravity

R_s ≡ solution gas, *scf/stb*

B_o ≡ oil formation volume factor, *rb/stb*

API ≡ oil specific gravity, ^{o}

Gas density, ρ_g

$$\rho_g = \frac{0.0764\gamma_g}{B_g} \tag{3.11}$$

where

γ_g ≡ gas specific gravity

B_g ≡ gas formation volume factor (rb/stb)

3.8 Bottom-Hole Pressure

Once the wellhead gas chamber pressure is obtained from equation 3.5, the bottom-hole build-up pressure, P_{BH}, can be obtained by adding the fluids' frictional pressure, P_σ, and the fluids' hydrostatic pressure, P_{hyd}, to the wellhead pressure, P_{wh}, as in equation 3.12. In general, the contribution of the frictional component is very small even for flowing wells. After shut-in, the flow rate declines quickly and the P_f soon becomes negligible. Computation done by Xiao *et al.* (1995) indicated that the addition of a frictional head has negligible effect on pressure build-up data. However, during the flowing period prior to build-up, the steady state flow model which includes friction effects is used. P_{hyd} varies with time because of influx and can be calculated at any time-step, t_j, from the known mixtures densities at each cell.

$$P_{BH} = P_{wh} + P_{hyd} + P_\sigma \tag{3.12}$$

where

P_{wh} ≡ wellhead gas chamber pressure (psi)

P_{hyd} ≡ fluids' hydrostatic pressure (psi)

P_σ ≡ fluids' frictional pressure (psi)

The PVT properties are essential in determining the fluids' hydrostatic pressure over the transient period. The final fluids' hydrostatic pressure, P_{hyd}, upon equilibrium condition is calculated from the gas-oil- contact (GOC) level and the oil and gas columns' gradients.

$$P_{hyd} = (h \times P_{gradient})_{gas} + (h \times P_{gradient})_{oil} \tag{3.13}$$

where

$P_{gradient}$ ≡ fluid pressure gradient (psi/ft)

h ≡ fluid column height (ft)

An examination of the calculation procedures shows that the entire calculation is iterative. An estimate reservoir build-up pressure must be assumed as an input to the reservoir fluid influx calculation in equation 2.16. Then, the gas chamber volume can be calculated as an effect of influx. The resulted wellhead pressure followed by the bottom-hole pressure are obtained. The calculated bottom-hole pressure will converge to the assumed reservoir build-up pressure to complete the whole set of calculation over one time-step. The mathematical workflow is repeated for the next time-step until the reservoir pressure is achieved when the well reaches equilibrium. Well equilibrium is achieved when the shut-in bottom-hole pressure is equal to the reservoir pressure. This reservoir pressure must also converge with the assumed reservoir pressure in equation 2.16, resulting in two iteration loops in the entire calculation. To verify this transient flow modeling technique, the calculated wellhead pressure from the model must match with the field measured wellhead closed-in pressure. Details calculations process are attached in Appendix A.

3.9 Modules Description

This transient flow modeling technique was programmed into several logical calculation modules to speed up the calculation time and for easy code debugging. Each calculation module comprised numbers of functions and classes to prepare the input parameters, perform

specific calculations and return the output results. Table 3.1 summarizes the six calculation modules designed to perform the transient flow modeling calculation. The examples of the calculation modules in visual basic codes are attached in Appendix A.

Table 3.1: Description of calculation modules for the transient flow modeling

No.	Modules	Description	Function
1	modShutIn	The main module to link and call all the other modules to complete the shut-in calculation.	Organize calculation modules no. 2 to 6 into a main module.
2	PVTProp	Contains all the PVT correlations and EoS to calculate fluid density, viscosity, gas compressibility, liquid volume factor, solution GOR and surface tension.	Calculate PVT properties in each of the cell in the well throughout the shut-in period.
3	modInflux	Contains the reservoir fluid influx calculation to quantify the liquid volume entering (if any) into the wellbore during well shut-in.	Calculate reservoir fluid influx into the well throughout the shut-in period.
4	modMaterial	Corresponds to the gas bubble migration and material balance calculations.	Calculate the fluid redistribution in the well throughout the shut-in period.

5	modPws	Contains the functions to calculate the wellbore shut-in pressure based on gradient calculation at each node. It adopts the bisectional method to speed up the calculation to find the solution point for wellbore shut-in pressure.	Calculate the bottom-hole build-up pressure throughout the shut-in period.
6	modMath	Contains all the operational mathematic equations.	Calculate logarithm and conversion values.

3.10 Well Selection and Data Requirements

This developed transient well modeling technique was assessed with actual field data. This second section presents on the well selection criteria to shortlist candidate wells that are within the range of applicability of the modeling. A set of criteria was established to screen and identify the most suitable wells to be used in the modeling verification stage. In addition, a guideline on data requirement is formulated to ensure that the acquired data and information from the candidate wells and fields were detailed and of good quality.

The established well selection criteria as recommended by PETRONAS operation team (Zainal, 2008) are tabulated in Table 3.2:

Table 3.2: Well selection criteria

No.	Criteria	Basis
1	Oil producer from single zone	Commingled zone and cross flows affect the modeling accuracy.
2	Less than 80 degree deviation	Tortuous horizontal wells add further modeling complications and truncate the validation results.

3	Naturally producing well (without gas lift)	There must be no additional gas into the producing fluids from the well.
4	Dry oil (low water-cut, less than 5%)	The transient modeling is applicable to two-phase flow with gas and oil only.
5	Availability of permanent downhole gauges	To record bottom-hole pressure build-up data for the transient flow modeling matching.
6	Availability of surface digital pressure recorder	To record the wellhead pressure build-up data for the transient flow modeling matching.
7	Minimum production related problem i.e. scale, wax, asphaltene, etc.	Avoid introduction of solids in the system that affect the modeling accuracy.

CHAPTER 4

RESULTS AND DISCUSSIONS

This section presents the results evaluation where three case study wells are used to evaluate the accuracy of the transient flow modeling technique in estimating the reservoir pressure.

4.1. Results Evaluation

Three oil wells were selected from Sumandak Main field, offshore Sabah, Malaysia, to evaluate the capability of the developed transient flow modeling technique. Sumandak Main is located in Sub-Block 6S-18 area, offshore Sabah as indicated in Figure 4.1. The details of Sumandak main are described in Appendix B.

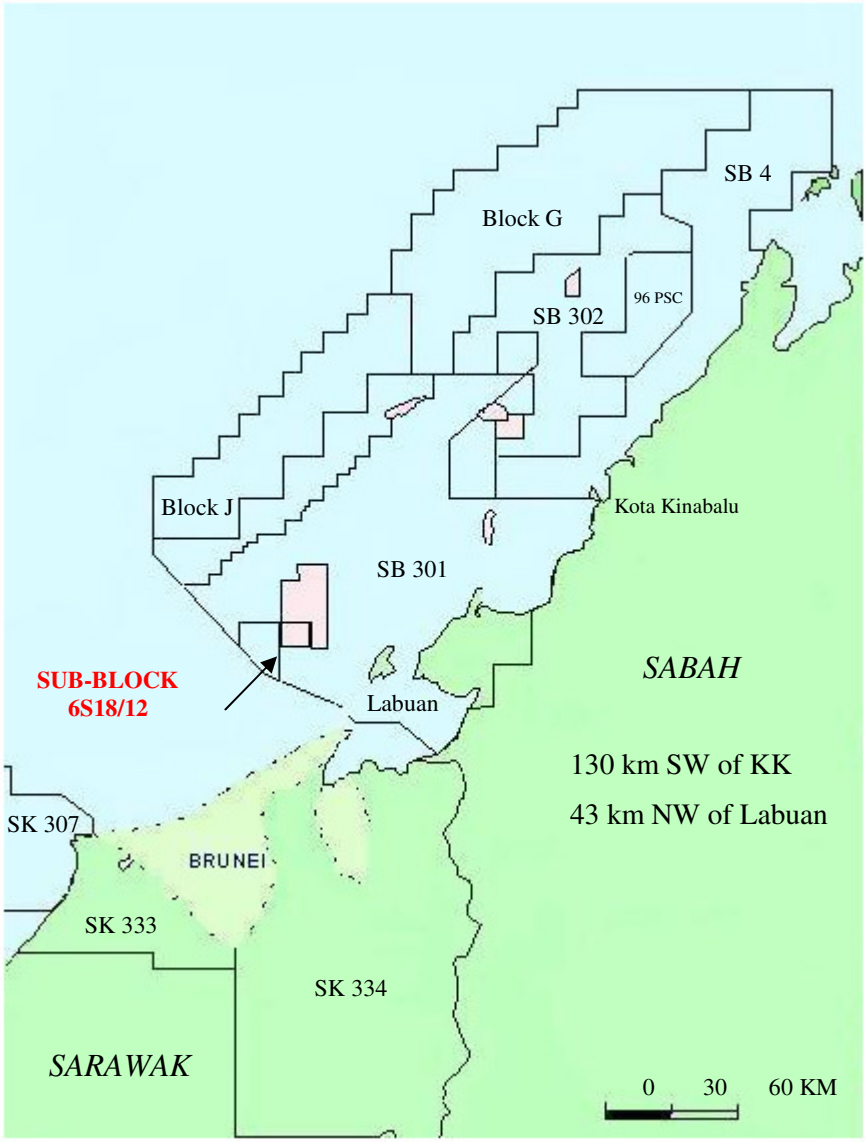

Figure 4.1: Location of Sumandak Main field (Lee Jean and Jiun Horng, 2009)

There are 24 oil producers in Sumandak Main, the three shortlisted oil wells/strings for the transient flow modeling verification were namely A-08, A-18L and A-20S. These wells were chosen because they were fairly new, flowing naturally (without gas-lift assistance) and equipped with digital surface data recorder. These wells had met all the well selection criteria detailed out in Chapter 3. Table 4.1 tabulates the data of these three wells.

Table 4.1: Data of the candidate wells (Lee Jean and Jiun Horng, 2009)

No.	Properties	Well A-20S	Well A-18L	Well A-08
1	Reservoir layer	Unit 3.1	Unit 3.2	Unit 1.0 & Unit 1.1
3	Permeability (mD)	681	129	767
4	Reservoir thickness (ft)	27	102	101(unit 1.0); 52(unit 1.1)
5	Porosity (fraction)	0.25	0.23	0.26
6	Viscosity (cp)	1.633	1.633	1.633
7	Formation volume factor (rb/stb)	1.095	1.095	1.095
8	Oil compressibility (psi^{-1})	5.74E-27	6.89E-27	9.13E-5
8	Rock compressibility (psi^{-1})	3E-6	3E-6	3E-6
10	Oil gravity (degree)	24.52	24.52	24.52
11	Specific gravity of produced gas	0.682	0.682	0.682
12	Reservoir solution gas oil ratio (rb/stb)	236	236	236
14	Skin	26.7	0.519	29.1
15	Wellbore radius (ft)	0.292	0.375	0.292
16	Radius of Investigation (ft)	759	1420	1732
17	Productivity Index (stb/d/psi)	2.7	2.0	4.0
18	PBU Date	Oct 2008	Nov 2008	Nov 2008

The first two selected wells, A-20S and A-18L, were dual string producers, with one well producing from the short string and the other well producing from the long string. The third selected well, A-08, was a single string producer producing commingling from two reservoir layers. These three wells shared the same PVT results conducted in year 2002 for Sumandak-1. The relevant PVT data is attached in Appendix C. The associate well

diagrams of well A-20S, A-18L and A-08 are attached is Appendix D, E and F respectively.

Well A-20 was a dual string well. The long string, A-20L, was excluded from the verification with the transient flow modeling due to poor quality of the build-up data. Both the recorded flowing tubing head pressure (FTHP) and closed-in tubing head pressure (CITHP) before and during shut-in were almost the same for A-20L as tabulated in Table 4.2. Thus, the build-up profile could not be generated for the transient flow modeling matching. The selected short string, A-20S, was producing naturally from Unit 3.1 sand. Well A-20S was the only well out of the three shortlisted wells equipped with permanent downhole gauge (PDG).

Table 4.2: Recorded tubing head pressure for well A-20L (Lee Jean and Jiun Horng, 2009)

No.	Description	Values
1	Flowing tubing head pressure, FTHP	258 psi
2	Closed-in tubing head pressure, CITHP	259 psi

The second selected candidate well was A-18L. Well A-18 is also a dual string well. The long string was selected as the candidate string due to the availability of the closed-in tubing head pressure data for transient flow modeling verification. The long string was producing naturally from Unit 3.2 sand and completed without permanent downhole gauge (Lee Jean and Jiun Horng, 2009).

Well A-08, the final selected candidate well, was a single string well completed in two sands, Unit 1.0 and Unit 1.1 sands. The well was producing commingle from both zones naturally. A-08 was completed without permanent downhole gauge installed (Lee Jean and Jiun Horng, 2009).

4.1.1. Steady State Flow Models

The steady state flow models for the three selected wells were constructed using Multiflo™, a nodal analysis software by Codeon GmbH. Nodal analysis, also known as system analysis, relies on forward steady state, two phase flow calculation from input parameters such as wellhead pressure and temperature, tubular internal diameter and flow rates of each phase (James and Hemanta, 1999). Overall, all the generated pressure traverse curves from the three wells were matched with the production data for a reliable well behavior projection.

For Well A-20S, the flowing bottom-hole pressure (FBHP) of 1550 psi was recorded before the well is shut-in. Hagedorn and Brown VLP correlation was used to match the constructed steady state flow model with the production data. The steady state flow model predicted a FBHP of 1521 psi, which was closely matched with the recorded FBHP of 1550 psi from PDG at 2% variance. Furthermore, the steady state flow model predicted production rate of 709 bpd, matched well with the reported production rate of 730 bpd with a minor 3% variance. The generated inflow and outflow curves from well A-20S steady state flow model are showed in Figure 4.2.

Meanwhile, Hagedorn and Brown VLP correlation was also used to match the steady state flow model of wells A-18L and A-08 based on the evaluation from well A-20S. These three wells were similar in terms of well configuration, reservoir and PVT properties as tabulated in Table 4.1.

Figure 4.2 shows the generated inflow and outflow curves from both well A-18L and A-08 steady state flow models. For well A-18L, the steady state flow model predicted a FBHP of 1097 psi and production rate of 1073 bpd at 249 psi FTHP. This result was closely matched with the recorded production rate of 1137 bpd at 249 psi FTHP. The steady state flow model of well A-08 predicted a FBHP of 1239 psi, whereas the production rate at 630 psi FTHP was 864 bpd. This result was also closely matched with the reported production rate of 850 bpd. This verified that the use of Hagedorn and Brown VLP correlation in both wells A-18L and

A-08 steady state models was suitable. The outputs of these three steady state flow models were exported into transient flow modeling to commence the transient flow calculation upon well shut-in.

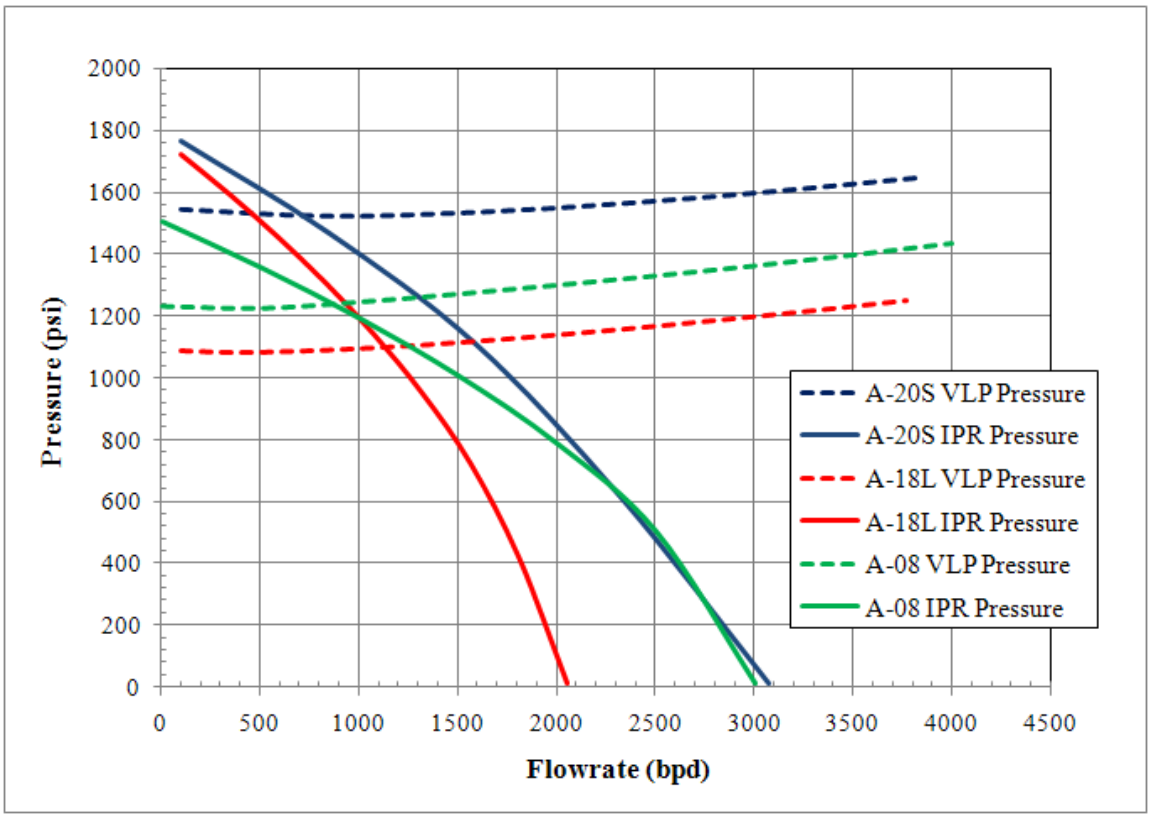

Figure 4.2: Inflow/outflow curves – Wells A-20S, A-18L and A-08

4.1.2. Reservoir Fluid Influx

When a well is shut-in for a pressure build-up, ideally the rate is reduced to zero instantaneously at the producing formation at the bottom of the well. However, since the well is shut-in at the surface, the flow from the reservoir into the well continues until the fluids in the wellbore are sufficiently compressed to balance with the formation pressure. Then the pressure in the well is large enough for the flow from the reservoir to be negligible (Slider, 1983). This phenomenon is called reservoir fluid influx, which occurs

briefly after the wellbore has been shut in at the surface. The influx is in the form of wellbore loading due to the compressibility of fluids inside the well bore. The wellbore has storage capacity equal to the volume within the wellbore in direct communication with the porous and permeable formation (Denis *et al.*, 1985). No wellbore storage effect can occur if the wellbore is shut in at the bottom of the well at the face of the formation. The influx may last for minutes or many hours depending on the nature of the fluid properties and the capacity of the flow string (Dake, 2001). For instance, in a gas saturated oil from a deep reservoir, the combination of highly variable compressibility and large storage volume to the surface will provide conditions conducive to a lengthy period of influx (Slider, 1983).

The influx calculation was obtained from stage 1 of the transient flow modeling calculation as illustrated in Figure 3.2. This influx phenomenon was clearly observed for all the three selected wells as shown in Figures 4.3 (a), (b) and (c) with respect to well A-20S, A-18L and A-08. All the three figures show a decreasing reservoir fluid influx over time, with significant influx emerged during the initial shut-in period. This might be due to the high initial pressure difference between the bottom-hole pressure and the reservoir pressure.

The influx period lasted for approximately 930 seconds in well A-20S. For well A-18L, there was a steep influx volume drop before the first 100 seconds after the well had been shut-in. The remaining effect lasted for approximately 2600 seconds, which the shut-in bottom-hole pressure (SIBHP) was equal to the reservoir pressure at the end of the influx.

For well A-08, a significant influx effect was observed from time 0 to 70 seconds after the well had been shut-in. From 100 seconds onwards, the influx rates were in the order of magnitude of 0.0001 ft^3only. The influx period lasted for approximately 310 seconds. The small magnitude of influx after the end of wellbore phase segregation shows that the phase segregation is a dominating factor (Xiao *et al.*, 1995).

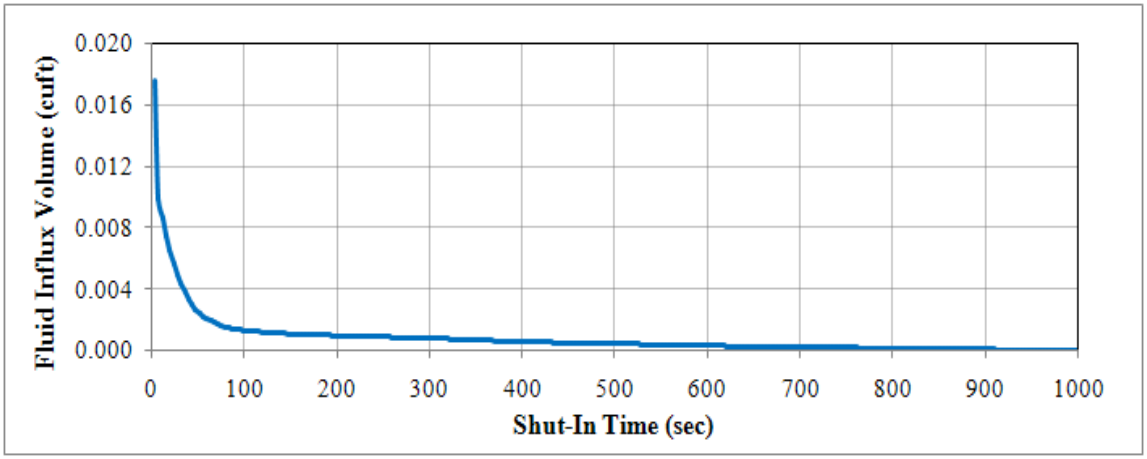

(a) Well A-20S

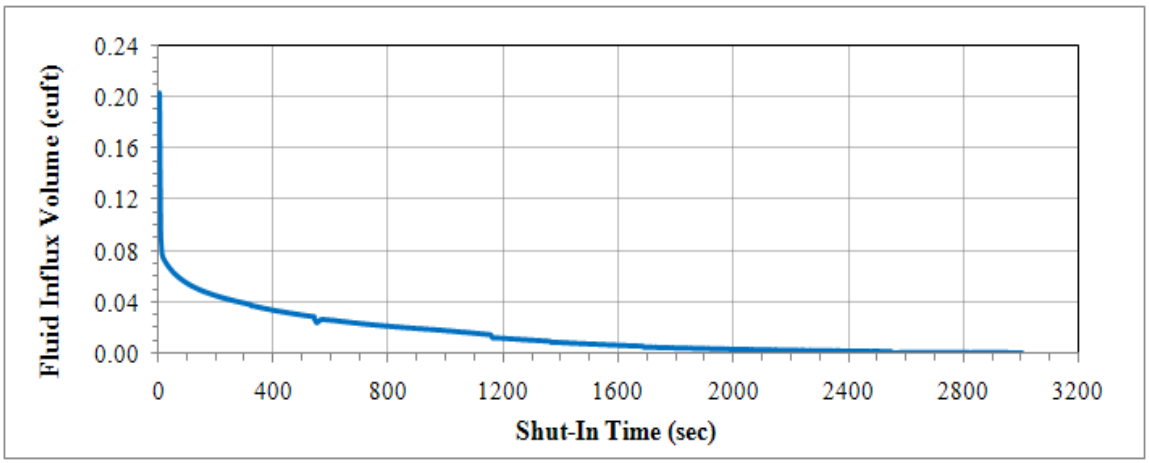

(b) Well A-18L

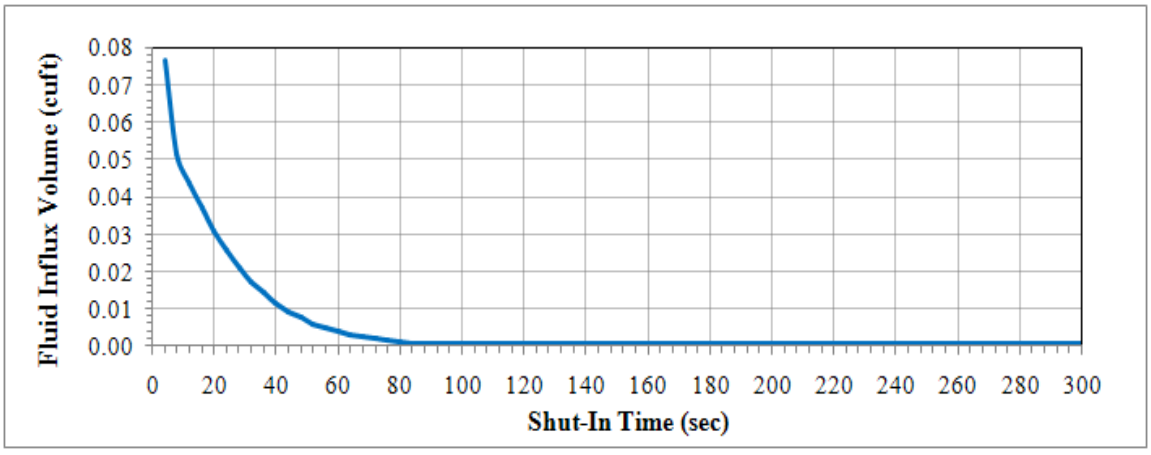

(c) Well A-08

Figure 4.3: Reservoir fluid influx over the shut-in period

(Ref: Stage 1 calculation - Figure 3.2)

4.1.3. Wellhead Gas Chamber

Upon shut-in, the gas migrated to the top of the tubing to form a gas chamber at wellhead, which is a single phase gas zone as observed by Xiao *et al.* (1995). During the well shut-in period, wellbore fluid-redistribution occurs rigorously as a result of fluids' densities difference and gravitational effect. This fluid redistribution process will cause wellbore pressurization as observed by Winterfeld (1989) during pressure build-up test simulated in a system consisting of a wellbore and a reservoir containing multiphase fluid. This might be due to the simultaneous flow of the relatively incompressible and heavier liquid phase with a relatively compressible and lighter vaporous phase (Winterfeld, 1989). Gas bubbles rise to the top cell to form a gas chamber. The volume of the gas chamber changes with time. The gas chamber receives gas from the cell below, which tends to increase the chamber volume. Meanwhile, the reservoir fluid influx from the reservoir and the expansion of gas in the rest of the well could tend to decrease the gas chamber volume because of upward migration. The net effect of these two opposing processes might be a net increase or decrease in the gas chamber volume (Hassan and Kabir, 1994). The movement of gas chamber represents the movement of the gas-liquid interface. Figure 4.4 shows a steadily increased gas chamber volume over the shut-in period in relation to the interface depth for wells A-20S, A-18L and A-08. The volume profile was generated from stage 2 of the transient flow modeling calculation in Figure 3.2.

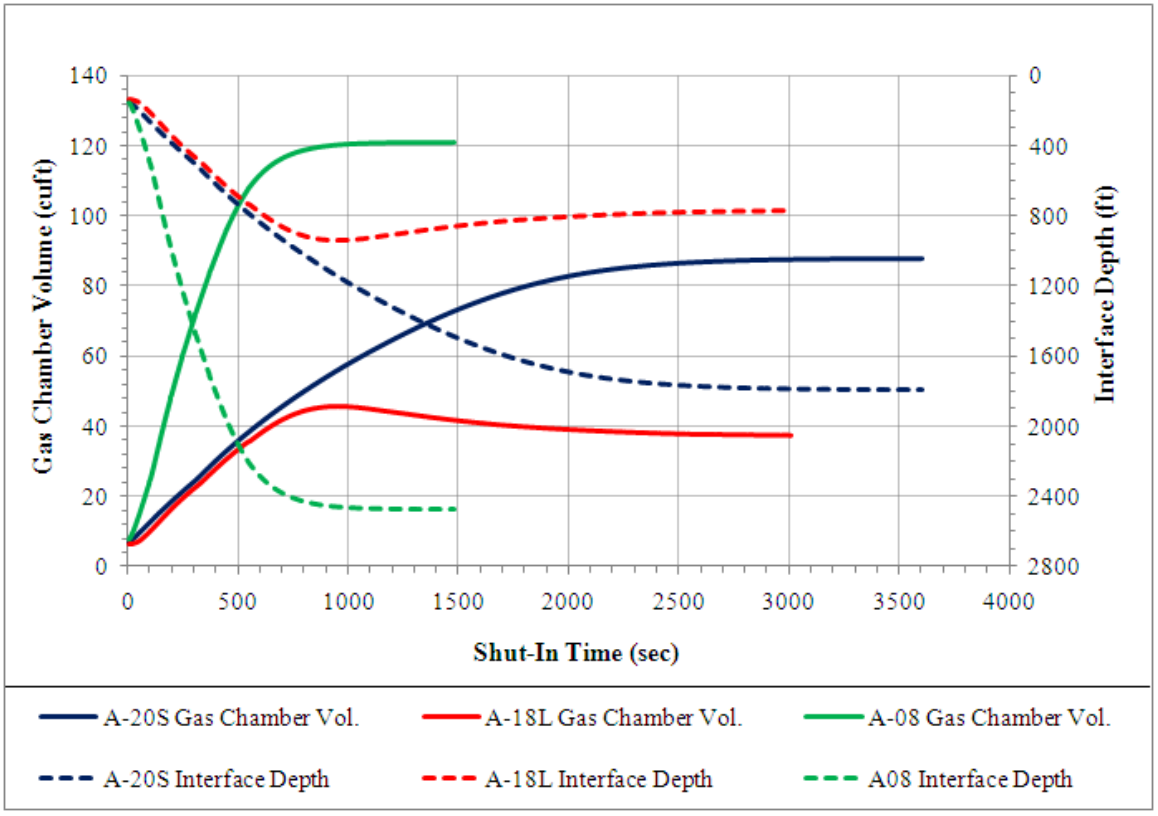

Figure 4.4: Wellhead gas chamber volume and interface depth changes over the shut-in period (Ref: Stage 2 calculation - Figure 3.2)

The wellhead gas chamber volume changes can be transacted into the gas-liquid interface movement over time. For well A-20S, the gas-liquid interface increased steadily and reached its maximum depth of 1795 ft at approximately 2400 seconds, corresponding exactly to the gas chamber volume. 2400 seconds is the duration of the well shut-in period to reach equilibrium.

However, well-A-18L showed a wellhead gas chamber volume expansion with a hump which ended at 1000 sections after shut-in. To understand this effect, the fluid interface movement was studied. The fluid interface depth profile showed that the wellhead gas chamber volume reached its maximum depth of 934 ft at approximately 1000 seconds (15 minutes) and started to decrease to 765 ft upon equilibrium at 2600 seconds (43 minutes). From 0 to 1000 seconds after shut-in, the gas migration towards the wellhead gas chamber was a dominating effect resulting in an increase in the wellhead gas chamber volume. After 1000 seconds, this gas migration effect was overshadowed by both the

effects of reservoir fluid influx and gas expansion in the rest of the tubing, resulting in a decrease in the wellhead gas chamber volume, and thus, the fluid interface level. Well A-18L had the lowest GOR among the three selected wells. This low GOR was equivalent to a low gas volume in the tubing during shut-in. Therefore, this low amount of gas volume was able to migrate and accumulate at the wellhead gas chamber in a relatively short duration of time, resulting in its effect lasted at 1000 seconds. This observation was supported by the work of Xiao and Reynolds (1992), which concluded that the decreasing gas chamber volume was due to the compression of the gas column after wellbore phase segregation.

Similar with well A-20S, well A-08 showed a steadily increased gas chamber volume over the shut-in period. This net increase in the gas chamber volume indicated that the effect of gas accumulation was dominating the effects of reservoir fluid influx and gas expansion in the rest of the tubing over the shut-in period. Since well A-08 was a relatively high GOR well, the duration for the gas to fully segregate to accumulate at the wellhead gas chamber was long. Thus, the effect of gas accumulation dominated over the shut-in period. The associate gas-liquid interface movement based on the wellhead gas chamber volume changes was compared. Corresponding exactly to the gas chamber volume, the gas-liquid interface reaches its maximum depth of 2475 ft at approximately 900 seconds (15 minutes) at equilibrium.

4.1.4. Wellhead and Bottom-hole Pressure

Finally, the wellhead and bottom-hole pressure build-up were obtained from stage 3 and 5 of the transient flow modeling calculation in Figure 3.2. Knowing the gas-liquid interface and the fluids' gradient along the tubing, the bottom-hole pressure build-up profile was generated by adding the fluids' static pressure to the wellhead pressure. Figure 4.5 and 4.6 show the pressure build-up profiles for both wellhead and bottom-hole for wells A-20S, A-18L and A-08.

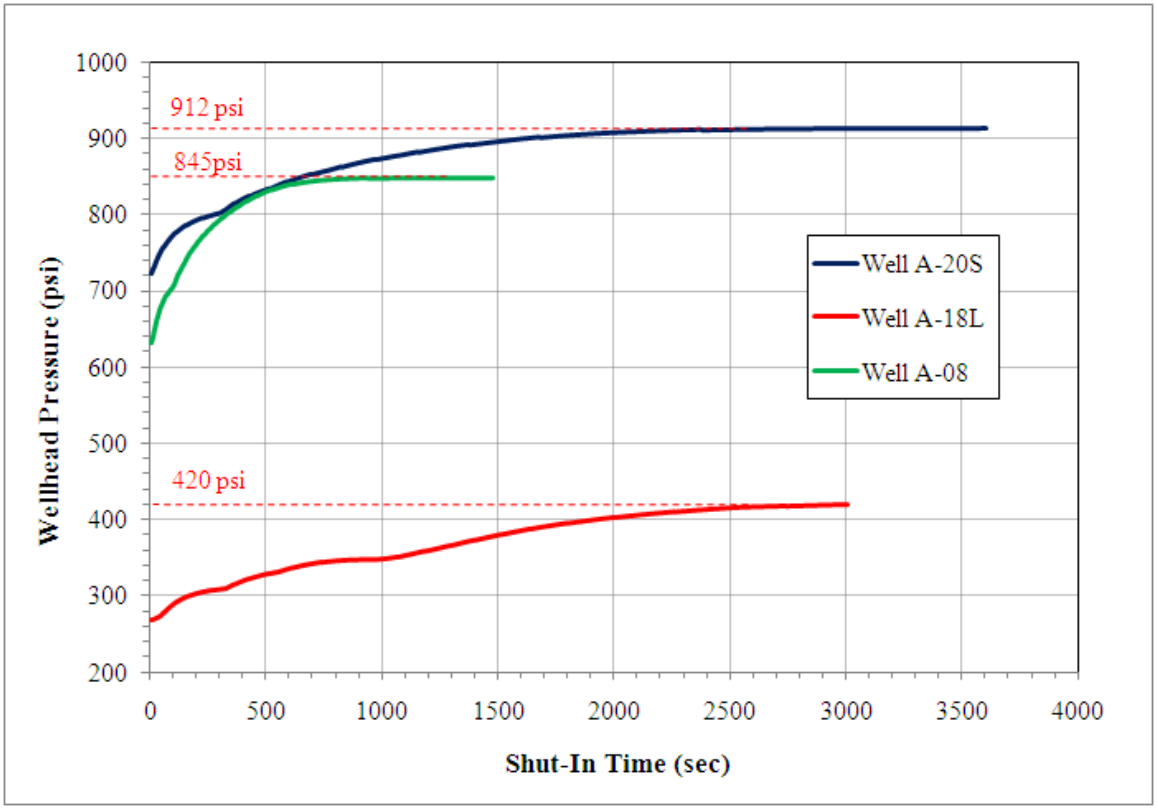

Figure 4.5: Wellhead pressure build-up over the shut-in period

(Ref: Stage 3 calculation - Figure 3.2)

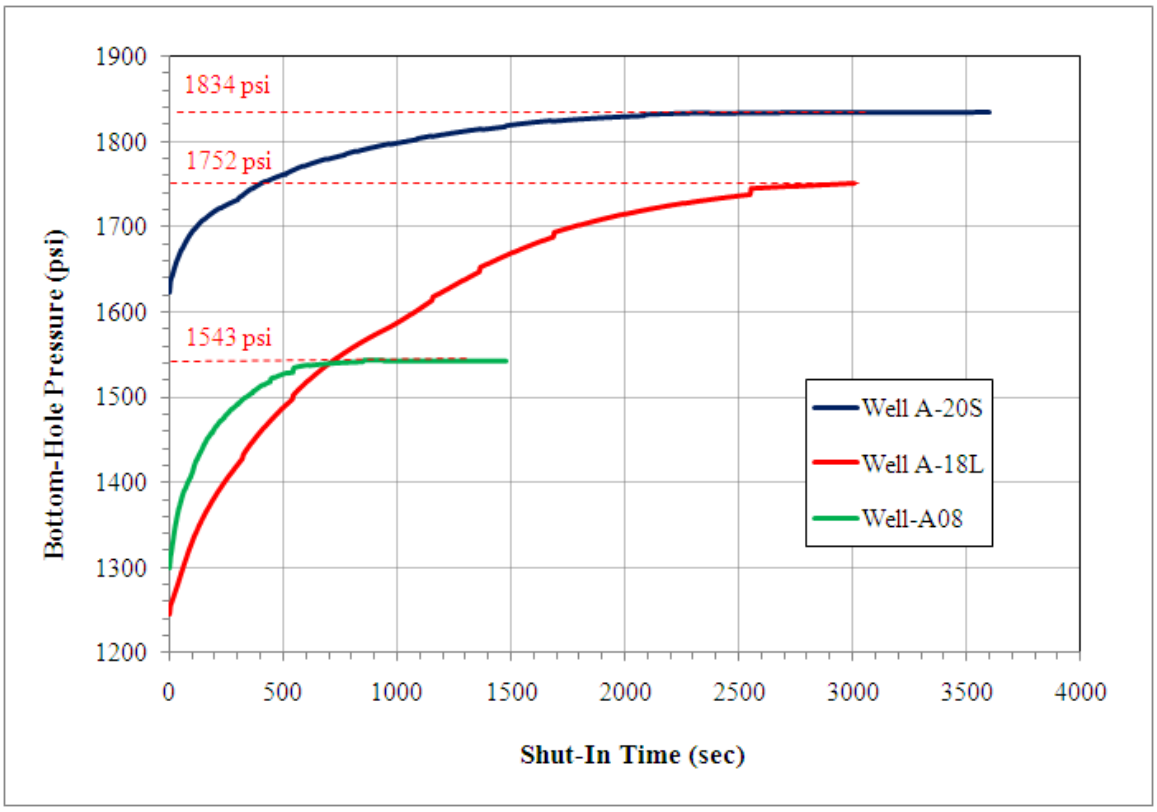

Figure 4.6: Bottom-hole pressure build-up over the shut-in period

(Ref: Stage 5 calculation - Figure 3.2)

For well A-20S, the wellhead pressure was stabilized at 912 psi towards the end of the build-up period. The reservoir pressure of 1834 psi was achieved when the well reached equilibrium at approximately 2400 seconds, equivalent to 40 minutes, after the well is shut-in. This 2400 seconds of the fluid redistribution period to reach equilibrium was equivalent with the duration of the gas chamber volume to stabilize.

Meanwhile, well A-18L showed a wellhead pressure of 420 psi was reached at the end of the build-up period. In addition, a pressure hump ending at 1000 seconds was observed corresponding exactly to the gas chamber volume changes as described in the previous section. The reservoir pressure of 1752 psi was achieved when the well reached equilibrium in approximately 2600 seconds after the well had been shut-in.

Similarly, well A-08 showed the wellhead pressure stabilized at 845 psi towards the end of the build-up period. After 900 seconds after shut-in, the reservoir pressure of 1543 psi was achieved.

All the wellhead and bottom-hole pressure build-up results from these three wells were verified with the actual field measure data and are discussed in detail in the next section.

4.1.5. Pressure Build-up Data Analysis and Verification

For well A-20S, the recorded pressure build-up survey data were obtained from the permanent downhole gauge installed at 1145.38 m-TVDDF over a shut-in period of more than 24 hours (Lee Jean and Jiun Horng, 2009). Figure 4.7 shows the actual recorded pressure build-up profile for the first 100 minutes.

It is important to note that the build-up pressure survey data was recorded at the gauge depth of 1145.38 m-TVDDF, whereas the developed transient flow modeling generated pressure build-up results was at the mid-perforation depth of 1195 m-TVDSS. Both depth references must be the same in order to compare the results correctly. Therefore, in order to adjust the pressure at gauge depth to the pressure at mid-perforation depth, a pressure adjustment calculation was done by assuming a fluid gradient of 0.365 psi/ft between the gauge and mid-perforation as detailed out in Appendix G.

With the pressure adjustment, all the pressure data recorded at gauge depth were added 163.84 psi to reflect the pressure at mid-perforation as in Figure 4.7. In this pressure build-up survey, the reservoir pressure of 1802 psi is reached at approximately 60 minutes after the well has been shut-in. After 60 minutes, the well had stabilized in which there was no change in the recorded pressure value.

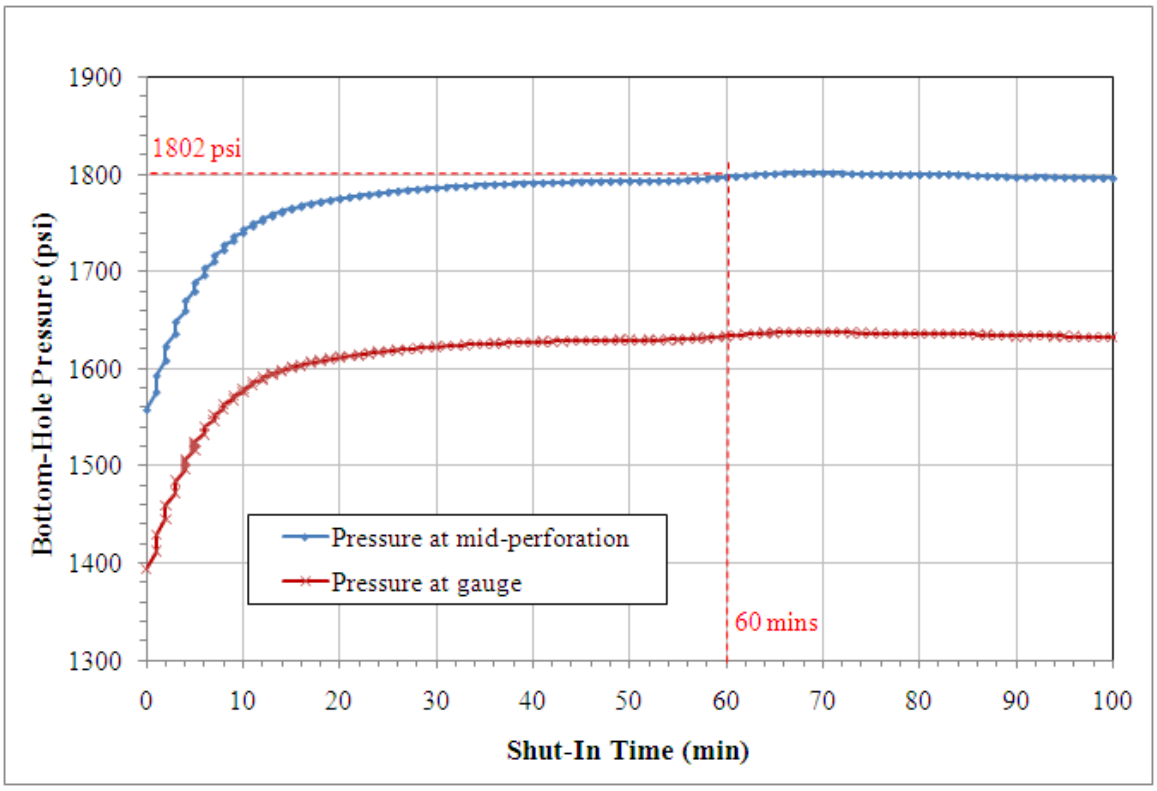

Figure 4.7: Well A-20S pressure build-up profile at gauge depth and mid-perforation depth (Jiun Horng, 2009)

Meanwhile, the close-in tubing head pressure (CITHP) was recorded at the end of the well shut-in period for a 6-hour duration as tabulated in Table 4.3.

Table 4.3: Well A-20S close-in tubing head pressure (Jiun Horng, 2009)

Date	Time (hour)	CITHP (psi)
22 October 2008	0800	907.4
22 October 2008	1400	906.6
22 October 2008	1800	906.0

These pressure build-up survey results were compared with the pressure build-up profiles generated by the developed transient flow modeling as tabulated in Table 4.4. It shows that both wellhead and bottom-hole pressure generated by the transient flow modeling matched within 2% variance with the actual pressure build-up survey results. This shows that the developed transient flow modeling could closely simulate the fluid redistribution of well A-20S over the shut-in period. The obtained reservoir pressure of 1834 psi for well A-20S was accurate supported by the permanent downhole gauge recorded pressure build-up survey result.

Table 4.4: Well A-20S transient flow modeling results verification

Parameters	Pressure Build-Up Survey Results	Transient Flow Modeling Results	Variance
Bottom-hole pressure	1802 psi (Figure 4.7)	1834 psi (Figure 4.6)	2% (32 psi)
Wellhead pressure	907 psi (Table 4.3)	912 psi (Figure 4.5)	1% (5 psi)

For well A-18L, the pressure build-up survey data recorded from this gauge were obtained from the pressure gauge hung on slickline at 1264.55 m-TVDDF. The period for analysis includes a-12 hour of flow and a-24 hour of build-up period (Lee Jean and Jiun Horng, 2009). Figure 4.8 shows the initial pressure build-up profile for the first 40 minutes. After 30 minutes, the well had stabilized in which there was no change in the recorded pressure value.

Similarly, the build-up pressure survey data were recorded at the gauge depth of 1264.55 m-TVDDF, whereas the transient flow modeling generated pressure build-up profile was at the mid-perforation depth of 1225 m-TVDSS. A pressure adjustment of 57.06 psi was added to the pressure at gauge depth to reflect the actual pressure at mid-perforation depth as illustrated

in Figure 4.8. It was assumed that the fluid gradient between the gauge and mid-perforation was 0.365 psi/ft (Lee Jean and Jiun Horng, 2009).

From this pressure build-up survey, the near wellbore reservoir pressure of 1773 psi was reached in approximately 30 minutes after the well is shut-in.

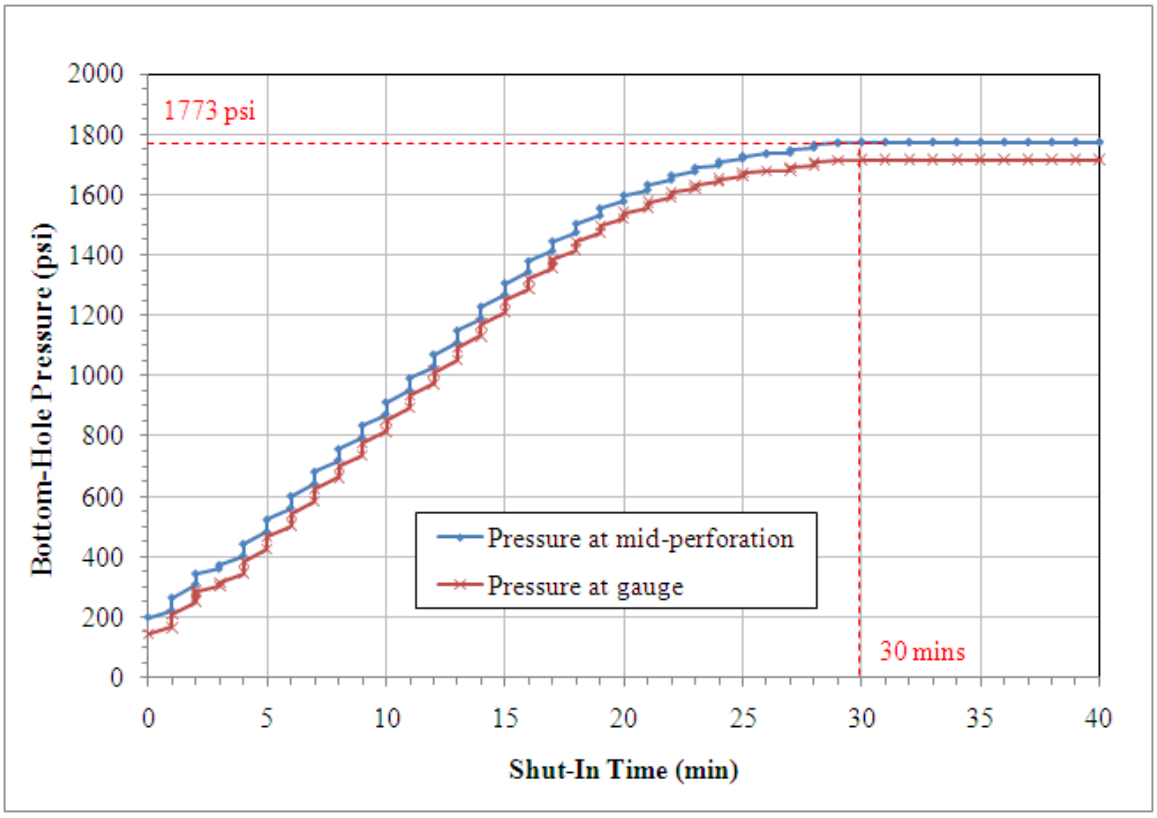

Figure 4.8: Well A-18L pressure build-up profile at gauge depth and mid-perforation depth (Jiun Horng, 2009)

In addition, the close-in tubing head pressure (CITHP) was recorded over a 4-hour duration as tabulated in Table 4.5.

Table 4.5: Well A-18L close-in tubing head pressure (Jiun Horng, 2009)

Date	Time (hour)	CITHP (psi)
13 November 2008	1400	441.3
13 November 2008	1800	445.3

These pressure build-up survey results were compared with the pressure build-up profiles generated by the developed transient flow modeling. Table 4.6 shows that both wellhead and bottom-hole pressures generated by the transient flow modeling matched within 21 to 23 psi difference with the actual pressure build-up survey data (within 5% variance). This suggested that the developed transient flow modeling could closely simulate the fluid redistribution of well-A18L over the shut-in period.

Table 4.6: Well A-18L transient flow modeling results verification

Parameters	Pressure Build-Up Survey Results	Transient Flow Modeling Results	Variance
Bottom-hole pressure	1773 psi (Figure 4.8)	1752 psi (Figure 4.6)	1% (21 psi)
Wellhead pressure	443 psi (Table 4.5)	420 psi (Figure 4.5)	5% (23 psi)

For the final selected well, well A-08, the pressure data recorded from this gauge were obtained from the pressure gauge hung on slickline at 1215.18 m-TVDDF. The period for analysis included a-12 hour of flow and a-24 hour of build-up period (Lee Jean and Jiun Horng, 2009). Figure 4.9 shows the initial pressure build-up profile for the first 40 minutes. After 24 minutes, the well had stabilized in which there was no change in the recorded pressure value. Again, this pressure build-up data were recorded at the gauge depth of 1215.18 m-TVDDF, whereas the developed transient flow modeling generated the pressure build-up

profile at the mid-perforation depth of 1199 m-TVDSS. A pressure adjustment of 85.05 psi was added to the pressure at gauge depth to reflect the actual pressure at mid-perforation depth in Figure 4.9.

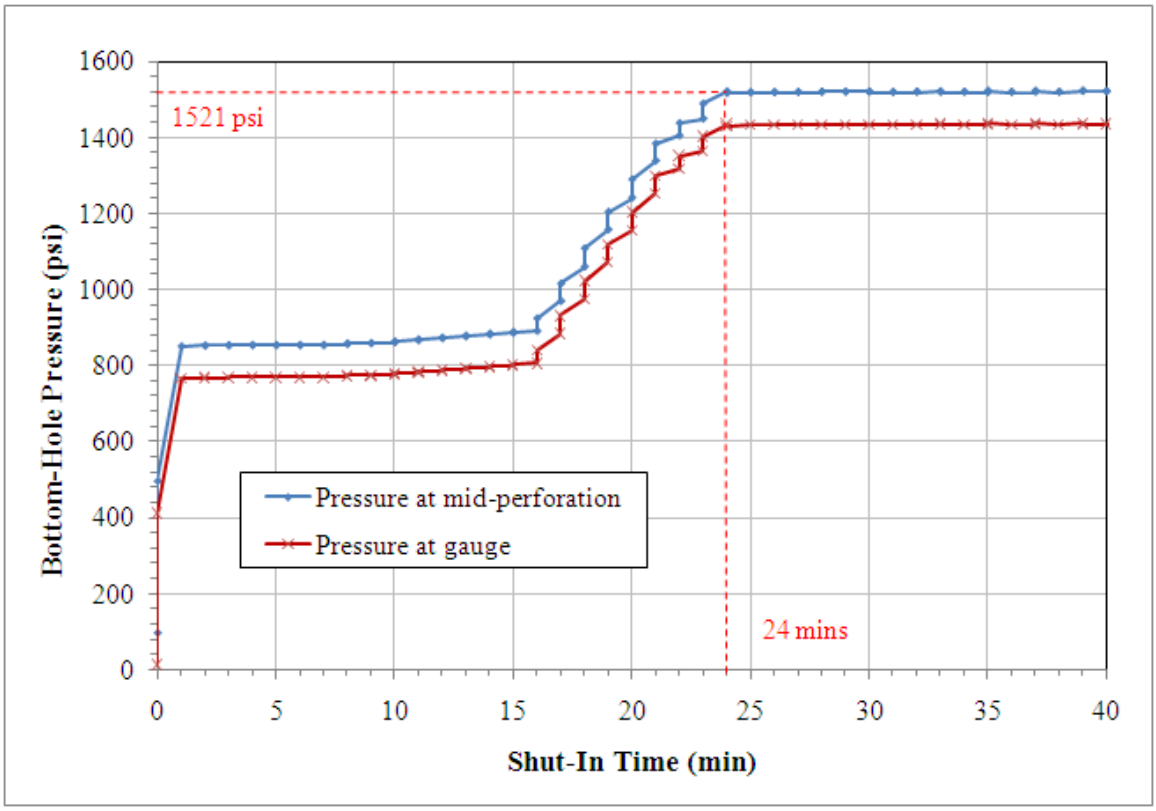

Figure 4.9: Well A-08 pressure build-up profile at gauge depth and mid-perforation depth (Jiun Horng, 2009)

During the pressure build-up survey, well A-07S, the nearest well to well A-08, was located 215 m away and was flowing at 676 bbl/d. This might contributed to the slightly noisy and scattered data in the recorded pressure trend. The radius of investigation at well A-08 was 528 m, which crossed that of well A-07S. From well A-08 pressure build-up survey, the reservoir pressure of 1521 psi was reached at approximately 24 minutes after the well was shut-in. Meanwhile, the close-in tubing head pressure was recorded over a 34-hour duration, giving the highest recorded pressure of 857 psi as tabulated in Table 4.7.

Table 4.7: Well A-08 close-in tubing head pressure (Jiun Horng, 2009)

Date	Time (hour)	CITHP (psi)
21 November 2008	0800	778.3
21 November 2008	1400	801.7
21 November 2008	1800	814.4
22 November 2008	0800	856.6
22 November 2008	1400	729.6
22 November 2008	1800	783.4

These pressure build-up survey results obtained from the field were compared with the pressure build-up profiles generated by the transient flow modeling. Table 4.8 shows that both wellhead and bottom-hole pressure generated by the transient flow modeling were matched within 1 % variance with the actual pressure build-up survey data. This verified that the transient flow modeling could closely simulate the fluid redistribution of well-A08 over the shut-in period, and the obtained reservoir pressure of 1543 psi is accurate supported by the downhole gauge recorded pressure build-up data.

Table 4.8: Well A-08 transient flow modeling results verification

Parameters	Pressure Build-Up Survey Results	Transient Flow Modeling Results	Variance
Bottom-hole pressure	1521 psi (Figure 4.9)	1543 psi (Figure 4.6)	1% (22 psi)
Wellhead pressure	857 psi (Table 4.7)	845 psi (Figure 4.5)	1% (12 psi)

In summary, the developed transient flow modeling was verified in modeling and simulating the transient behaviors encountered during well shut-in. This demonstrated

that the transient flow modeling-generated reservoir pressure could match well with the actual pressure build-up survey data.

As reported by Mantecon (2007), dynamic simulation results from transient flow modeling were typically used to support project decision in the areas of flow delivery through field life, liquid surges, hydrates, wax, integrity and safety. Instead of application in flowing condition as reported by Mantecon (2007), the transient flow modeling developed in this research is a virtual down-hole gauge which can simulate the bottom-hole shut-in condition. This transient flow modeling accounted for continually decreasing influx after shut-in, the variation of void distribution within the wellbore with depth and the combined effects of influx and gas bubble migration on the wellhead and bottom-hole pressure. The developed transient flow modeling was verified of capable in calculating the bottom-hole build-up pressure from the available surface wellhead build-up pressure measurement.

CHAPTER 5

CONCLUSIONS AND RECOMMENDATIONS

This research has developed and tested a transient flow modeling technique to predict reservoir pressure.

- The transient flow model to simulate fluid redistribution in a shut-in well to estimate the reservoir pressure has been formulated with modification on Hassan and Kabir (1994) model. The transient flow model is able to calculate five parameters: reservoir fluid influx, wellhead gas chamber volume, fluids' interface movement, wellhead build-up pressure and bottom-hole build-up pressure over the shut-in duration.

- The developed transient flow model mathematical workflow was transformed into visual basic code and linked with steady state model to become a fully functional transient flow modeling tool. The transient flow model mathematical workflow was programmed into six logical calculation modules. Each calculation modules comprised numbers of functions and classes to prepare the input parameters, perform specific calculations and generate the results. The calculation process was programmed in-sequence to simulate the whole transient behavior of a shut-in well until equilibrium condition was met at the end of the wellbore pressure build-up period.

- The reservoir pressure generated by the transient flow model has been verified to match within 10% variance with the pressure build-up survey results from three Sumandak oil wells. Three producing oil wells were selected from Sumandak Main field, Offshore Sabah, Malaysia, to evaluate the capability of the developed transient flow model. The developed transient flow model was able to generate the profiles of reservoir fluid influx, wellhead gas chamber volume, fluids' interface depth, wellhead and bottom-hole pressure build-up over the shut-in period for the three selected wells.

These results were compared with the gauge measured data during shut-in from the field. Both wellhead and bottom-hole pressure generated from the transient flow modeling were matched within 10% variance with the field data. This suggested that the developed transient flow model could closely simulate the fluid redistribution of a shut-in well and estimate a reliable reservoir pressure.

This transient flow model could be an alternative technique to well intervention measurement in obtaining reservoir pressure data. Using this transient flow model, the reservoir pressure could be computed from the readily available steady state flow properties and wellhead pressure build-up data. Indeed, this transient flow model expanded the conventional application areas of transient flow model.

Recommendation for future work is to extend the current transient flow model application limit from two-phase flow (oil-gas phase) to three-phase flow (oil-gas-water phase).

REFERENCES

1. Abdul, M. and Ghassan, H. (1985, April 30). *Evaluation of PVT correlations*, [Online]. Paper 14478. Available: http://www.onepetro.org

2. Ahmed, T. "Comparative study of eight equations of state for predicting hydrocarbon volumetric phase behavior", *SPE Reservoir Engineering*, pp. 337-348, Feb. 1988.

3. Ahmed, T. *Hydrocarbon phase behavior*, Gulf Publishing Company, 1989.

4. Ali, D. "PVT and phase behavior of petroleum reservoir fluids"*, Elsevier Science B. V.*, pp. 67-80. 1998.

5. Bikbulatov S., Khasanov M., Zagurenko A. (2005) Flowing bottom-hole pressure calculation for a pumped well under multiphase flow. [Online]. Available: http://arxiv.org/ftp/physics/papers/0504/0504083.pdf

6. Bin, H., Sagen, J., Chupin, G., Haugset, T., Ek, A., Sommersel, T., Zheng, G. X. and Mantecon, J. C. "Integrated wellbore/reservoir dynamic simulation", presented at the Asia Pacific Oil and Gas Conference and Exhibition, Jakarta, Indonesia, October 30-November 1, 2007, Paper SPE 109162-MS.

7. Boyun, G., William, C. L. and Ali, G. "Petroleum production engineering – A computer-assisted approach", *Gulf Professional Publishing*, pp. 6-70. 2007.

8. Boxall, J., Davies, S, Koh, C. and Sloan, E. D. "Predicting when and where hydrate plugs form in oil-dominated flowlines", presented at the 2008 Offshore Technology Conference, Houston, TX, May 5-8, 2008, Paper OTC 19514-MS.

9. Chamoux and Patrick. "Deep Sea Subsea Wells: DHSCSSV or Not"*,* presented at the SPE International Conference on Health, Safety, and Environment in Oil and Gas

Exploration and production, Caracas, Venezuela, June 7-10, 1998, Paper SPE 46615-MS.

10. Chupin, G., Hu, B., Haugset, T., Sagen, J. and Claudel, M. "Integrated wellbore/reservoir model predicts flow transients in liquid-loaded gas wells", presented at the 2007 SPE Annual Technical Conference and Exhibition, Anaheim, CA, November 11-14, 2007, Paper SPE 110461-MS.

11. Dake L. P. "The practice of reservoir engineering", *Elsevier Science & Technology,* vol. 145, pp. 253-268. 2001.

12. Danielson, T. J., Brown, L. D. and Bansal, K. M. "Flow management: Steady-state and transient multiphase pipeline simulation", presented at the 2000 Offshore Technology Conference, Houston, TX, May 1-4, 2000, Paper OTC 11965.

13. Davies, S. R., Boxall, J. A., Dieker, L. E., Sum, A. K., Koh, C. A., Sloan, E. D., Creek, J. L. and Zheng, G. X. "Improved predictions of hydrate plug formation in oil-dominated flowlines", presented at the 2009 Offshore Technology Conference, Houston, TX, May 4-7, 2009, Paper OTC 19990-MS.

14. Denis, M., Wittmann, M. J. and George, S. "Interpretation of pressure build-up test using in-situ measurement of afterflow", *Journal of Petroleum Technology*, pp. 143-152, Jan. 1985.

15. Duns, H. J. and Ros, N. C. J. "Vertical Flow of Gas and Liquid Mixtures in Wells", in *Proc. 6th World Petroleum Congress,* Frankfurt, 1963, pp. 451.

16. Eidsmoen, H. and Roberts, I. "Issues relating to proper modelling of the profile of long gas condensate pipelines", presented at the 2005 PSIG Annual Meeting, San Antonio, TX, November 7-9, 2005, Paper PSIG 0501.

17. Ellul, I. R., Saether, G. and Shnippen, L. P. "The modeling of multiphase systems under steady-state and transient conditions – A tutorial", presented at the 2004 PSIG annual Meeting, Palm Springs, CA, October 20-22, 2004, Paper PSIG 0403.

18. Fard, M. P., Godhavn, J. M. and Sagatun, S. I. "Modeling of severe slug and slug control with OLGA", *SPE Production & Operations Journal*, vol. 21, no. 3, 2006.

19. Gaspari, E. F., Oliveira, G. P. H. A., Monteiro, M. R. B. and Dourado, R.J. "Evaluating transient multiphase model performance for the Brazilian offshore environment", presented at the 2006 Offshore Technology Conference, Houston, TX, May 1-4, 2006, Paper OTC 17956.

20. Ghetto, G. D., Paone, F. and Villa, M. "Reliability analysis on PVT correlations", presented at the European Petroleum Conference, London, UK, October 25-27, 1994, Paper SPE 28904.

21. Glaso, O. "Generalised pressure-volume-temperature correlations", *Journal of Petroleum Technology,* pp. 785-795, May 1980.

22. Hagesæter, L., Knud, L., Nygård, F. and Eidsmoen, H. "Flow assurance modeling: Reality check and aspects of transient operations of gas/condensate pipelines" presented at the 2006 Offshore Technology Conference, Houston, TX, May 1-4, 2006, Paper OTC 17894-PP.

23. Harmathy, T. Z. "Velocity of large drops and bubbles in media of infinite or restricted extend", *AIChE J.*, vol. 6, pp. 281, 1960.

24. Harun, A. F., Krawietz, T. E. and Erdogmus, M. "Hydrate remediation in deepwater Gulf of Mexico dry-tree wells: Lesson learned," presented at the 2006 Offshore Technology Conference, Houston, TX, May 1-4, 2006, Paper OTC 17814.

25. Hassan, A. R. and Kabir, C. S. *Fluid flow and heat transfer*, Society of Petroleum Engineers, Inc., 2002, pp. 2, 7-9, 24-25, 55-60.

26. Hassan, A. R. and Kabir, C. S. "Modeling changing storage during a shut-in test", *SPE Formation Evaluation*, pp. 279-284, Dec. 1994.

27. Havre, K. and Dalsmo, M. "Active feedback control as the solution to severe slugging", presented at the 2001 SPE Annual Technical Conference and Exhibition, New Orleans, LO, September 30-October 3, 2001, Paper SPE 71540.

28. Hurzeler, K. "Subsea Intervention – The Balance of Effectiveness, Risk and Cost", presented at the 2010 Offshore Technology Conference, Houston, TX, May 3-7, 2010, Paper OTC 20419-MS.

29. James, P. B. and Hemanta, M. "Multiphase flow in wells", *SPE Monograph*, vol. 17, pp. 2, 1999.

30. Jiun Horng, C. (2009). Sumandak daily welltest data, *PETRONAS Carigali Sdn. Bhd.* [CD-ROM].

31. Jordan, M. M., Collins, I. R., Gyani, A. and Graham, G. M. "Coreflood studies examine new technologies that minimize intervention throughout well life cycle", SPE Production and Operations, vol. 21, no. 2, pp. 161-173, 2006.

32. Kaya, A.S., Sarica, C., and Brill, J.P. "Mechanistic modeling of two-phase flow in deviated wells", SPE Production and Facilities, vol. 16, no. 3, pp. 156-165, 2001.

33. Lasater, J. A. "Bubble point pressure correlation", *Journal of Petroleum Technology*, pp. 65-67, May 1958.

34. Lee Jean, W. and Jiun Horng, C. "Sumandak main SUDP-A sub block 6S-18 offshore Sabah pressure build-up", PETRONAS Carigali Sdn. Bhd., 2009.

35. Macary, S. M. and El-Batanoney, M. H. "Derivation of PVT correlations for the Gulf of Suez crude oils", *Journal of the Japan Petroleum Institute (formerly the Sekiyu Gakkaishi-Journal of the Japan Petroleum Institute)*, vol. 36, no. 6, 1993.

36. Mantecon, J. C. "The virtual well: Guidelines for the application of dynamic simulation to optimize well operations, life cycle design, and production", presented at the 2007 SPE Annual Technical Conference and Exhibition, Anaheim, CA, November 11-14, 2007, Paper SPE 109829-MS.

37. Mattar, L. "IPR's and all that "The 'direct' and 'inverse' problem" ", presented at the 38th Annual Technical Meeting of the Petroleum Society of CIM, Calgary, June 7-10, 1987, Paper 87-38-13.

38. McCain, W. D. Jr. *The properties of petroleum fluids*, 2nd Edition. Oklahoma: PennWell Publishing Co., 1990.

39. Meng, W. H. and Zhang, J. J. “Modeling and mitigation of severe riser slugging: A case study”, presented at the 2001 SPE Annual Technical Conference and Exhibition, New Orleans, LO, September 30-October 3, 2001, Paper SPE 71564.

40. Meunier, D., Wittmann, M. J. and Steward, G. “Interpretation of pressure build-up test using in-situ measurement of afterflow”, *Journal of Petroleum Technology*, pp. 143, Jan. 1985.

41. Moody, L.F. “Friction factors for pipe flow”, *Trans., ASME*, vol. 66, no. 8, pp. 671, 1944.

42. Mukherjee, H. and Brill, J. P. “Liquid holdup correlations for inclined two-phase flow”, *Journal of Petroleum Technology*, pp. 1003-1008, May 1983.

43. Orkiszewski, J. “Predicting two-phase pressure drops in vertical pipe”. *Journal of Petroleum Technology*, pp. 829-828, June 1967.

44. Petrosky, G. E. and Farshad, F. F. “Pressure-volume-temperature correlations for Gulf of Mexico crude oils”, *SPE Reservoir Evaluation & Engineering*, pp. 416-420, Oct. 1998.

45. Redlich, O. and Kwong, J., “On the thermodynamics of solutions. An Equation of State. Fugacities of Gaseous Solutions,” *Chemical Reviews*, vol. 44, pp. 233-247, 1949.

46. Reeves, H., Siegmund, M., Dawson, I. and Openshaw, G. “Future Intervention Options for Remote Subsea Facilities”, presented at the 2003 Offshore Technology Conference, Houston, TX, May 5-8, 2003, Paper OTC 15176-MS.

47. Schmidt, G. and Wenzel, H., “A modified Van der Waals type Equation of State,” *Chem. Eng. Sci.*, vol. 135, pp. 1503-1512, 1980.

48. Shah, Y. T., Stiegel, G. J. and Sharma, M. M. “Backmixing in gas-liquid reactors”, *AIChE J.*, vol. 24, pp. 369, 1978.

49. Slider, H. C. *Worldwide practical petroleum reservoir engineering methods*, 2nd Edition. Oklahoma: PennWell Publishing Co., 1983, pp. 157, 159.

50. Standing, M. B. “A pressure-volume-temperature correlation for mixtures of Californian oils and gasses”, *Drill. and Prod.,* pp. 275-287, 1947.

51. Standing, M. B. “Inflow performance relationships for solution-gas drive wells”, *Journal of Petroleum Technology*, pp. 1399-1400, Nov. 1970.

52. Taitel, Y. and Bornea, D. “Counter current gas-liquid vertical flow, model for flow pattern and pressure drop”, Int. J. Multiphase Flow, vol. 9, pp. 637, 1983.

53. Taitel, Y., Sarica, C., and Brill, J. P. “Slug flow modeling for downward inclined pipe flow: theoretical considerations”, *International Journal of Multiphase Flow*, vol. 26, issue 5, pp. 833-844, May 2000.

54. Tang, Y. and Danielson, T. “Pipelines slugging and mitigation: Case study for stability and production optimization”, presented at the 2006 SPE Annual Technical Conference and Exhibition, San Antonio, TX, September 24-27, 2006, Paper SPE 102352-MS.

55. Van der Waals, J. D. “On the continuity of the liquid and gaseous state”, Ph.D. dissertation, Sigthoff, Leiden, 1873.

56. Vasquez, M. and Beggs, H. D. “Correlations for Fluid Physical Property Prediction”, *Journal of Petroleum Technology*, pp. 968-970, Jun. 1980.

57. Vogel, J. V. “Inflow performance relationships for solution-gas drive wells”, *Journal of Petroleum Technology*, pp. 83-92, Jan. 1968.

58. Winterfeld, P. H. “Simulation of pressure buildup in a multiphase wellbore/reservoir system”, SPE Formation Evaluation Journal, pp. 247-252, 1989.

59. Xiao, J. J., Fuentes, F. A., Alhanati, F. and Reynolds, A. C. “Modeling and analyzing pressure buildup data affected by phase redistribution in the wellbore”, SPE Advanced Technology Series, vol. 4, no. 1, pp. 28-37, 1995.

60. Xiao, J. J. and Reynolds, A.C. “New methods for the analysis of closed chamber tests”, presented at the 1992 Western Regional Meeting, Bakersfield, CA, March 30-April 1, 1992, Paper SPE 24059.

61. Zabaras, G. J. and Mehta, A. P. “Effectiveness of bullheading operations for hydrate management in DVA and subsea wells”, presented at the 2004 Offshore Technology Conference, Houston, TX, May 3-6, 2004, Paper OTC 16689.

62. Zainal, S. (2008, January 17). *Data gathering workshop: Development of an enhanced dynamic well model.* PETRONAS Research Sdn. Bhd. Minutes of Meeting.

63. Zainal, S. (2010, February 2). *Project closing workshop: Development of an enhanced dynamic well model.* PETRONAS Research Sdn. Bhd. Minutes of Meeting.

APPENDIX A

CALCULATION MODULES

MODULE: modShutIn

```
' Module modShutIn

  Public Sub MainSI()

    ' INPUT
    Dim P(25, 2000) As Double
    Dim T(25, 2000) As Double
    Dim SGFG(25, 2000) As Double
    Dim IFT(25, 2000) As Double

    Dim T_WH(2000) As Double
    Dim SGFG_WH(2000) As Double
    Dim DENO(25, 2000) As Double
    Dim DENG(25, 2000) As Double

    Dim DENW(25, 2000) As Double
    Dim TD(2000) As Double
    Dim MD(2000) As Double
    Dim Vsl(25) As Double

    Dim Vsg(25) As Double
    Dim Dia(25) As Double
    Dim LC(25) As Double
    Dim dBT As Double

    Dim BO(25, 2000) As Double
    Dim BG(25, 2000) As Double
    Dim BW(25, 2000) As Double
    Dim PA(25, 2000) As Double

    Dim P_Grad(25, 2000) As Double
    Dim Mole_WH(2000) As Double
    Dim P_WH(2000) As Double
    Dim VG_WH(2000) As Double

    Dim Z_WH(2000) As Double
    Dim FL(25) As Double
    Dim L As Integer
```

```
    Dim CN As Integer

    Dim RSCODE As Integer
    Dim BOCODE As Integer
    Dim BWCODE As Integer

    Dim API As Double
    Dim GOR As Double ' unused
    Dim SGPG As Double
    Dim SGW As Double
    Dim RSI As Double

    Dim InfluxIn As New Influx

    ' OUTPUT Variables

    Dim V_Gas(25, 2000) As Double
    Dim Results(2000) As SIResult
Call ExcelReadSI(P, T, SGFG, IFT, DENO, DENG, DENW, TD, MD, Vsl, Vsg, Dia,
LC, dBT, BO, BG, BW, PA, P_Grad, FL, L, CN, RSCODE, BOCODE, BWCODE, API,
GOR, SGPG, SGW, RSI, InfluxIn, P_WH, T_WH, SGFG_WH)

Call CalcSI(P, T, SGFG, IFT, DENO, DENG, DENW, TD, MD, Vsl, Vsg, Dia, LC, dBT,
BO, BG, BW, PA, P_Grad, FL, L, CN, RSCODE, BOCODE, BWCODE, API, GOR,
SGPG, SGW, RSI, InfluxIn, P_WH, T_WH, SGFG_WH, V_Gas, Results)

  End Sub

Public Sub CalcSI(ByRef P As Variant, ByRef T As Variant, ByRef SGFG As Variant,
ByRef IFT As Variant, ByRef DENO As Variant, ByRef DENG As Variant, ByRef
DENW As Variant, ByRef TD() As Double, ByRef MD() As Double, ByRef Vsl() As
Double, ByRef Vsg() As Double, ByRef Dia() As Double, ByRef LC() As Double,
ByRef dBT As Double, ByRef BO As Variant, ByRef BG As Variant, ByRef BW As
Variant, ByRef PA As Variant, ByRef P_Grad As Variant, ByRef FL() As Double,
ByRef L As Integer, ByRef CN As Integer, ByRef RSCODE As Integer, ByRef
BOCODE As Integer, ByRef BWCODE As Integer, ByRef API As Double, ByRef GOR
As Double, ByRef SGPG As Double, ByRef SGW As Double, ByRef RSI As Double,
ByRef InfluxIn As Influx, ByRef P_WH() As Double, ByRef T_WH() As Double, ByRef
SGFG_WH() As Double, ByRef V_Gas As Variant, ByRef Results() As SIResult)

    'Public Sub CalcSI()

    ' LOCAL VARIABLES
    Dim BT As Integer
    Dim DENM(25, 2000) As Double
    Dim PB(25, 2000) As Double
    Dim RS(25, 2000) As Double
    Dim RSW(25, 2000) As Double
    Dim V_Cell(25, 2000) As Double
```

```
    Dim V_bubble(25, 2000) As Double
    Dim V_Liquid(25, 2000) As Double
    Dim VG_R(25, 2000) As Double
    Dim VG_L(25, 2000) As Double
    Dim Z(25, 2000) As Double

    Dim DelLC(2000) As Double
    Dim PWF(2000) As Double
    Dim QO(2000) As Double   'in influx in bbl/day
    Dim Mole_WH(2000) As Double
    Dim tD1(2000) As Double
    Dim Sum_L(2000) As Double
    Dim Sum_G(2000) As Double
    Dim Sum_Pstatic(2000) As Double
    Dim VG_WH(2000) As Double
    Dim Z_WH(2000) As Double

    Dim FG(25) As Double
    Dim P_Cell(25) As Double
    Dim YCH(1) As Double

    Dim I As Integer
    Dim NN As Integer
    Dim Steps As Integer

    Dim BT_S As Double
    Dim LFgas As Double
    Dim dBTSet As Double
    Dim PWS_In As Double
    Dim SGDG As Double
    Dim Sum_tbg As Double
    Dim VDA As Double
    Dim V_DIFF As Double
    Dim tSGFG As Double
    Dim tPB As Double

    ' KEY OUTPUT
    Dim PWS(2000) As Double
    Dim SumdBT As Double
    Dim Q(2000) As Double
    Dim Result As SIResult
'----- Calc fluid properties in each cell for the rest of the wellbore -----
Call PrepCellValues(CN, FG, FL, Dia, LC, V_Cell, V_Gas, V_Liquid, Z, T, PA, SGFG)

'----- Assign cell properties for Wellhead Node at time = 0 sec -----
Call Prepare_WH_Initial(V_Gas, P_WH, T_WH, SGFG_WH, VG_WH, Z_WH,
Mole_WH)

'----- Initial volume balance check -----
```

```
Call InitialVolBalance(NN, CN, Sum_tbg, V_Cell, Sum_G, Sum_L, V_Liquid, V_Gas)

'----- Calc static head instantly after shut in well, in psi
Call InitialPWS(CN, Sum_Pstatic, P_Grad, LC, PWS, P_WH)

'----- Calc RS(CN, 0) for bottom most cell. This is for use in material module
Call PVTProp.CALC_SOLUTION_GOR_AND_GWR(RSCODE, T(CN, 0), API,
PA(CN, 0), SGPG, 14.7, 60, 1, 1, RSI, 1, 0, YCH, 0, 0, 1, 0, RS(CN, 0), RSW(CN, 0),
SGDG, tSGFG, tPB)

    SGFG(CN, 0) = tSGFG
    PB(CN, 0) = tPB

For I = 1 To CN
Call PVTProp.CALC_SOLUTION_GOR_AND_GWR(RSCODE, T(I, 0), API, PA(I, 0),
SGPG, 14.7, 60, 1, 1, RSI, 1, 0, YCH, 0, 0, 1, 0, RS(I, 0), RSW(I, 0), SGDG, tSGFG,
tPB)
        SGFG(I, 0) = tSGFG
        PB(I, 0) = tPB

    Next I

Call PVTProp.CALC_SOLUTION_GOR_AND_GWR(RSCODE, T_WH(0), API,
P_WH(0), SGPG, 14.7, 60, 1, 1, RSI, 1, 0, YCH, 0, 0, 1, 0, RS(1, 0), RSW(I, 0), SGDG,
tSGFG, tPB)

    SGFG_WH(0) = tSGFG

     Z_WH(0) = modZ_HY.ZHY(T_WH(0), P_WH(0), SGFG_WH(0))


    '-------------------------------------------------------------------------------------------------
    '*** Part B: Gas Migration Calculation after shut-in well ***

    'Sum total liquid entry from reservoir at t = 0, begining shut in well, in cuft
    ' SumQ = 0  ' unused

    NN = 2 'this cell exchanging  mass with gas chamber
    SumdBT = 0   'total elapsed time, in sec
    dBTSet = dBT

    '-----------------------------------------------------------------------------
    '---------- Iteration over time starts here -----------
    '-----------------------------------------------------------------------------

    Call ExcelListInitialResults(CN, V_Gas, Sum_G, Sum_L, Sum_tbg, VG_WH)

    For BT = 1 To L   'time index, for number of time step cycle
```

```
        dBT = dBTSet
        BT_S = dBT   'BT_S to temporary store the BT value for influx calc

        For I = 1 To CN
          T(I, BT) = T(I, 0)   'assume temp constant for all time steps
          PA(I, BT) = PA(I, BT - 1)   'note that PA(1, BT) is the average pressure for
          wellhead gas chamber
          P(I, BT) = P(I, BT - 1)   'note that P is the pressure at node base
          Z(I, BT) = Z(I, BT - 1)
          Z_WH(BT) = Z_WH(BT - 1)
          DENO(I, BT) = DENO(I, BT - 1)
          DENG(I, BT) = DENG(I, BT - 1)
          DENW(I, BT) = DENW(I, BT - 1)
        Next I

        'Also for wellhead node
        P_WH(BT) = P_WH(BT - 1)
        T_WH(BT) = T_WH(0)
        Z_WH(BT) = Z_WH(BT - 1)

        For I = NN To CN
          V_Cell(I, BT) = V_Cell(I, 0)   'V_Cell is constant with time
        Next I

        'to calc bubble rise vel, ft/sec
        For I = 1 To CN
          V_bubble(I, BT) = 1.53 * (32.2 * (DENO(I, BT - 1) - DENG(I, BT - 1)) * _
                    IFT(I, 0) * 0.0022 / (DENO(I, BT - 1)) ^ 2) ^ 0.25
        Next I

Call PwsBisect(InfluxIn, PWS_In, P, dBT, V_Gas, BT, SumdBT, NN, CN, Vsg, Vsl,
V_bubble, PA, T, LC, V_Cell, Z, Q, Sum_G, tD1, V_DIFF, QO, PWS, LFgas, RSI, RS,
Dia, VG_WH, Mole_WH, P_WH, Z_WH, BG, P_Grad, TD, RSW, SGFG, BO, BW, PB,
FG, DENO, DENG, DENW, DENM, RSCODE, BOCODE, BWCODE, API, SGPG,
SGW, T_WH, SGFG_WH, SGDG, VDA, Steps)
        SumdBT = SumdBT + dBT

        ' save results
        Set Result = New SIResult

        Result.V_Gas = V_Gas(1, BT)
        Result.SumdBT = SumdBT
        Result.Sum_G = Sum_G(BT)
        Result.Sum_L = Sum_L(BT)
        Result.Sum_tbg = Sum_tbg
        Result.Q = Q(BT)
        Result.P_WH = P_WH(BT)
        Result.PWS = PWS(BT)
        Result.VG_WH = VG_WH(BT)
```

```
'        Result.Z = Z(NN, BT)
'        Result.LC = LC(1)

         Set Results(BT) = Result

         Call ExcelListVGas(CN, BT, V_Gas)
         Call ExcelListSIResult(BT, Result)
         Call ExcelListZ(CN, BT, SumdBT, TD, Z)
         Call ExcelListLC1(BT, SumdBT, LC)
         Call ExcelListSGFG(CN, BT, SumdBT, TD, SGFG_WH, SGFG)

         If LC(1) > TD(1) Then
           LFgas = ((LC(1) - TD(NN - 1)) / (TD(NN) - TD(NN - 1)))
         End If

         Application.StatusBar = "Calculating: BT=" & BT & " Pwh=" & P_WH(BT) & "
         Pws=" & PWS(BT)

         If Math.Abs(VDA) < 0.01 Or Steps > 20 Then

           NN = NN + 1
           V_Cell(NN, BT) = V_Cell(NN, 0)
           LFgas = 0
         End If

      Next BT

   End Sub


Private Sub Prepare_WH_Initial(ByRef V_Gas As Variant, ByRef P_WH() As Double,
ByRef T_WH() As Double, ByRef SGFG_WH() As Double, ByRef VG_WH() As
Double, ByRef Z_WH() As Double, ByRef Mole_WH() As Double)
      VG_WH(0) = V_Gas(1, 0)
      '----- Calc Z and moles for welhead node at time = 0 sec -----
      Z_WH(0) = modZ_HY.ZHY(T_WH(0), P_WH(0), SGFG_WH(0))
      Mole_WH(0) = P_WH(0) * VG_WH(0) / (23.6591 * Z_WH(0) * (T_WH(0) +
460.67))   'in kg.mole

   '   LC(1) = V_Gas(1, BT) / (3.142 * (Dia(1) / 24) ^ 2)

   End Sub

Private Sub PrepCellValues(ByVal CN As Integer, ByRef FG() As Double, ByRef FL()
As Double, ByRef Dia() As Double, ByRef LC() As Double, ByRef V_Cell As Variant,
ByRef V_Gas As Variant ByRef V_Liquid As Variant, ByRef Z As Variant, ByRef T As
Variant, ByRef PA As Variant, ByRef SGFG As Variant)
      Dim I As Integer
```

```
    For I = 1 To CN
      FG(I) = 1 - FL(I)   'liquid vol fraction
      V_Cell(I, 0) = 22 / 7 * (Dia(I) / 12) ^ 2 / 4 * LC(I) 'node vol in cuft
      V_Gas(I, 0) = FG(I) * V_Cell(I, 0)    'gas vol in cell, cuft
      V_Liquid(I, 0) = FL(I) * V_Cell(I, 0)  'liquid vol in cell, cuft
    Next I

        '----- Calc compressibility, Z for each node -----
    For I = 1 To CN
      Z(I, 0) = modZ_HY.ZHY(T(I, 0), PA(I, 0), SGFG(I, 0))
    Next I
  End Sub

Private Sub InitialVolBalance(ByVal NN As Integer, ByVal CN As Integer, ByRef
Sum_tbg As Double, ByRef V_Cell As Variant, ByRef Sum_G() As Double, ByRef
Sum_L() As Double, ByRef V_Liquid As Variant, ByRef V_Gas As Variant)
    Dim I As Integer

    Sum_tbg = 0
    For I = 1 To CN
      Sum_tbg = Sum_tbg + V_Cell(I, 0)  'total tbg vol, cuft ( = Vgas + Vliquid)
    Next I

    Sum_G(0) = 0   'total gas vol in cuft, at t = 0 sec
    Sum_L(0) = 0   'total liquid vol in cuft, at t = 0 sec
    For I = 1 To CN
      Sum_L(0) = Sum_L(0) + V_Liquid(I, 0)
    Next I

    For I = 2 To CN
      Sum_G(0) = Sum_G(0) + V_Gas(I, 0) 'except gas chamber gas
    Next I
  End Sub


Private Sub InitialPWS(ByVal CN As Integer, ByRef Sum_Pstatic() As Double, ByRef
P_Grad As Variant, ByRef LC() As Double, ByRef PWS() As Double, ByRef P_WH()
As Double)
    Dim I As Integer

    Sum_Pstatic(0) = 0
    For I = 1 To CN
      Sum_Pstatic(0) = Sum_Pstatic(0) + P_Grad(I, 0) * LC(I)
    Next I

    PWS(0) = Sum_Pstatic(0) + P_WH(0)
  End Sub

' End Module
```

MODULE: modInflux

```
' Module modInflux

Public Sub CalcInflux(ByVal InfluxIn As Influx, ByVal CN As Double, ByVal BT As
Double, ByVal dTempo As Double, ByRef PWS() As Double, ByRef tD1() As Double,
ByRef Q0() As Double)

    ' PRES              Reservoir pressure  (psi)
    ' P                 Node pres @ shutin  (psi)
    ' influxIn.PORO     influxIn.POROsity (frac)
    ' CT                System total compressibility  (psi^-1)
    ' VISO              Oil Viscosity (cp)
    ' BO                Oil formation volume factor   (rb/stb)
    ' RW                Wellbore radius (ft)
    ' influxIn.K        Permeability (mD)
    ' H                 Reservoir thicinfluxIn.Kness (ft)
    ' Q1                Oil rate befofre SI  (stb/d)
    ' S                 SinfluxIn.Kin (-)
    ' QO                Oil rate influx (stb/d)
    ' Inputs
    'Dim Pres As Double
    'Dim influxIn.PORO As Double
    'Dim CT As Double
    'Dim VISO As Double
    'Dim BO As Double
    'Dim RW As Double
    'Dim influxIn.K As Double
    'Dim Q1 As Double
    'Dim H As Double
    'Dim S As Double
    'Local Variables
```

```
    Dim pD_1 As Double
    Dim pD_2 As Double
    Dim pD_3 As Double
    Dim Sum_QP As Double
    Dim m As Double
    Dim I As Integer
    'Tabulate inputs data
    ' Call InfluxIn(influxIn.Pres, influxIn.PORO, CT, VISO, BO, RW, influxIn.K, Q1, H, S)
    'Calc liquid influx
    dTempo = dTempo / 3600 'convert time from sec to hour
    'Initialize tD and QO immediatly after well shut-in
    tD1(0) = 0
    Q0(0) = 0
    tD1(BT) = InfluxIn.TD(dTempo)
    m = InfluxIn.m()
    pD_1 = InfluxIn.pD(tD1(1))
    Q0(1) = (InfluxIn.Pres - PWS(BT - 1)) / (m * (pD_1 + InfluxIn.S))

    If BT > 1 Then
      Sum_QP = 0
      For I = 1 To BT - 1
        pD_2 = InfluxIn.pD(tD1(BT - 1) - tD1(I - 1))
        If pD_2 < 0 Then
          pD_2 = InfluxIn.pD(tD1(BT - 1) - tD1(I - 2))
        End If
        Sum_QP = Sum_QP + (Q0(I) - Q0(I - 1)) * pD_2
      Next I
      pD_3 = InfluxIn.pD(tD1(BT) - tD1(BT - 1))
      Q0(BT) = Q0(BT - 1) + (InfluxIn.Pres - PWS(BT)) / (m * (pD_3) + InfluxIn.S) - (1 /
     (pD_3 + InfluxIn.S)) * Sum_QP    'Eq 4 (Hassan)

    End If
  End Sub
' End Module
```

MODULE: modMaterial

```
' Module modMaterial

Public Sub CalcGVol(ByVal InfluxIn As Influx, ByVal BT As Integer, ByVal SumdBT
As Double, ByVal NN As Integer, ByVal CN As Integer, ByRef Vsg As Variant, ByRef
Vsl As Variant, ByRef V_bubble As Variant, ByRef PA As Variant, ByRef T As Variant,
ByRef LC As Variant, ByRef V_Cell As Variant, ByRef Z As Variant, ByVal StepdBT
As Double, ByRef V_GasActive As Double, ByRef V_Gas As Variant, ByRef VG_L As
Variant, ByRef Q As Variant, ByRef Sum_G As Variant, ByRef tD1() As Double, ByRef
V_DIFF As Double, ByRef QO() As Double, ByRef VDA As Double, ByRef PWS() As
Double, ByVal LFgas As Double, ByRef RSI As Double, ByRef RS As Variant, ByRef
BO As Variant, ByRef BG As Variant)

    'Local variable
    ReDim Cell_Frac(CN) As Double
    ReDim VG_R(CN) As Double
    Dim QG As Double
    Dim I As Integer
    Dim CO As Double
    Dim dTempo As Double
    Dim DIFF_VL As Double
    Dim L_bubble As Double
    Dim Multi As Double
    Dim V_CellF As Double
    Dim V1_Temp As Double

    CO = 2   'for concurrent 2 phase flow as suggested by Hassan and Kabir
    For I = 1 To
      Vsl(I) = 0
    Next I

    For I = NN To CN
      Cell_Frac(I) = (CO * (Vsg(I) - Vsl(I)) + V_bubble(I, BT)) * StepdBT / LC(I)
      L_bubble = (V_bubble(I, BT) * StepdBT)
      If LC(I) < L_bubble Then
        ' MsgBox ("Cell jumping @ " & SumdBT & " sec . Calc continue using max gas
        travelling rate")
      End If
    Next I
```

```
For I = NN To CN - 1
   VG_R(I + 1) = Cell_Frac(I + 1) * V_Gas(I + 1, BT - 1) * (PA(I + 1, BT) / PA(I,
  BT)) * (T(I, BT) / T(I + 1, BT)) * (Z(I, BT) / Z(I + 1, BT))
   VG_L(I, BT) = Cell_Frac(I) * V_Gas(I, BT - 1)
   ' VG_L(NN, BT) = 0
   V_Gas(I, BT) = V_Gas(I, BT - 1) + (VG_R(I + 1) - VG_L(I, BT))
Next I

V_Gas(CN, BT) = V_Gas(CN, BT - 1) - Cell_Frac(CN) * V_Gas(CN, BT - 1)

For I = NN To CN
   If V_Gas(I, BT) <= 10 ^ -10 Then V_Gas(I, BT) = 0
Next I

'----- Calc new wellhead volume in cuft -----

dTempo = SumdBT
dTempo = dTempo + StepdBT   'total elapsed time, in sec

Call CalcInflux(InfluxIn, CN, BT, dTempo, PWS, tD1, QO)

QO(BT) = QO(BT) ' * BO(CN, BT - 1)  'convert to in-situ bbl
Q(BT) = QO(BT) * 5.6 * BO(CN, BT - 1) / 86400   'convert from bbl/day to cuft/sec
(insitu bbl)

If Q(BT) < 0 Then
   Q(BT) = 0
End If

Sum_G(BT) = 0

QG = (Q(BT) / 5.6) * (RSI - RS(CN, BT - 1)) * BG(CN, BT - 1)   'insitu cuft gas
Sum_G(BT) = Sum_G(BT) + QG

'----- Sum all gases in rest of wellbore after each timestep -----
For I = NN To CN
   Multi = IIf(I = NN, (1 - LFgas), 1)
   Sum_G(BT) = Sum_G(BT) + V_Gas(I, BT) * Multi
Next I

 DIFF_VL = 0   'decrease in the volume of the wellbore liquid owing to increased
wellbore pressure, later pre-calc using PVT module


 V1_Temp = V_GasActive   'previous wellhead gas chamber vol, in cuft (time step
 BT-1)
```

```
    V_GasActive = V_GasActive + Sum_G(BT - 1) - Sum_G(BT) - Q(BT) * StepdBT +
   DIFF_VL 'Eq 11 (Hassan)  'change in gas chamber vol

    If V_GasActive < 0 Then
      MsgBox ("Influx higher than wellhead gas chamber volume")
      Exit Sub
    End If

    V_DIFF = V_GasActive - V1_Temp   'vol increase in wellhead gas chamber, in cuft

    V_CellF = 0
    For I = 1 To NN
      V_CellF = V_CellF + V_Cell(I, 0)
    Next I

    VDA = V_CellF - V_GasActive 'void space in active cell available for gas filling

 End Sub

'End Module
```

MODULE: modPws

```
' Module modPws

Private Sub CalcGradient(ByVal RSCODE As Integer, ByVal BOCODE As Integer,
ByVal BWCODE As Integer, ByVal API As Double, ByVal SGPG As Double, ByVal
SGW As Double, ByVal RSI As Double, ByVal T_Node As Double, ByVal
V_Gas_Node As Double, ByVal V_Cell_Node As Double, ByVal LC_Node As Double,
ByVal TopPressure As Double, ByVal Assumed_Gradient As Double, ByRef RS_Node
As Double, ByRef RSW_Node As Double, ByRef SGFG_Node As Double, ByRef
SGDG As Double, ByRef BG_Node As Double, ByRef BO_Node As Double, ByRef
BW_Node As Double, ByRef Z_Node As Double, ByRef PB_Node As Double, ByRef
FG_Node As Double, ByRef DENO_Node As Double, ByRef DENG_Node As Double,
ByRef DENW_Node As Double, ByRef DENM_Node As Double, ByRef
Average_Pressure As Double, ByRef BottomPressure As Double, ByRef
Calculated_Gradient As Double)
    'Local Variables
    Dim converged As Boolean
    Dim loops As Integer
    Dim Guess_BottomPressure As Double
    Dim YCH(1) As Double

    converged = False
    loops = 0

    Do
    Guess_BottomPressure = TopPressure + Assumed_Gradient * LC_Node
    Average_Pressure = (TopPressure + Guess_BottomPressure) / 2

      ' Calculate the solution GOR
Call PVTProp.CALC_SOLUTION_GOR_AND_GWR(RSCODE, T_Node, API,
Average_Pressure, SGPG, 14.7, 60, 1, 1, RSI, 1, 0, YCH, 0, 0, 1, 0, RS_Node,
RSW_Node, SGDG, SGFG_Node, PB_Node)

Call PVTProp.PVT_LIQUID_VOLUME_FACTOR(BOCODE, BWCODE, T_Node,
API, Average_Pressure, SGPG, 14.7, 60, PB_Node, RSI, RS_Node, 1, 0, 1, BO_Node,
BW_Node)

      Z_Node = modZ_HY.ZHY(T_Node, Average_Pressure, SGFG_Node)
      BG_Node = 14.7 / 520 * ((T_Node + 460) * Z_Node / Average_Pressure)
      DENO_Node = PVTProp.DENSO(API, SGPG, RS_Node, BO_Node)
```

```
      DENG_Node = PVTProp.DENSG(SGPG, BG_Node)
      DENW_Node = PVTProp.DENSW(SGW, BW_Node)

      FG_Node = V_Gas_Node / V_Cell_Node
      DENM_Node = FG_Node * DENG_Node + (1 - FG_Node) * DENO_Node
      Calculated_Gradient = DENM_Node / 144  'in psi/ft

      If Math.Abs(Assumed_Gradient - Calculated_Gradient) < 0.001 Then
        converged = True

      ElseIf (Assumed_Gradient - Calculated_Gradient) > 0 Then
        Assumed_Gradient = Assumed_Gradient - 1 / 2 ^ loops

      ElseIf (Assumed_Gradient - Calculated_Gradient) < 0 Then
        Assumed_Gradient = Assumed_Gradient + 1 / 2 ^ loops

      End If

      loops = loops + 1
      If loops >= 50 Then
        Exit Sub
      End If
    Loop Until converged

    BottomPressure = Guess_BottomPressure
  End Sub

Public Sub PwsBisect(ByVal InfluxIn As Influx, ByVal PWS_In As Double, ByRef P As
Variant, ByRef dBT As Double, ByRef V_Gas As Variant, ByVal BT As Integer, ByVal
SumdBT As Double, ByVal NN As Integer, ByVal CN As Integer, ByRef Vsg() As
Double, ByRef Vsl() As Double, ByRef V_bubble As Variant, ByRef PA As Variant,
ByRef T As Variant, ByRef LC() As Double, ByRef V_Cell As Variant, ByRef Z As
Variant, ByRef Q() As Double, ByRef Sum_G() As Double, ByRef tD1() As Double,
ByRef V_DIFF As Double, ByRef QO() As Double, ByRef PWS() As Double, ByVal
LFgas As Double, ByVal RSI As Double, ByRef RS As Variant, ByRef Dia() As Double,
ByRef VG_WH() As Double, ByRef Mole_WH() As Double, ByRef P_WH() As
Double, ByRef Z_WH() As Double, ByRef BG As Variant, ByRef P_Grad As Variant,
ByRef TD() As Double, ByRef RSW As Variant, ByRef SGFG As Variant, ByRef BO
As Variant, ByRef BW As Variant, ByRef PB As Variant, ByRef FG() As Double,
ByRef DENO As Variant, ByRef DENG As Variant, ByRef DENW As Variant, ByRef
DENM As Variant, ByVal RSCODE As Integer, ByVal BOCODE As Integer, ByVal
BWCODE As Integer, ByVal API As Double, ByVal SGPG As Double, ByVal SGW As
Double, ByRef T_WH() As Double, ByRef SGFG_WH() As Double, ByVal SGDG As
Double, ByRef VDA As Double, ByRef Steps As Integer)

    Dim X0 As Double, H As Double, X1 As Double, X2 As Double, Y0 As Double, Y1
    As Double
    Dim Iswitch As Integer
    Dim FNF0 As Double
```

```
    Dim FNF1 As Double
    Dim A As Double, B As Double
    Dim L As Double
    Dim dBT_S As Double   'temporary storage for dBT

    dBT_S = dBT

    Iswitch = 0
    H = 100 ' Starting Interval
    A = P(CN, BT - 1) '115 ' Starting point set to steady state
    B = 10000 ' End point
    X0 = A - H
    X1 = X0 + H

    dBT = dBT_S

Call PWS1(InfluxIn, X0, P, dBT, V_Gas, BT, SumdBT, NN, CN, Vsg, Vsl, V_bubble,
PA, T, LC, V_Cell, Z, Q, Sum_G, tD1, V_DIFF, QO, PWS, LFgas, RSI, RS, Dia,
Mole_WH, P_WH, Z_WH, BG, P_Grad, TD, RSW, SGFG, BO, BW, PB, FG, DENO,
DENG, DENW, DENM, RSCODE, BOCODE, BWCODE, API, SGPG, SGW, T_WH,
SGFG_WH, SGDG)

    FNF0 = X0 - PWS(BT)
    dBT = dBT_S

Call PWS1(InfluxIn, X1, P, dBT, V_Gas, BT, SumdBT, NN, CN, Vsg, Vsl, V_bubble,
PA, T, LC, V_Cell, Z, Q, Sum_G, tD1, V_DIFF, QO, PWS, LFgas, RSI, RS, Dia,
Mole_WH, P_WH, Z_WH, BG, P_Grad, TD, RSW, SGFG, BO, BW, PB, FG, DENO,
DENG, DENW, DENM, RSCODE, BOCODE, BWCODE, API, SGPG, SGW, T_WH,
SGFG_WH, SGDG)
    FNF1 = X1 - PWS(BT)

    X0 = X1
    If FNF0 * FNF1 <= 0 Then
      X0 = X0 - H
      H = H / 10
      Iswitch = Iswitch + 1
      If Iswitch >= 5 Then
        X1 = X0 + H
        GoTo 110
      End If
    End If
    If X1 > B Then
      L = 0
      X2 = 0
      MsgBox ("Pws > Max Pws allowed")
      Exit Sub
    End If
    GoTo 70
```

```
    Y0 = FNF0
    Y1 = FNF1
    X2 = (X0 * Y1 - X1 * Y0) / (Y1 - Y0)

    dBT = dBT_S

Call PWS2(InfluxIn, X2, P, dBT, V_Gas, BT, SumdBT, NN, CN, Vsg, Vsl, V_bubble,
PA, T, LC, V_Cell, Z, Q, Sum_G, tD1, V_DIFF, QO, PWS, LFgas, RSI, RS, Dia,
Mole_WH, P_WH, Z_WH, BG, P_Grad, TD, RSW, SGFG, BO, BW, PB, FG, DENO,
DENG, DENW, DENM, RSCODE, BOCODE, BWCODE, API, SGPG, SGW, T_WH,
SGFG_WH, SGDG, VDA, Steps)
  End Sub

Private Sub PWS1(ByVal InfluxIn As Influx, ByVal PWS_In As Double, ByRef P As
Variant, ByRef dBT As Double, ByRef V_Gas As Variant, ByVal BT As Integer, ByVal
SumdBT As Double, ByVal NN As Integer, ByVal CN As Integer, ByRef Vsg() As
Double, ByRef Vsl() As Double, ByRef V_bubble As Variant, ByRef PA As Variant,
ByRef T As Variant, ByRef LC() As Double, ByRef V_Cell As Variant, ByRef Z As
Variant, ByRef Q() As Double, ByRef Sum_G() As Double, ByRef tD1() As Double,
ByRef V_DIFF As Double, ByRef QO() As Double, ByRef PWS() As Double, ByVal
LFgas As Double, ByVal RSI As Double, ByRef RS As Variant, ByRef Dia() As Double,
ByRef Mole_WH() As Double, ByRef P_WH() As Double, ByRef Z_WH() As Double,
ByRef BG As Variant, ByRef P_Grad As Variant, ByRef TD() As Double, ByRef RSW
As Variant, ByRef SGFG As Variant, ByRef BO As Variant, ByRef BW As Variant,
ByRef PB As Variant, ByRef FG() As Double, ByRef DENO As Variant, ByRef DENG
As Variant, ByRef DENW As Variant, ByRef DENM As Variant, ByVal RSCODE As
Integer, ByVal BOCODE As Integer, ByVal BWCODE As Integer, ByVal API As
Double, ByVal SGPG As Double, ByVal SGW As Double, ByRef T_WH() As Double,
ByRef SGFG_WH() As Double, ByVal SGDG As Double)
    Dim V_Cell_Node As Double
    Dim V_Gas_Node As Double
    Dim LC_Node As Double
    Dim T_Node As Double
    Dim Sum_L(2000) As Double
    Dim V_Liquid(25, 2000) As Double
    Dim VG_L(25, 2000) As Double
    Dim StepdBT As Double
    Dim V_GasActive As Double
    Dim V_GasNN As Double
    Dim AddMole As Double
    Dim Z_WH_Loop As Double
    Dim Z_Diff As Double
    Dim iterate As Integer
    Dim K As Integer
    Dim RS_Node As Double
    Dim RSW_Node As Double
    Dim SGFG_Node As Double
    Dim BG_Node As Double
    Dim BO_Node As Double
```

```
    Dim BW_Node As Double
    Dim Z_Node As Double
    Dim PB_Node As Double
    Dim FG_Node As Double
    Dim DENO_Node As Double
    Dim DENG_Node As Double
    Dim DENW_Node As Double
    Dim DENM_Node As Double
    Dim TopPressure As Double
    Dim Average_Pressure As Double
    Dim Calculated_Gradient As Double
    Dim BottomPressure As Double
    Dim DelLC(25) As Double
    Dim Sum_Pstatic(2000) As Double
    Dim TotDelLC As Double
    Dim Multi As Double
    Dim VDA As Double
    Dim Steps As Integer
    Dim I As Integer
    Dim Assumed_Gradient As Double

    PWS(BT) = PWS_In

    Steps = 0
    StepdBT = dBT

    V_GasActive = V_Gas(1, BT - 1)   'this is wellhead gas chamber
    V_GasNN = V_Gas(NN, BT - 1)

Call CalcGVol(InfluxIn, BT, SumdBT, NN, CN, Vsg, Vsl, V_bubble, PA, T, LC,
V_Cell, Z, StepdBT, V_GasActive, V_Gas, VG_L, Q, Sum_G, tD1, V_DIFF, QO, VDA,
PWS, LFgas, RSI, RS, BO, BG)

    If VDA >= 0 Then
      GoTo 10
    End If

    If VDA < 0 Then
      'try to narrow down steps
      For Steps = 1 To 20
        If VDA < 0 Then
          StepdBT = StepdBT - (dBT / 2 ^ Steps)
        Else
          StepdBT = StepdBT + (dBT / 2 ^ Steps)
        End If

        V_GasActive = V_Gas(1, BT - 1)
        V_Gas(NN, BT - 1) = V_GasNN
```

```
        Call CalcGVol(InfluxIn, BT, SumdBT, NN, CN, _
              Vsg, Vsl, V_bubble, _
              PA, T, LC, V_Cell, Z, StepdBT, _
              V_GasActive, V_Gas, VG_L, Q, _
              Sum_G, tD1, V_DIFF, QO, VDA, PWS, _
              LFgas, RSI, RS, BO, BG)

        If Math.Abs(VDA) < 0.01 Then
          Exit For
        End If
      Next Steps
    End If

10:

    V_Gas(1, BT) = V_GasActive
    LC(1) = V_Gas(1, BT) / (3.142 * (Dia(1) / 24) ^ 2)
    dBT = StepdBT

    For I = NN To CN
      V_Liquid(I, BT) = V_Cell(I, BT) - V_Gas(I, BT)
      If V_Liquid(I, BT) < 0 Then
        V_Liquid(I, BT) = 0
      End If
    Next I

    Sum_L(BT) = 0
    For I = 1 To CN
      Sum_L(BT) = Sum_L(BT) + V_Liquid(I, BT)
    Next I

    '-------------------------------------------------------------------------------------------
    '*** Part C: Wellhead Pressure Calc in psi ***
    '
    ' Additional gas mole in wellhead from first cell
    ' AddMole = P(NN, BT) * VG_L(NN, BT) / (23.6591 * Z(NN, BT) * (T(NN, BT) +
   460.67))   'in kg.mole
    ' AddMole = P_WH(BT) * V_DIFF / (23.6591 * Z_WH(BT) * (T_WH(BT) +
   460.67))   'in kg.mole
    'AddMole = P_WH(BT) * VG_L(NN, BT) / (23.6591 * Z_WH(BT) * (T_WH(BT) +
   460.67))  'in kg.mole
    AddMole = P(NN, BT) * V_DIFF / (23.6591 * Z(NN, BT) * (T(NN, BT) + 460.67))
   'in kg.mole

    'Total gas mole in wellhead after timestep
    Mole_WH(BT) = Mole_WH(BT - 1) + AddMole

    'Calc new wellhead pressure in psi
```

```
For iterate = 1 To 20
   P_WH(BT) = (P_WH(BT - 1) * Mole_WH(BT) * V_Gas(1, BT - 1) * Z_WH(BT))
 / (Mole_WH(BT - 1) * V_Gas(1, BT) * Z_WH(BT - 1))
   Z_WH_Loop = modZ_HY.ZHY(T_WH(BT), P_WH(BT), SGFG_WH(0))
   Z_Diff = Z_WH(BT) - Z_WH_Loop
   If Math.Abs(Z_Diff) < 0.001 Then
      Exit For
   End If
   If Z_Diff > 0 Then
      Z_WH(BT) = Z_WH(BT) - 1 / 2 ^ iterate
   End If

   If Z_Diff < 0 Then
      Z_WH(BT) = Z_WH(BT) + 1 / 2 ^ iterate
   End If

Next iterate

' Z(1, BT) = Z_WH_Loop
      Z(1, BT) = Z_WH(BT)
' Z(1, BT) = 1
'  Call ExcelShowWellHead(P_WH(BT), Z(1, BT), BT)




'-------------------------------------------------------------------------------------------------
'*** Part D: Static Bottomhole Pressure Calc in psi ***      '

''''''''''''''''''''''''''''''''''''''''''''''''''''''''''''''''''''''''''''''''''''''''''''''''''''
' Calculate PVT and insitu properties
''''''''''''''''''''''''''''''''''''''''''''''''''''''''''''''''''''''''''''''''''''''''''''''''''''
BG(1, BT) = 14.7 / 520 * ((T(1, BT) + 460) * Z(1, BT) / P(1, BT))
P_Grad(1, BT) = (SGPG * 0.0764 / BG(1, BT)) / 144

TopPressure = P_WH(BT) + P_Grad(1, BT) * LC(1)
P(1, BT) = TopPressure

For K = 2 To NN - 1   'for cells full with 100% gas
   P(K, BT) = P(K - 1, BT) + P_Grad(1, BT) * (TD(K) - TD(K - 1))
Next

For K = NN To CN
   Assumed_Gradient = P_Grad(K, BT - 1)

   If K = NN Then
      LC_Node = TD(NN) - LC(1)
      If LC_Node < 0 Then LC_Node = 0
```

```
        Else
          LC_Node = LC(K)
        End If

        T_Node = T(K, BT)
        Multi = IIf(I = NN, (1 - LFgas), 1)
        V_Gas_Node = V_Gas(K, BT) * Multi
        V_Cell_Node = V_Cell(K, BT)

Call CalcGradient(RSCODE, BOCODE, BWCODE, API, SGPG, SGW, RSI, T_Node,
V_Gas_Node, V_Cell_Node, LC_Node, TopPressure, Assumed_Gradient, RS_Node,
RSW_Node, SGFG_Node, SGDG, BG_Node, BO_Node, BW_Node, Z_Node,
PB_Node, FG_Node, DENO_Node, DENG_Node, DENW_Node, DENM_Node,
Average_Pressure, BottomPressure, Calculated_Gradient)

        RS(K, BT) = RS_Node
        RSW(K, BT) = RSW_Node
        SGFG(K, BT) = SGFG_Node
        BG(K, BT) = BG_Node
        BO(K, BT) = BO_Node
        BW(K, BT) = BW_Node
        Z(K, BT) = Z_Node
        PB(K, BT) = PB_Node
        FG(K) = FG_Node
        DENO(K, BT) = DENO_Node
        DENG(K, BT) = DENG_Node
        DENW(K, BT) = DENW_Node
        DENM(K, BT) = DENM_Node
        PA(K, BT) = Average_Pressure
        P_Grad(K, BT) = Calculated_Gradient
        TopPressure = BottomPressure
        P(K, BT) = BottomPressure
      Next K

      TotDelLC = 0
      Sum_Pstatic(BT) = P_Grad(1, BT) * LC(1)
      For I = NN To CN   'from the rest of tubing cells
        If I = NN Then
          DelLC(I) = TD(NN) - LC(1)
          If DelLC(I) < 0 Then DelLC(I) = 0
        Else
          DelLC(I) = LC(I)
        End If
        Sum_Pstatic(BT) = Sum_Pstatic(BT) + P_Grad(I, BT) * DelLC(I)
        TotDelLC = TotDelLC + DelLC(I)
      Next I

      PWS(BT) = P_WH(BT) + Sum_Pstatic(BT)
    End Sub
```

```
Private Sub PWS2(ByVal InfluxIn As Influx, ByVal PWS_In As Double, ByRef P As
Variant, ByRef dBT As Double, ByRef V_Gas As Variant, ByVal BT As Integer, ByVal
SumdBT As Double, ByVal NN As Integer, ByVal CN As Integer, ByRef Vsg() As
Double, ByRef Vsl() As Double, ByRef V_bubble As Variant, ByRef PA As Variant,
ByRef T As Variant, ByRef LC() As Double, ByRef V_Cell As Variant, ByRef Z As
Variant, ByRef Q() As Double, ByRef Sum_G() As Double, ByRef tD1() As Double,
ByRef V_DIFF As Double, ByRef QO() As Double, ByRef PWS() As Double, ByVal
LFgas As Double, ByVal RSI As Double, ByRef RS As Variant, ByRef Dia() As Double,
ByRef Mole_WH() As Double, ByRef P_WH() As Double, ByRef Z_WH() As Double,
ByRef BG As Variant, ByRef P_Grad As Variant, ByRef TD() As Double, ByRef RSW
As Variant, ByRef SGFG As Variant, ByRef BO As Variant, ByRef BW As Variant,
ByRef PB As Variant, ByRef FG() As Double, ByRef DENO As Variant, ByRef DENG
As Variant, ByRef DENW As Variant, ByRef DENM As Variant, ByVal RSCODE As
Integer, ByVal BOCODE As Integer, ByVal BWCODE As Integer, ByVal API As
Double, ByVal SGPG As Double, ByVal SGW As Double, ByRef T_WH() As Double,
ByRef SGFG_WH() As Double, ByVal SGDG As Double, ByRef VDA As Double,
ByRef Steps As Integer)

    Dim V_Cell_Node As Double
    Dim V_Gas_Node As Double
    Dim LC_Node As Double
    Dim T_Node As Double
    Dim Sum_L(2000) As Double
    Dim V_Liquid(25, 2000) As Double
    Dim VG_L(25, 2000) As Double
    Dim StepdBT As Double
    Dim V_GasActive As Double
    Dim V_GasNN As Double
    Dim AddMole As Double
    Dim Z_WH_Loop As Double
    Dim Z_Diff As Double
    Dim iterate As Integer
    Dim K As Integer
    Dim RS_Node As Double
    Dim RSW_Node As Double
    Dim SGFG_Node As Double
    Dim BG_Node As Double
    Dim BO_Node As Double
    Dim BW_Node As Double
    Dim Z_Node As Double
    Dim PB_Node As Double
    Dim FG_Node As Double
    Dim DENO_Node As Double
    Dim DENG_Node As Double
    Dim DENW_Node As Double
    Dim DENM_Node As Double
    Dim TopPressure As Double
    Dim Average_Pressure As Double
```

```
    Dim Calculated_Gradient As Double
    Dim BottomPressure As Double
    Dim DelLC(25) As Double
    Dim Sum_Pstatic(2000) As Double
    Dim TotDelLC As Double
    Dim Multi As Double
    Dim I As Integer
    Dim Assumed_Gradient As Double

    PWS(BT) = PWS_In

    Steps = 0
    StepdBT = dBT

    V_GasActive = V_Gas(1, BT - 1)
    V_GasNN = V_Gas(NN, BT - 1)

Call CalcGVol(InfluxIn, BT, SumdBT, NN, CN, Vsg, Vsl, V_bubble, PA, T, LC,
V_Cell, Z, StepdBT, V_GasActive, V_Gas, VG_L, Q, Sum_G, tD1, V_DIFF, QO, VDA,
PWS, LFgas, RSI, RS, BO, BG)

    If VDA >= 0 Then
      GoTo 10
    End If

    If VDA < 0 Then
      For Steps = 1 To 20
        If VDA < 0 Then
          StepdBT = StepdBT - (dBT / 2 ^ Steps)
        Else
          StepdBT = StepdBT + (dBT / 2 ^ Steps)
        End If

        V_GasActive = V_Gas(1, BT - 1)
        V_Gas(NN, BT - 1) = V_GasNN

Call CalcGVol(InfluxIn, BT, SumdBT, NN, CN, Vsg, Vsl, V_bubble, PA, T, LC,
V_Cell, Z, StepdBT, V_GasActive, V_Gas, VG_L, Q, Sum_G, tD1, V_DIFF, QO, VDA,
PWS, LFgas, RSI, RS, BO, BG)

        If Math.Abs(VDA) < 0.01 Then
          Exit For
        End If
      Next Steps
    End If

10:
    V_Gas(1, BT) = V_GasActive
    LC(1) = V_Gas(1, BT) / (3.142 * (Dia(1) / 24) ^ 2)
```

```
    dBT = StepdBT
    For I = NN To CN
      V_Liquid(I, BT) = V_Cell(I, BT) - V_Gas(I, BT)
      If V_Liquid(I, BT) < 0 Then
        V_Liquid(I, BT) = 0
      End If
    Next I
    Sum_L(BT) = 0
    For I = 1 To CN
      Sum_L(BT) = Sum_L(BT) + V_Liquid(I, BT)
    Next I

  End Sub
' End Module
```

MODULE: modMath

```
'Module modMath

  Public Function Log10(ByVal x As Double) As Double
    Log10 = Math.Log(x) / Math.Log(10#)
  End Function

  Public Function ALog10(ByVal x As Double) As Double
    ALog10 = Math.Log(x) / Math.Log(10#)
  End Function

  Public Function LogN(ByVal x As Double) As Double
    LogN = Math.Log(x) / Math.Log(2.718282)
  End Function

  Public Function Min(ByVal x As Double, ByVal y As Double) As Double
    If x > y Then
      Min = y
    Else
      Min = x
    End If
  End Function

'End Module
```

APPENDIX B

DESCRIPTION OF SUMANDAK MAIN

SUMANDAK MAIN

SUDP-A

SUB-BLOCK 6S-18

OFFSHORE SABAH

Sumandak Main is located in Sub-Block 6S-18 area, offshore Sabah. It is located 43km Northwest of Labuan and 12 km from Samarang field. Discovered in September 2001 by 3 appraisal wells namely SMDK-1, SMDK-2 and SMDK-2ST1. The field produced its first oil on the 30th of November, 2006. The average water depth is 51.3 m.

Sumandak Main is located at the most northern part of the Sumandak Area, which is known to be an oil field with the presence of small gas caps. Based on the development drilling results, the hydrocarbon bearing reservoirs are from U1.0 to U6.0 layers (Lee Jean and Jiun Horng, 2009). All reservoir layers share a common oil water contact at 1300.8 m-TVDSS, and 2 gas oil contacts at 1222 m-TVDSS and 1269 m-TVDSS. The reservoir datum is at 1213 m-TVDSS.

Sumandak Main is a stratigraphic play type with multi layering reservoirs dipping 10 - 15 degrees to the East and overlain by massive shale sediments of Stage IVC. The sand bodies deposited in the Sumandak Area are a series of shallow marine sediments with wave influence and “possible” deltaic packages.

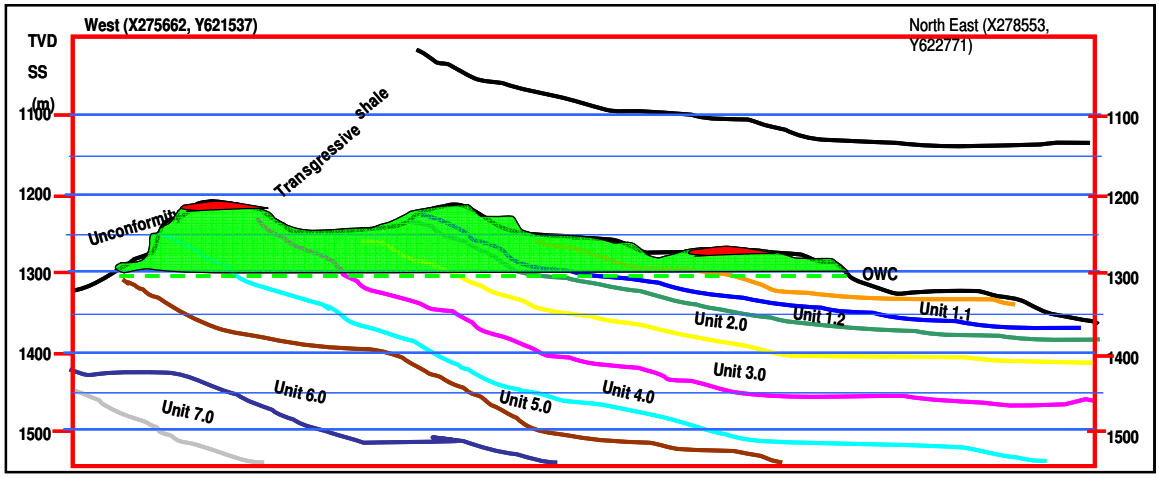

Figure B1: Cross Section of Sumandak Main

Tectonically, Sumandak fields lie in a relatively undisturbed area except for a major fault occurrence, known as the Morris Fault, which is located 1.5km west of the structure.

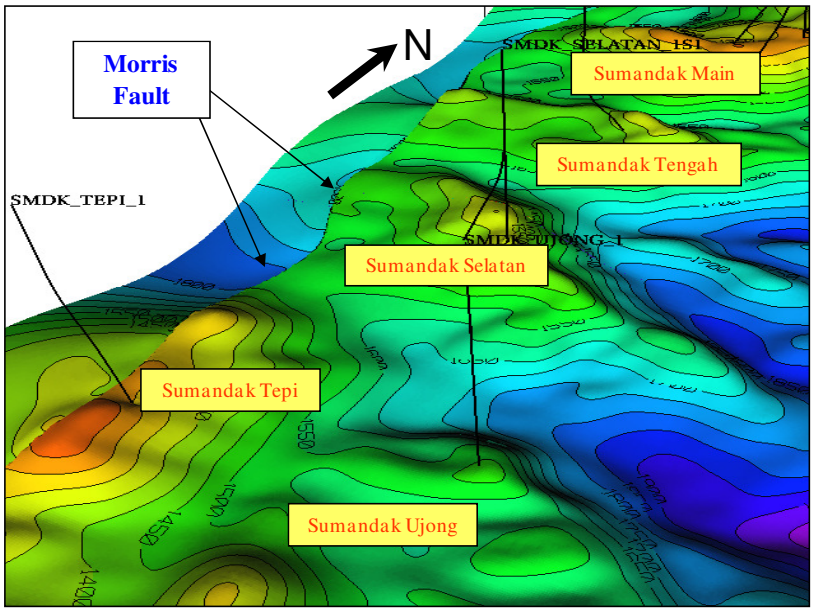

Figure B2: Fault Location

APPENDIX C

PVT DATA

DIFFERENTIAL VAPORISATION TEST AT 149 ^{o}F

Pressure (psig)	Oil Density (g/cc)	Oil FVF (bbl/stb)	Solution Gas Oil Ratio (scf/stb)	Gas FVF (cf/scf)	Gas Gravity	Z Factor
5000	0.860	1.071	236	-	-	-
4000	0.584	1.079	236	-	-	-
3000	0.848	1.087	236	-	-	-
2000	0.842	1.094	236	-	-	-
1800	0.841	1.096	236	-	-	-
1740	0.839	1.098	236	-	-	-
1400	0.841	1.093	220	0.011	0.602	0.896
1200	0.843	1.086	191	0.013	0.603	0.906
1000	0.844	1.080	160	0.016	0.603	0.919
800	0.845	1.076	127	0.020	0.605	0.935
600	0.846	1.068	100	0.027	0.607	0.952
400	0.848	1.060	67	0.040	0.617	0.966
200	0.851	1.054	30	0.079	0.636	0.983
100	0.854	1.047	14	0.149	0.652	0.991
0	0.870	1.042	0	1.150	0.713	1.000

OIL AND GAS VISCOSITYAT AT 149 ^{o}F

Pressure (psig)	Viscosity (cp)		Oil / Gas Viscosity Ratio
	Oil	Gas	
5000	2.306	-	-
4000	2.098	-	-
3000	1.875	-	-
2000	1.680	-	-
1740	1.633	-	-
1400	1.763	0.0147	119.93
1000	1.983	0.0139	142.93
600	2.243	0.0132	169.92
200	2.573	0.0127	202.60
100	2.689	0.0125	215.12

SINGLE-STAGE SEPARATOR TEST

Pressure (psig)	Separator Temperature (^{o}F)	Gas Oil Ratio (scf/stb)[1]	Separator Volume Factor (bbl/stb)[2]	Formation Volume Factor (bbl/stb)[3]	Stock Tank Oil Gravity (^{o}API)
50	87	223	1.001	-	-
0	60	7	1.000	1.084	24.52

1. Cubic feet of gas at 14.73 psia, 60 ^{o}F per barrel of oil at indicated pressure and temperature.
2. Barrel of oil at indicated temperature and pressure per barrel of stock tank oil at 60 ^{o}F.
3. Barrels of saturated oil at 1740 psig and 149 ^{o}F per barrel of stock tank oil at 60 ^{o}F.

APPENDIX D

WELL DIAGRAM: WELL A-20S

COMPLETION SCHEMATIC - SUMANDAK A-20 (PS16)
DUAL STRING - OIL PRODUCER

Well ID:	Smdk A-20	CSG:26" Drive Pipe 202.3# X-56 @ 162.4 mMDDF	9-5/8"43.5#L-80 V-Top@ 1693.50 mMDDF
Field / Platform :	Sumandak-A / SUDPA Slot#16	18-5/8"87 #K-55 BTC @ 354.0 mMDDF	Build & Hold - Max Angle 57.68° at 1689.20 mMDDF
Rig Name :	Tioman-6 (Tender)	13-3/8" 68.0#L-80 K-fox @ 1532.0 mMDDF	Screen : W-ford 9-5/8" WWS 316 SS 200 Micron
Water Depth (m) :	53.0 meter	Compl Equipment : Halliburton	X-Mas Tree : Solar Alert 3-1/8" 5000 psi
Drill Floor Height :	34.2.meter-AMSL	Completion Date 08 Feb 2008	Tubing: 3-1/2" 9.2 ppf, L-80, K-Fox
Drill Floor to Tubing Hanger :	14.6 meter-AMSL	Completion Fluid : 3% KCL+NaCL of 9.0 ppg	
Spud Date :	25-Jan-08	Packer Fluid: Completion Fluid with corr inhib + oxygen scav+bactericide - 9.0 ppg	

SHORT STRING 3-1/2" TBG, 9.2PPF, L-80, FOX			DEPTH mTVDDF	DEPTH mMDDF
MIN ID IN	MAX OD IN	EQUIPMENT		
2.923	13.550	TUBING HANGER	14.60	14.60
2.900	4.135	FLOW COUPLING		
2.813	5.030	SCSSV-TRSV	145.61	145.61
2.813	3.960	X-NIPPLE	343.95	344.15
2.900	5.230	GLM#1 (1" 12/64" 840 psi)	491.47	495.98
2.900	5.230	GLM#2 (1" 12/64" 820 psi)	718.11	773.66
2.900	5.230	GLM#3 (1" 12/64" 800 psi)	845.38	960.53
2.900	5.230	GLM#4 (1" 12/64" 785 psi)	973.81	1148.57
		PIP TAG IN 13-3/8" CASING	1,063.49	1280.00
2.900	5.230	GLM#5 (1" 12/64" orifice)	1,133.43	1381.34
8.755	12.125	13-3/8 X 9-5/8" ZXP LINER HANGER	1,199.16	1479.29
		PIP TAG	1,207.39	1491.60
8.755	10.330	9-5/8" CSG PUP 43.5# L-80 V-TOP	1,207.40	1491.62
8.755	10.330	9-5/8" BLANK CSG 43.5# L-80 V-TOP	1,209.41	1494.62
8.755	11.780	SWELL PACKER TOP SEAL	1,244.82	1548.13
		BOTTOM SEAL	1,246.91	1551.31
2.813	3.960	X-NIPPLE	1,246.13	1550.12
RESERVOIR UNIT- 3.0 (GAS)- 15.69 MT		TOP RES LAYER - 1553.16	1,248.13	
		BTM RES LAYER - 1568.85	1,257.98	
8.755		TOP SEAL	1,257.50	1568.08
8.755	11.500	SWELL PACKER		
		BOTTOM SEAL	1,259.50	1571.27
		TOP RES LAYER - 1570.13	1,258.78	
RESERVOIR UNIT- 3.0 (OIL) - 31.60 MTR				
		BTM RES LAYER - 1601.73	1,278.19	
2.813	4.550	SSD-XD ASSY (CLOSED)	1,268.34	1585.45
8.755	11.780	TOP SEAL	1,277.76	1601.02
		SWELL PACKER		
		BOTTOM SEAL	1,279.69	1604.21
2.690	3.960	2.75" XN NIPPLE	1,279.71	1604.24
2.871	3.920	POP ASSY	1,280.33	1605.26
2.992	3.500	PERFORATED PUP JOINT		
-	3.500	BULL PLUG		
		EOT	1,281.33	1606.93
		TOP RES LAYER - 1603.28	1,279.13	
RESERVOIR UNIT-3.1 (OIL) - 8.24 MTR				
		BTM RES LAYER - 1611.52	1,284.08	
8.755	11.780	TOP SEAL	1,284.48	1612.19
		SWELL PACKER		
		BOTTOM SEAL	1,286.38	1615.38
		PIP TAG	1,286.67	1615.87
		TOP RES LAYER - 1615.11	1,286.22	
RESERVOIR UNIT-3.2 (OIL) - 33.54 MTR				
		BTM RES LAYER - 1648.65	1,305.90	
8.755	11.780	TOP SEAL	1,306.23	1649.22
		SWELL PACKER		
		BOTTOM SEAL	1,308.07	1652.41
		TOP RES LAYER - 1652.11	1,307.90	
RESERVOIR UNIT-4.0 (OIL) 35.51 MTR				
		BTM RES LAYER - 1687.62	1,327.65	
8.755	10.333	9-5/8" CSG PUP 43.5# L-80 V-TOP	1,327.99	1688.24
2.875	10.333	PACK OFF BUSHING	1,328.83	1689.79
8.755	9.625	9-5/8" REAMER SHOE (bottom)	1,330.81	1693.50

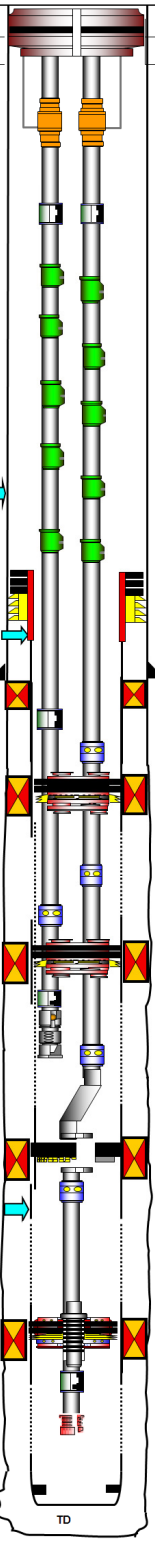

DEPTH mMDDF	DEPTH mTVDDF	ANGLE (°)	LONG STRING 3-1/2" TBG, 9.2PPF, L-80, FOX EQUIPMENT	MIN ID IN	MAX OD IN
14.60	14.60		TUBING HANGER	2.923	13.550
			FLOW COUPLING	2.900	4.135
155.32	155.32	0.9	SCSSV-TRSV	2.813	5.030
353.79	353.53	4.7	X-NIPPLE	2.813	3.960
505.90	500.56	21.7	GLM#1 (1" 12/64" 830 psi)	2.900	5.230
778.54	721.55	45.6	GLM#2 (1" 12/64" 845 psi)	2.900	5.230
964.96	848.42	47.5	GLM#3 (1" 12/64" 855 psi)	2.900	5.230
1154.46	977.85	47.0	GLM#4 (1" 12/64" 870 psi)	2.900	5.230
1390.59	1,139.75	47.6	GLM #5 (1" 12/64" orifice)	2.900	5.230
1479.29	1,199.16		13-3/8 X 9-5/8" ZXP LINER HANGER	8.755	12.125
1532.0	1,234.25		13-3/8" CSG SHOE		
1559.53	1,252.13		SSD-XD ASSY (CLOSED)	2.813	3.960
1568.96	1,258.05	52.1	9-5/8" BHD DUAL HYD PKR - S/S SET L/S REL	2.885	8.475
1571.63	1,259.73		TOP OF SCREEN (2 X 35FT +1 X 21 FT)		
			9-5/8" WWS SCREEN 316-SS 200 MICRON	8.833	10.396
1577.80	1,263.60		SSD-XD ASSY (CLOSED)	2.813	4.550
1599.57	1,276.88		BOTTOM OF SCREEN		
1601.90	1,278.29	53.4	9-5/8" BHD DUAL HYD PKR - S/S SET L/S REL	2.885	8.475
			9-5/8" CSG PUP 43.5# L-80 V-TOP	8.755	10.330
1604.53	1,279.88		TOP OF SCREEN		
			9-5/8" WWS SCREEN 316-SS 200 MICRON (1 X 21 FT)	8.742	10.396
1609.42	1,282.83		SSD-XD ASSY (CLOSED)	2.813	4.550
1610.97	1,283.75		BOTTOM OF SCREEN		
			9-5/8" BLANK CSG 43.5# L-80 V-TOP	8.755	10.330
1612.88	1,284.89	54.35	9-5/8" AHC SINGLE HYDRAULIC PKR	2.960	8.300
1617.44	1,287.59		SSD-XD ASSY (CLOSED)	2.813	4.550
1615.87	1,286.67		TOP OF SCREEN		
			9-5/8" WWS SCREEN 316-SS 200 MICRON (3 X 35 FT)	8.833	10.396
1647.96	1,305.49		BOTTOM OF SCREEN		
1649.24	1,306.24		LTSA c/w 7 SEAL UNITS	2.880	4.250
1650.00	1,306.68	54.4	9-5/8" BWS PERMANENT PKR + SBE + HMS	4.000	8.120
1654.98	1,309.53		XN NIPPLE (2.75" SEAL BORE)	2.690	3.960
1655.94	1,310.08		TOP OF SCREEN (3 X 35 FT)		
1657.24	1,310.82		SELF ALIGNING MULE SHOE (EOT)	2.940	3.970
1658.16	1,311.34		EOT		
			9-5/8" WWS SCREEN 316-SS 200 MICRON	8.833	10.396
1688.24	1,327.97		BOTTOM OF SCREEN		
1695.00	1,331.61	57.7	TOTAL DEPTH		

Prepared by : M Azrul / Djuhana Syafei / Khairul A Rashid
4-Jun-10

APPENDIX E

WELL DIAGRAM: WELL A-18L

COMPLETION SCHEMATIC - SUMANDAK A-18 (PS-07)
DUAL STRINGS OIL PRODUCER

Well ID:	Smdk A-18(PS 07)	CSG:26" Drive Pipe 202.3# X-56 @ 162.4 mMDDF		7" 26.0# L-80 V-Top @ 1366 mMDDF
Field :	Sumandak-A SUDP-A Slot# 08	13-3/8"54.5#K-55 BTC @ 752.0 mMDDF		Build & Hold - Max Angle 70.38° at 1634.40 mMDDF
Rig Name :	Tioman-6 (Tender)	9-5/8"40.0#L-80 V-Top@1305 mMDDF		Screen : Weatherford 7" WWS 316 SS 175 Micron
Water Depth (m) :	53.0 meter	Compl Equipment : Halliburton		X-Mas Tree :Solar Alert 3-1/8" 5000 psi
Drill Floor Height :	34.2.meter-AMSL	Completion Date : xx November 2007		Tubing: 3-1/2" 9.2 ppf, L-80, K-Fox
Drill Floor to Tubing Hanger :	14.5 meter-AMSL	Completion Fluid : 3% KCL+NaCL of 9.0 ppg		
Spud Date :	17-Nov-07	Packer Fluid: Completion Fluid with corr inhib + oxygen scav+bactericide - 9.0 ppg		

SHORT STRING 3-1/2" TBG, 9.2PPF, L-80, FOX			DEPTH mTVDDF	DEPTH mMDDF		DEPTH mMDDF	DEPTH mTVDDF	ANGLE (°)	LONG STRING 3-1/2" TBG, 9.2PPF, L-80, FOX		
MIN ID IN	MAX OD IN	EQUIPMENT							EQUIPMENT	MIN ID IN	MAX OD IN
2.923	13.500	TUBING HANGER							TUBING HANGER	2.923	13.500
2.880	3.920	FLOW COUPLING	149.52	150.00		155.00	149.48		FLOW COUPLING	2.880	3.920
2.813	5.030	SCSSV-TRSV							SCSSV-TRSV	2.813	5.030
2.813	3.960	X-NIPPLE	347.82	350.00		355.00	352.77		X-NIPPLE	2.813	3.960
2.900	5.230	GLV #1(1" 12/64" 825 psi)	437.94	441.53		470.00	465.56	15.4	GLV #1(1" 12/64" 825 psi)	2.900	5.230
2.900	5.230	GLV #2(1" 12/64" 750 psi)	712.82	726.29		754.03	739.56	15.1	GLV #2(1" 12/64" 755 psi)	2.900	5.230
2.900	5.230	GLV #3(1" 12/64" 720psi)	907.06	928.87		938.65	916.23	21.4	GLV #3(1" 12/64" 725psi)	2.900	5.230
2.900	5.230	GLV #4(1" 12/64" 690 psi)	1060.46	1103.87		1115.33	1069.58	37.4	GLV #4(1" 12/64" 690 psi)	2.900	5.230
2.900	5.230	GLV #5(1" 12/64" orifice)	1211.04	1336.48		1355.07	1219.94	63.7	GLV #5(1" 12/64" orifice)	2.900	5.230
		PIP TAG	1241.27	1403.60							
2.813	4.550	SSD-XD ASSY (CLOSED)		1404.0		1392.00	1236.37		X-NIPPLE	2.813	3.960
2.885	8.545	9-5/8" BHD DUAL HYD PKR. (S/S SET - L/S REL 72 KLBS)	1244.69	1412.0		1412.00	1244.69	65.6	9-5/8" BHD DUAL HYD PKR. (S/S SET - L/S REL 72 KLBS)	2.885	8.545
2.690	3.960	XN NIPPLE	1245.51	1414.0							
2.871	3.920	POP ASSY	1245.92	1415.0							
2.992	3.500	PERFORATED PUP JOINT									
-	3.500	CATCHER SUB									
		EOT	1246.73	1417.0							
						1441.16	1256.49	65.6	9-5/8 X 7" LINER HANGER ASSY	6.188	8.350
		PIP TAG	1260.77	1451.9							
						1482.00	1272.61	66.7	9-5/8" CSG SHOE		
6.276	7.656	7" 26PPF L-80 BLANK PIPE									
		TOP SEAL	1281.71	1505.45							
6.276	8.150	SWELL PACKER				1507.00	1282.32		SSD ASSY (CLOSED)	2.813	4.550
		BOTTOM SEAL	1282.89	1508.45		1510.43	1283.67	67.0	TOP OF SCREEN	6.276	8.250
		PIP TAG IN THE SCREEN									
		TOP OIL LAYER - 1509.89 m	1238.57								
RESERVOIR UNIT- 3.0 (OIL) (47m)			1292.13	1532.24					WWS SCREEN 316-SS 175 MICRON (4 x 35 ft)	6.276	8.250
						1554.08	1300.31		BOTTOM OF SCREEN	6.276	8.250
									RA MARKER SUB	4.520	2.986
		TOP SEAL	1300.86	1555.58				67.6	7" BHR SINGLE HYDRAULIC PKR	2.835	5.875
6.276	8.150	SWELL PACKER				1557.00	1301.37				
		BTM OIL LAYER - 1557.07 m	1301.40								
		BOTTOM SEAL	1301.95	1558.58		1560.00	1302.46		TOP OF SCREEN	6.276	8.250
		TOP OIL LAYER - 1558.80 m	1302.03			1562.46	1303.35		SSD ASSY (CLOSED)	2.813	4.550
RESERVOIR UNIT- 3.1 (OIL) (4.8m)									WWS SCREEN 316-SS 175 MICRON (21 ft x 1)	6.276	8.250
		BTM OIL LAYER - 1563.60m	1303.76			1566.34	1304.75		BOTTOM OF SCREEN	6.276	8.250
		TOP SEAL	1305.65	1568.85							
6.276	8.150	SWELL PACKER				1570.00	1306.07	68.4	7" BHR SINGLE HYDRAULIC PKR	2.835	5.875
		BOTTOM SEAL	1306.74	1571.85							
						1572.32	1306.91	68.4	TOP OF SCREEN	6.276	8.250
						1573.00	1307.15		XN NIPPLE (2.75" SEAL BORE)	2.690	3.960
		TOP OIL LAYER - 1571.48 m	1306.61			1575.00	1307.88		POP ASSEMBLY	3.000	3.920
RESERVOIR UNIT- 3.2 (OIL) (31m)									WWS SCREEN 316-SS 175 MICRON (35 ft x 2) + (21 ft x 1)	6.276	8.250
		BTM OIL LAYER - 1602.60 m	1317.59								
						1600.50	1316.69		BOTTOM OF SCREEN	6.276	8.250
		TOP SEAL	1317.38	1602.00							
6.276	8.150	SWELL PACKER									
		BOTTOM SEAL	1318.43	1605.00							
6.276	7.656	7" 26 ppf L80 15ft x 1 + 10 ft x 2 Pup Joint									
6.276	7.656	7" 26 ppf L80 42 ft Blank Pipe									
2.875	7.656	PACK OFF BUSHING									
6.276	7.656	7" CASING PUP JOINT 15 FT LONG									
6.276	7.000	REAMER SHOE									
						1610.93	1320.49		PBTD		
						1639.00	1329.99	70.4	TOTAL DEPTH		

Prepared by :M Farris Bakar/ Djuhana Syafei/ Khairul Azmi
16-Nov-07

APPENDIX F

WELL DIAGRAM: WELL A-08

COMPLETION SCHEMATIC - SUMANDAK A-08 (PS-11)
SINGLE SELECTIVE STRING OIL PRODUCER

Well ID:	Smdk A-08	CSG:26" Drive Pipe 202.3# X-56 @ 162.4 mMDDF	7" 26.0# L-80 V-Top @ 1365 mMDDF
Field / Platform :	Sumandak-A / SUDP-A Slot-04	13-3/8" 54.5# K-55 BTC@ 750 mMDDF	Build & Hold - Max Angle 15.0° at 461.4 mMDDF
Rig Name :	Tioman-6 (Tender)	9-5/8"40.0#L-80 V-Top@1277.8 mMDDF	TD : 1370.0 mMDDF
Water Depth (m) :	53.0 meter	Compl Equipment : Halliburton	Screen : Weatherford 7" WWS 316 SS 175 Micron
Drill Floor Height :	34.2.meter-AMSL	Completion Date : 18 May 2007	X-Mas Tree : Cameron 3-1/8" 5000 psi
Drill Floor to Tubing Hanger :	14.6 meter-AMSL	Completion Fluid : 3% KCL+NaCL of 9.0 ppg	Tubing: 3-1/2" 9.2 ppf, L-80, K-Fox
Spud Date :	3-May-07	Packer Fluid: Completion Fluid with corr inhib + oxygen scav+bactericide - 9.0 ppg	

SHORT STRING			DEPTH		DEPTH	ANGLE	LONG STRING		
			mMDDF		mMDDF	(°)	3-1/2" TBG, 9.2PPF, L-80, FOX		
MIN ID IN	MAX OD IN	EQUIPMENT					EQUIPMENT	MIN ID IN	MAX OD IN
					14.60		TUBING HANGER	2.832	11.000
							FLOW COUPLING	2.900	4.135
					150.36		SCSSV-TRSV	2.813	5.030
					149.95				
					300.44		X-NIPPLE	2.813	3.960
					299.37				
					410.51		GLM#1 (1" GLV#1 IPO 12/64" 840 PSI)	2.900	5.230
					408.31				
					681.21		GLM#2 (1" GLV#2 IPO 12/64" 810 PSI)	2.900	5.230
					666.86				
					873.28		GLM#3 (1" GLV#3 IPO 12/64" 775 PSI)	2.900	5.230
					850.61				
					1031.36		GLM#3 (1" GLV#3 IPO 12/64" 745 PSI)	2.900	5.230
					1003.81				
					1188.95		GLM#4 (1" GLV#4 12/64" ORIFICE)	2.900	5.230
					1156.50				
					1199.36		SSD-XD ASSY (CLOSED)	2.813	4.550
					1166.52				
		PIP TAG	1200.06						
			1167.26						
					1212.55		9-5/8" BHR SINGLE HYD PKR.	2.880	8.380
					1179.34				
6.188	8.350	9-5/8 X 7" LINER HANGER ASSY			1231.40				
					1197.56				
		PIP TAG	1240.40						
			1206.24						
			1277.80		1277.80		CSG SHOE 9-5/8" 40# L-80 VAM TOP		
			1242.32		1242.32				
6.276	7.688	7" 26PPF L-80 BLANK PIPE							
		TOP SEAL	1290.10						
6.276	8.150	SWELL PACKER	1254.17		1290.86		SSD-XD ASSY (OPEN)	2.813	4.550
		BOTTOM SEAL	1293.10		1264.90				
		TOP OIL LAYER - 1295.5	1257.06						
		1259.37			1294.68		TOP OF SCREEN	6.276	8.250
					1258.58				
RESERVOIR UNIT- 1.1 (OIL) - 32.0 MTR							WWS ULTRA GRIP 316-SS 175 MICRON	6.276	6.276
							(3 x 35 FT)		
		1290.17							
		BTM OIL LAYER - 1327.5			1327.39(1290.07)		BOTTOM OF SCREEN	6.276	8.250
					1328.35		PIP TAG		
					1290.99				
		TOP SEAL	1330.32(1292.88)						
6.276	8.150	SWELL PACKER			1331.33		7" BHR HYDR SET PACKER	2.940	6.000
		BOTTOM SEAL	1333.32(1295.77)		1293.86				
6.276	7.688	7" 26PPF L-80 PUP JOINT			1336.42(1298.75)		2.75" XN-NIPPLE	2.690	3.893
					1338.00(1300.27)		TOP OF SCREEN	6.276	8.250
		TOP OIL LAYER - 1338.5							
		1300.75			1337.65(1299.93)		POP ASSEMBLY	3.000	3.920
					1337.91(1300.18)		EOT		
RESERVOIR UNIT- 1.2 (OIL) - 16.5 MTR							WWS ULTRA GRIP 316-SS 200 MICRON	6.276	6.276
							(1 x 35 FT+ 1 X 21 FT)		
		1316.61							
		BTM OIL LAYER - 1355.0			1355.23(1316.84)		BOTTOM OF SCREEN	6.276	8.250
		TOP SEAL	1358.16(1319.65)						
6.276	8.150	SWELL PACKER							
		BOTTOM SEAL	1361.16(1322.54)						
2.875	7.688	PACK OFF BUSHING							
6.276	7.688	7" CASING PUP JOINT 5 FT LONG							
-	7.000	REAMER SHOE							
		BTM REAMER SHOE	1365.00(1326.23)				PBTD		
				TD	1370.00(1331.03)		TOTAL DEPTH		

Prepared by : M Farris Bakar/M Azrul Nuriyadi/Djuhana Syafei
19-May-07

APPENDIX G

PRESSURE ADJUSTMENT CALCULATION

Well A-20S

Data:

Water depth	=	53 meter
Drill floor height	=	34.2 meter – AMSL
Mid-perforation depth	=	1195 m-TVDSS
Gauge depth	=	1145.38 m-TVDDF
Fluid gradient	=	0.365 psi/ft

Correct gauge depth to the same refernce depth of mid-perforation depth:

Gauge depth	=	1145.38 m-TVDDF
	=	(1145.38 – 53 – 34.2) m-TVDSS
	=	1058.18 m-TVDSS

Calculate pressure difference between gauge and mid-perforation:

Depth difference	=	1195 m-TVDSS - 1058.18 m-TVDSS
	=	136.82 meter
	=	448.89 ft
Pressure difference	=	(448.89 ft) x (0.365 psi/ft)
	=	163.84 psi